Requirements for Copernicus Ocean Colour Vicarious Calibration Infrastructure

31st July 2017

Study funded by the European Commission and EUMETSAT under contract EUM/CO/16/4600001772/EJK

PREAMBLE

All requirements stated in this report come from current knowledge of the science of ocean colour and state-of-the-art instrumental performance. The choice is made to focus on the System Vicarious Calibration (SVC) approach, which is a calibration of the system comprising the satellite instrument and the processing algorithm. SVC has been operationally used by Space Agencies in the last decade to meet ocean colour mission requirements in open waters. Given our current knowledge, SVC is the most achievable approach to be implemented in the future in the frame of the Copernicus programme. As part of the processing algorithm, the atmospheric correction plays a crucial role in the success of any SVC; its robustness, validation and continuous improvement shall be conducted in parallel of the SVC, including over complex coastal waters of interest to many users. Most of present requirements are based on the standard atmospheric correction algorithm (Gordon and Wang, 1994; Antoine and Morel, 1999), also currently used by Space Agencies for open waters and climate-related studies, notably in the Sentinel-3 mission. This document focuses on in-water technology because current above-water technology does not allow the production of continuous measurements of water-leaving radiance with the same accuracy, when performed in deep oligotrophic/mesotrophic waters and well away from the coast. Limitations are mostly dictated by deployment technologies, rather than by the above-water methodology. Should science and technology significantly progress in this domain, departure from these specific requirements could be acknowledged, as far as the required accuracy on ocean colour data is proven to be respected. This report must be considered as a living document which would integrate such a progress.

CONTRIBUTING AUTHORS

EUMETSAT Technical officer: Ewa Kwiatkowska

Study team:

Constant Mazeran	Solvo (Antibes – France); study responsible, editor
Carsten Brockmann	Brockmann Consult (Geesthacht – Germany)
Kevin Ruddick	Royal Belgian Institute for Natural Sciences (RBINS, Brussels – Belgium)
Ken Voss	University of Miami (Coral Gables – Florida)
Francis Zagolski	Solvo (Antibes – France)

Review expert team (in alphabetical order):

David Antoine	Curtin University (Perth – Western Australia) & CNRS, Laboratoire d'Océanographie de Villefranche (LOV, Villefranche/Mer - France)
Agnieszka Bialek	National Physical Laboratory (NPL, Teddington - UK)
Vittorio Brando	Istituto di Scienze dell'Atmosfera e del Clima - Consiglio Nazionale delle Ricerche (ISAC-CNR, Bologna - Italy)
Craig Donlon	European Space Agency (ESA, Noordwijk - The Netherlands)
Bryan Franz	National Aeronautics & Space Administration / Goddard Space Flight Center (NASA/GSFC, Greenbelt - MD)
Carol Johnson	National Institute of Standards and Technology (NIST - Optical Radiation Group, Gaithersburg - MD)
Hiroshi Murakami	Japan Aerospace Exploration Agency (JAXA, Earth Observation Center, Ohashi - Japan)
Young-Je Park	Korea Institute of Ocean Science and Technology (KIOST, Ansan - South Korea)
Menghua Wang	National Oceanic & Atmospheric Administration (NOAA center for Satellite Applications & Research, College Park - MD)
Giuseppe Zibordi	European Commission, Joint Research Center (JRC, Ispra - Italy)

ACKNOWLEDGEMENTS

This study was funded by the European Commission and EUMETSAT under contract EUM/CO/16/4600001772/EJK. Members of the Review expert team, as well as Ken Voss, have actively participated in the development of this document on a volunteer basis and are kindly acknowledged for sharing their expertise. We are also grateful to Vincenzo Vellucci (UPMC, Laboratoire d'Océanographie de Villefranche, France) for his helpful comments on the report.

EXECUTIVE SUMMARY

The European Commission, via its Copernicus programme, has invested in decades of commitment to operational Earth Observation from space. As part of this programme, Ocean Colour (OC) instruments on-board the Sentinel-3 missions as well as Sentinel-2 have become an essential source of data at global and regional scales for continuous monitoring, forecasting and alerting on the ocean biogeochemistry. Through the Copernicus Marine Environment Monitoring Service (CMEMS), these data are expected to support the implementation of European marine and environmental policies, to contribute to climate studies and to empower economical activities such as fisheries, aquaculture, health, shipping, water supply, tourism and offshore operations.

Achieving the Copernicus objectives in a context of increasing climate variability requires, however, climate-quality ocean colour data with emphasis on accuracy and stability, both for long-term and cross-mission time series. The main challenge resides in the necessary stringent calibration and characterisation of the sensors, because the marine signal is only a small fraction of the radiometry acquired by the satellite at the top of atmosphere. It is acknowledged that limiting the uncertainty of water-leaving radiance to below 5% (Global Climate Observing System GCOS requirements) cannot be achieved today with pre-launch and on-board instrument calibration alone. OC instruments require a complementary System Vicarious Calibration (SVC), i.e. an indirect calibration of the sensor and the processing algorithm through highly accurate and long-term sea-truth measurements.

This document is targeted as a traceable reference for the development and operation of a future European SVC infrastructure that would enable Copernicus to reach its operational objectives. The purpose is twofold: first, to clearly justify the need of SVC in the Copernicus programme; and second, to formally specify the scientific, technical and operational requirements for the SVC infrastructure. This document has been written and reviewed in cooperation with the international ocean colour community to ensure state-of-the-art Copernicus requirements and standardisation in joint efforts such as within the Committee on Earth Observation Satellites (CEOS).

The requirements are driven by the uncertainty budget of the SVC process, from the in situ radiometric measurement to the computation of mission-averaged vicarious calibration gains. All sources of uncertainty are listed, following principles of metrology and encompassing the various aspects of SVC:

- The SVC process: requirements on the measurement uncertainties and on the methodology;
- The SVC field infrastructure: requirements on the radiometer design, characterisation and calibration, on the platform and environmental conditions;
- The SVC data processing: requirements on data processing and gain computation;
- The SVC operation and maintenance: requirements on the field operation and maintenance, data access, management, including human aspects to ensure a sustainable service.

The overall uncertainty approach presented in this document, and the detailed uncertainty numbers provided whenever possible, are intended as a guideline to assess the performance of any SVC system for Ocean Colour. The numbers written in the companion Excel file to this report shall be understood as examples, based on state-of-the-art practice, to minimise the uncertainty to an acceptable level.

This document strongly builds upon the experience of the Marine Optical BuoY (MOBY) buoy in the USA and the "*BOUée pour l'acquiSition d'une Série Optique à Long termE*" (BOUSSOLE) buoy in Europe. In view of planning a successful operational SVC in Europe within the Copernicus programme, the experience gained over the past two decades demonstrates the crucial need to ensure sustainable resources (staff, knowledge and infrastructure) to build long-term data series over multi-mission lifetime.

1. INTRODUCTION

1.1. JUSTIFICATION OF OCEAN COLOUR VICARIOUS CALIBRATION

Ocean Colour (OC) satellites provide a unique synoptic view of the Earth's ocean biological conditions and support both climate studies (summarised by the Global Climate Observing System, GCOS, 2011, 2016), marine and coastal water quality monitoring (e.g. Kratzer et al., 2014) and industries such as fisheries, aquaculture, shipping, water supply, tourism, offshore operations, health and real estate (IOCCG, 2008). In Europe, the Copernicus programme is delivering, through its Space component, operational marine data and services for these industries and other environmental policies (Marine Strategy Framework Directive, Water Framework Directive, Common Fisheries Policy, EU Integrated Marine Policy). Ocean Colour data is thus an important component of the Copernicus Marine Environment Monitoring Service (CMEMS) providing information on living marine environments.

Vicarious calibration must be used to achieve the required ocean colour product uncertainties (IOCCG, 2012; INSITU-OCR, 2012). Without vicarious calibration, these uncertainties are unobtainable today with only direct pre-launch and on-board space sensor calibrations. Ocean colour technology exploits the spectral modification of sunlight by water constituents such as phytoplankton chlorophyll, suspended sediments and coloured dissolved organic matter (CDOM). However, this modification of the sunlight in the water column is further changed by surface and atmospheric optical processes before finally being measured by the spaceborne radiometer. The main ocean colour variable is water-leaving radiance which is used to derive the bio-optical water constituents. Water-leaving radiances contribute only a small fraction to the total radiometric signal measured at Top Of Atmosphere (TOA), about 10% in the blue/green spectrum in open clear waters and less in the red and near infra-red. Hence, achieving the standard ocean colour mission requirements requires very stringent calibration and characterisation of the spaceborne sensor, spectrally dependent and well below 0.5% (Zibordi et al., 2015). Climate applications impose even more stringent requirements. Sensor pre-launch laboratory calibrations and in-flight on-board calibrations do not achieve these uncertainties today.

Ocean Colour Vicarious Calibration (OC-VCAL) complements pre-launch and on-board calibrations by using highly accurate in situ measurements of water-leaving radiances. These measurements are the principal source of sea-truth for the vicarious approach. OC-VCAL reduces residual biases in water-leaving radiances.

OC-VCAL enables meeting the ocean colour mission requirements (Donlon *et al*., 2011). As an example, most ocean colour applications require long-term data records in order to detect trends and anomalies. When building long-term data records, it is crucial to harmonise and ensure traceability of the products of the various space missions against a sustainable source of sea-truth measurement. In the frame of the Copernicus programme, the long-term time series of data will be produced by a series of similar but physically different instruments (Sentinel-3 A, B, C, D) and by third party contributing missions.

An example in Figure 1 is based on Sentinel-3A OLCI and Aqua MODIS product time series. Average values of remote sensing reflectances are plotted for the blue band at 442.5 nm (the reflectances are derived from water-leaving radiances). The blue line shows MODIS reflectances—all of which have been vicariously calibrated. The red line shows corresponding OLCI reflectances for two periods of time: firstly, for May 2016 – June 2017 for which the data have not yet been vicariously calibrated and secondly, for June – July 2017, for which the data have been vicariously calibrated. During the period in which OLCI was not vicariously calibrated, there is a bias of about 25% in remotely sensed reflectance compared to MODIS (which is vicariously calibrated). Vicarious calibration applied to OLCI from June 2017 yields excellent harmonisation with MODIS.

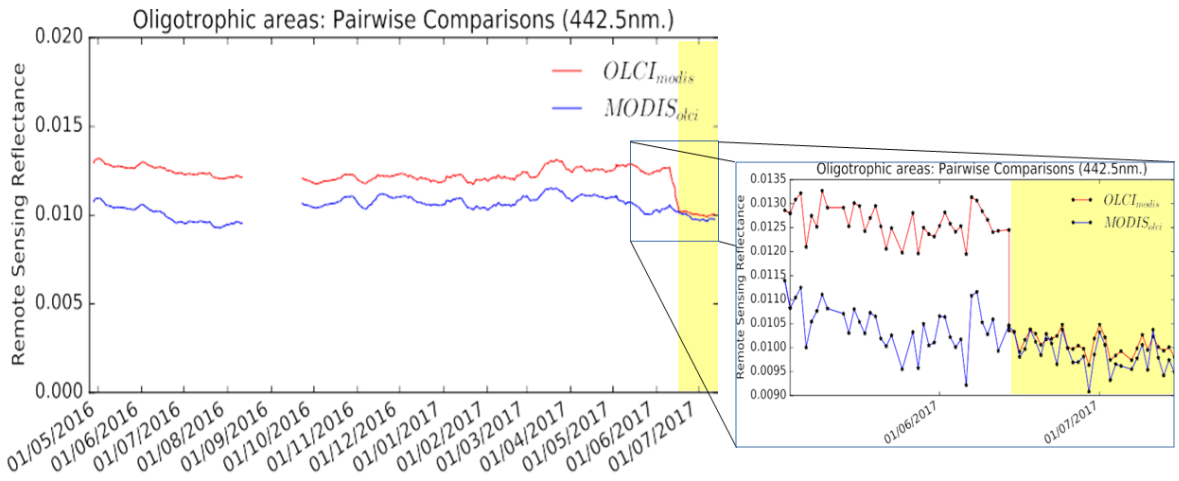

Figure 1. Time-series of pairwise OLCI (red) and MODIS (blue) remote-sensing reflectance at 442.5 nm over oligotrophic areas. Vicarious calibration is applied to MODIS from the beginning, while it has been implemented to OLCI only from mid-June 2017 (yellow overlay). EUMETSAT monitoring.

OC-VCAL also strongly impacts all downstream ocean colour products, as illustrated on Figure 2 for chlorophyll-a concentration. Accurate water-leaving radiances allow the derivation of accurate bio-optical products and the attainment of ocean colour mission requirements (Donlon *et al*., 2011).

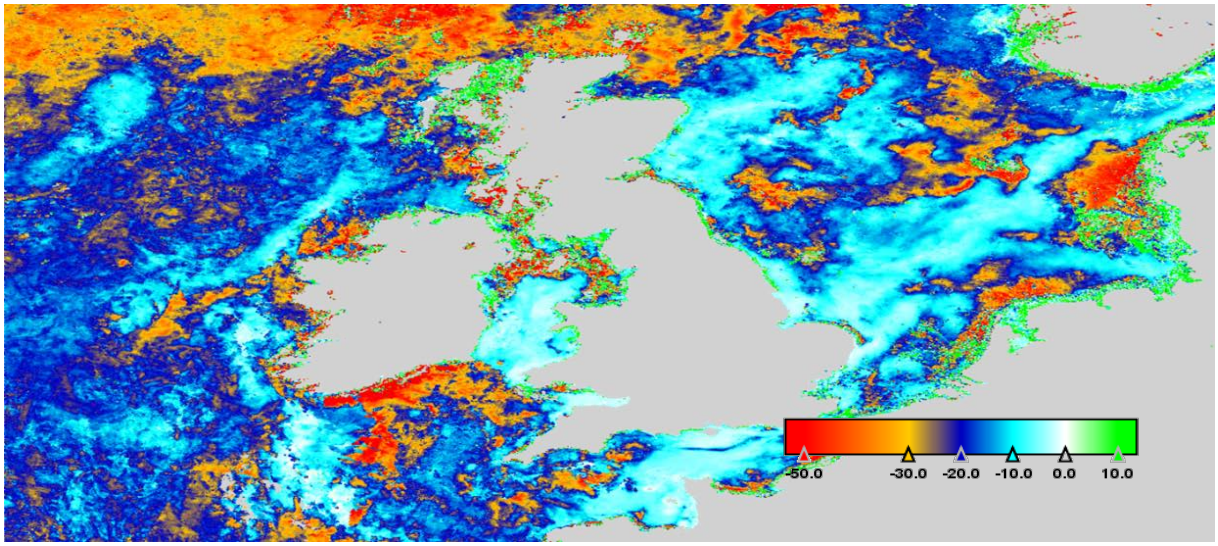

Figure 2. Impact of vicarious calibration on chlorophyll-a concentration, as measured by MERIS over the Eastern North Atlantic and North Sea in May 2008. The relative change (in %) is due to disabling vicarious calibration. When it is disabled, 82% of the pixels change by more than 10% in chlorophyll-a magnitude and 42% by more than 20%.

1.2. SCOPE OF THE DOCUMENT

1.2.1. EUMETSAT STUDY

This report and its companion Excel annex are the project deliverables of the study "*Requirements for Copernicus Ocean Colour Vicarious Calibration Infrastructure*" lead by EUMETSAT from September 2016 to July 2017. The goal of this study is to generate a complete scientific, technical and operational requirements document that can be used as a traceable reference for all steps and aspects of an OC-VCAL infrastructure development and operations for the Copernicus Programme.

After summarising the background on OC-VCAL (this introductory section 1), this report describes the traceability chain of the OC-VCAL process (section 2). Ensuring SI traceability in the sea-truth data is necessary so that OC-VCAL can contribute to SI traceability of the Copernicus data and services. This document then details the requirements for the four main aspects of OC-VCAL:

1. The OC-VCAL process itself, i.e. the methodology combining ground-truth measurements and Earth Observation (EO) data to reach the desired quality in marine products; for this we exclusively rely on System Vicarious Calibration (SVC), which is to date the only solution able to meet the specified accuracy (section 3);
2. The OC-VCAL field infrastructure, which is the core element providing sea-truth data with the highest radiometric quality (section 4);
3. The OC-VCAL data processing, i.e. the very concrete process that produces vicarious gains over the mission lifetime with associated uncertainties (section 5);
4. The OC-VCAL operation and service, i.e. the implementation of the OC-VCAL facility within Copernicus, associated with maintenance, interfaces, timelines and management aspects (section 6).

The requirements covered in this document support long-term and multi-mission OC-VCAL. Among the various applications that require and benefit from OC-VCAL, we target here climate change investigation, as it is the most demanding in terms of temporal stability of the calibration. It is worth noting that regional or mission-specific applications could have special requirements from those expressed here.

The missions covered in this document are primarily the Sentinel-3/OLCI series, then Sentinel-2/MSI and Copernicus Third Party Missions such as VIIRS. Since the Level-2 OLCI data are currently not available to us, a part of the analysis conducted on this report is based on ENVISAT/MERIS, which constitutes a strong heritage for OLCI and shares most of technical specifications.

1.2.2. REQUIREMENT ENGINEERING THROUGH UNCERTAINTY

OC-VCAL aims at correcting systematic bias and reducing uncertainty of the ocean colour radiometry (OCR). The fundamental principle implemented for this requirement document is that the uncertainty of the mission-averaged vicarious gains is the main driver and the justification for all requirements of the OC-VCAL infrastructure and its location. Hence the goal is to exhaustively list all components of the full OC-VCAL process and to provide guidance on how to deal with their associated uncertainty, in view of building a complete uncertainty budget (see section 2). It should be noted that this report cannot provide a definitive quantified uncertainty budget, since no specific infrastructure and location has been selected. A tentative uncertainty budget is provided in the Excel annex with numbers based on state-of-the-art radiometry. This annex must be used as a

methodology demonstration, on one hand for checking that any existing infrastructure actually fulfils the required accuracy for OC-VCAL, and on the other hand for providing guidelines in the design of any future infrastructure. In the following, we will always refer to standard uncertainty (i.e. coverage factor *k=1*, see Bell, 2001, for an introduction to the concept of uncertainty).

In this report, the entire OC-VCAL context is considered (Figure 3): quality of OC products for Copernicus should drive requirements in the OC-VCAL process, which itself must drive the requirements of the OC-VCAL field infrastructure and its location. This means, in particular, that the uncertainty budget of the OC-VCAL process should drive the design of field infrastructure and the selection of the site, and not the other way round.

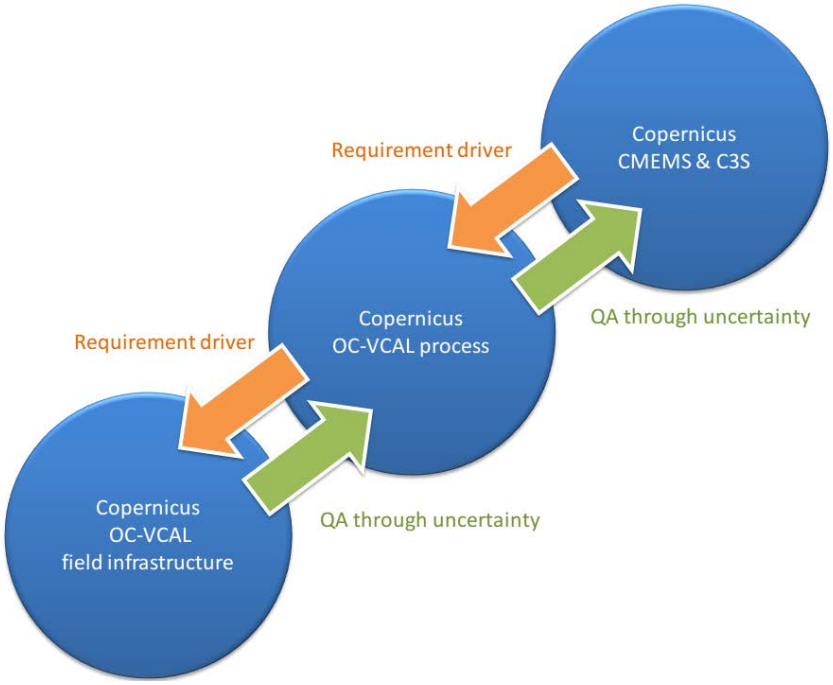

Figure 3. Requirements logic of the present study

This approach is crucial because both instrumentation and protocols quickly evolve and one technical solution cannot be set in stone based on its current performance (see for example Bialek et al., 2013, for how to go from the classical 2% uncertainty in radiometric calibration towards 1% with the recent STAIRS system, Levick et al., 2014). On the other hand, lessons learnt on existing infrastructures are extremely valuable and should be used to check if their uncertainties meet the requirements in quality (see the quality assessment in Figure 3).

Following this experience, this report focuses on requirements for under-water systems. Indeed above-waters systems are generally deployed from permanent platforms in coastal waters, where the coastal waters largely increase the sources and level of uncertainty of the radiometry (see sections hereafter on spatial homogeneity, temporal stability) and make these systems irrelevant for vicarious calibration targeting climate applications. On the other hand, when performed in deep oligotrophic/mesotrophic waters and well away from the coast, current above-water technology does not allow the production of continuous measurements of water-leaving radiance with the same accuracy achievable with in-water systems. Limitations are mostly dictated by deployment technologies, rather than by the above-water methodology.

1.2.3. REQUIREMENT FORMATTING AND NUMBERING

For each requirement, a short paragraph details the physical phenomena or process of the OC-VCAL component, possibly with equations, references and illustrations. Then the requirement itself is numbered with a unique code (used in the traceability chain and uncertainty budget) as follows:

OC-VCAL-RD-1. Requirement Description; written as a short and specific statement.

OC-VCAL-RU-1. Requirement Uncertainty; the uncertainty associated with the respective component. This can be either a requirement on the acceptable level of uncertainty (target) or on the need to characterise the uncertainty, without a target.

OC-VCAL-RV-1. Requirement Verification; providing the method to verify the requirement is well met.

1.3. REQUIRED QUALITY FOR COPERNICUS OCEAN COLOUR PRODUCTS AND SERVICES

1.3.1. OPEN WATER AND CLIMATE-ORIENTED APPLICATIONS

The accuracy goal of OLCI products stated in the Sentinel-3 Mission Requirements Traceability Document (MRTD; Donlon, 2011) is 5 x 10^{-4} in absolute value for the marine reflectance (more precisely between 5 x 10^{-4} and 1 x 10^{-3}, from Antoine and Morel 1999) and 30% in chlorophyll concentration (threshold) over open waters. These numbers come from MERIS heritage and are based on the discrimination of 30 classes of chlorophyll between 0.03 and 30 mg/m^3 in Case-1 waters with a band-ratio algorithm. This is roughly equivalent to the historical 5% relative uncertainty in marine reflectance in the blue required by NASA/GSFC (e.g. Gordon, 1997) over clear and open waters, related to the 30% uncertainty on Chlorophyll concentration, and more recently formally required by GCOS (2016) in the blue and green for producing Climate Data Records (CDRs). Very importantly, these requirements only refer to the blue and green bands, used to compute chlorophyll. To date it seems difficult to justify any requirements over the whole solar spectrum from an application perspective, e.g. at 400 nm and in the red bands, although a reasonable uncertainty should be ensured for these bands to be confidently used in the future; for instance NASA has required a similar 5% uncertainty in the red bands for the in situ measurement, including all sources of uncertainties (NASA, 2014). It should be emphasised that the uncertainty of the satellite marine reflectance is spectrally correlated when derived by standard atmospheric correction (IOCCG 2010), so that, in practice, we can consider that the requirements in the blue drive requirements at other bands. Finally note that when dealing with clear waters, the radiometry in the red is so small that expressing uncertainties in absolute values is more meaningful and recommended.

In parallel of ensuring low uncertainties, high stability of the satellite ocean colour data is required for detecting long-term changes or trends (see Figure 4). Stability is defined by Ohring et al. (2004) as “the measure of repeatability and reproducibility of the metrological characteristics of the instrument with time”. These authors assign a requirement on stability per decade of 20% of that on uncertainty, recognising that this number is somewhat arbitrary and “should be periodically reevaluated”. Under this rule, the required 5% uncertainty on marine reflectance translates into a 1% stability per decade.

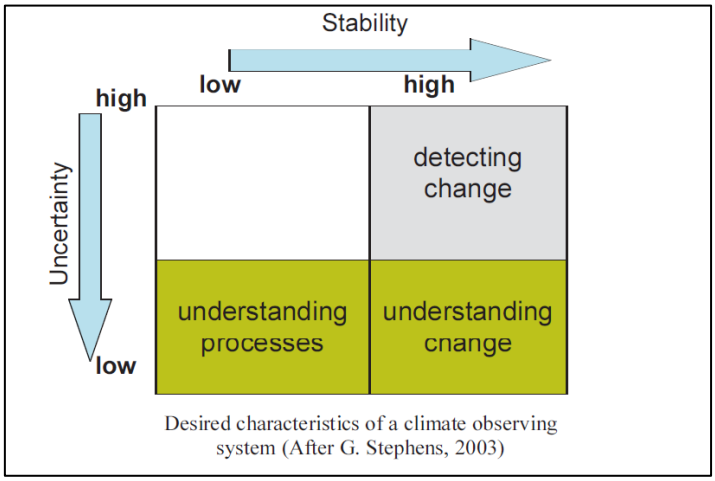

Figure 4. Complementarity between uncertainty and stability for climate observing system. From Ohring et al. (2004)

More recently, numerical models of Dutkiewicz (2016) predict a change in remote-sensing reflectance lower than 0.1% per year for most of the world ocean (computed in the blue, see Figure 5), i.e. a change lower than 1% per decade. This number suggests that a sensor stability worse than 1% per decade would render much of the climate change signal indecipherable from the satellite observation.

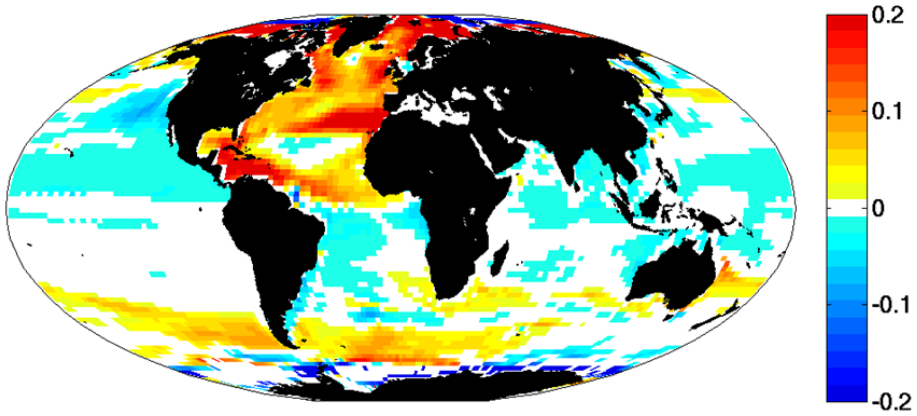

Figure 5. Percent of change per year in Rrs(475) over the 21st century, computed by a numerical model. From Dutkiewicz 2016.

The target of 0.5% stability per decade stated by GCOS (2011) is a more ambitious further step. It is acknowledged that these numbers should be justified by dedicated studies (see e.g. Mélin 2016 for trends estimates in chlorophyll-a).

1.3.2. COASTAL APPLICATIONS

Remote sensing of coastal waters is still challenging, because of the complexity of the water signal (not only driven by chlorophyll but also sediments and dissolved organic matter), and of the generally complex atmosphere due to land influences. Hence, the requirements on the sensor calibration for coastal applications cannot be easily translated from those for the open water (see next section). Furthermore, the required uncertainty of remote-sensing data over coastal areas is still not well defined today. For instance, the white paper for a Copernicus Coastal Service (Mangin et al., 2014) expresses the need to assess uncertainties but does not specify quantitative requirements. Hence the present document does not consider further the coastal applications as a key driver for the design of a vicarious calibration infrastructure (although the impact of vicarious calibration over such waters shall be assessed, see section 3.3.3). Nevertheless, the infrastructure defined in this report should contribute to the best calibration of all data, open water or coastal, as documented through past experience of many ocean colour missions.

It is recommended that for coastal services, the effort is put on the algorithm development and validation to ensure accurate retrievals over a variety of complex water types and atmospheres.

1.4. PHYSICS OF OCEAN COLOUR

Satellite OC sensors are passive optical imaging instruments, measuring the radiation exiting the ocean-atmosphere coupled system. These measurements are performed at discrete spectral bands, λ_i, from the blue to the near-infrared (NIR) or even the short-wave-infrared (SWIR) part of the solar spectrum. The primary quantity measured by the sensor is a spectral radiance, L, i.e. a radiant energy per unit time, per unit projected area, per unit solid angle and per unit wavelength, whose SI derived unit is $mW.m^{-2}.sr^{-1}.nm^{-1}$.

The spectral radiance $L(\lambda_i)$ at a given discrete band λ_i actually results from spectral integration of the radiance spectrum $L(\lambda)$ weighted by the spectral response function (SRF) of the band, SRF_i (see for instance S3 Cal/Val Team, 2016, for OLCI):

$$L(\lambda_i) = \frac{\int L(\lambda)\, SRF_i(\lambda) d\lambda}{\int SRF_i(\lambda) d\lambda} \quad (1)$$

In this equation, integration over the whole spectrum assumes that SRF_i is zero outside a bounded domain centered on λ_i; note that λ_i is here essentially used as an index for the i^{th} channel , and that its value simply comes from the integration of λ, weighted by SRF_i as above. Hence, $L(\lambda_i)$ is the spectral radiance measured at this equivalent wavelength λ_i.Producing a physically calibrated, ortho-geolocated, and spatially re-sampled spectral radiance L_t from the raw signal acquired by the sensor at TOA is the object of the Level-0 and Level-1 processing steps. This depends on the exact orbital, mechanical, and optical design of the mission, and is out of the scope of the present study. One important assumption in the present context is that the Level-1 calibration should correct for any temporal degradation in the optical system. As such, L_t is the input of the Level-2 processor, whose primary goal is to provide as output the water-leaving radiance L_w and associated bio-optical products.

Starting from L_t, the physics of the ocean colour process embedded in the Level-2 processor can be summarised as:

$$L_t(\lambda_i) = t_g(\lambda_i) \cdot \left(L_R(\lambda_i) + L_a(\lambda_i) + L_{Ra}(\lambda_i) + t_{up}(\lambda_i) L_w(\lambda_i)\right) \quad (2)$$

In this equation, t_g is the product of downward and upward transmittances for the gaseous absorption (mainly ozone and nitrogen dioxide, but also other gases such as oxygen and water vapour for some particular bands, see Fisher et al., 2010 for OLCI). L_R, L_a and L_{Ra} are the radiances for respectively the pure molecular (or Rayleigh) scattering, the pure aerosol atmosphere and the multiple-scattering between air molecules and aerosols (i.e. the Rayleigh-aerosol coupling term), over a wind-roughened black sea surface, hence accounting for the multiple Fresnel reflection of incident sky radiance at the air-water interface (i.e. the sky glint). L_w is the water-leaving radiance (non-normalised) and t_{up} the total (i.e. direct plus diffuse parts, and Rayleigh plus aerosol contributions) upward transmittance of the atmosphere (Tanré et al., 1990; Vermote et al., 1997; Lenoble et al., 2007). For the sake of brevity, this formulation ignores implicitly the diffuse reflection by whitecaps and the direct Sun glint contribution, which can be achieved by flagging the pixels contaminated by high wind speed and observed in the angular geometry of the specular reflection; these conditions are indeed not favoured in the context of OC-VCAL as we shall see hereafter.

For the sake of brevity, all equations of this document are written without explicit dependence on angular variables (i.e. Sun zenith angle θ_s, view zenith angle θ_v and relative azimuth angle $\Delta\varphi$), except when strictly necessary.

The desired radiometric quantity is the fully normalised water-leaving radiance L_{wN}, i.e. for a Sun at zenith, in absence of the atmosphere and for a mean Sun-Earth distance (Morel and Gentili 1996):

$$L_{wN}(\lambda_i) = \frac{L_w(\lambda_i)}{t_{down}(\lambda_i)\mu_s C_s C_Q(\lambda_i)} \quad (3)$$

where t_{down} is the total (i.e. direct plus diffuse, Rayleigh plus aerosol) downward transmittance of the atmosphere, μ_s the cosine of the solar zenith angle, C_s a coefficient accounting for the variation in the Sun-Earth distance and C_Q the corrective factor for the Bidirectional Reflectance Distribution Function (BRDF) of sea-water (Morel et al., 2002). This latter factor depends on the inherent optical properties (IOPs) of in-water constituents and is, in practice, deduced by an iterative process applied on the directional radiance L_w. Thus, another writing of Eq. (2) in terms of normalised radiance is:

$$L_t(\lambda_i) = t_g(\lambda_i) \cdot \left(L_R(\lambda_i) + L_a(\lambda_i) + L_{Ra}(\lambda_i) + t(\lambda_i)\mu_s C_s C_Q(\lambda_i) L_{wN}(\lambda_i)\right) \quad (4)$$

in which t stands for the total atmospheric transmittance due to molecular and aerosol extinctions along the two atmospheric paths (downwelling and upwelling directions):

$$t(\lambda_i) = t_{up}(\lambda_i) * t_{down}(\lambda_i) \quad (5)$$

Note that within Copernicus, the official Sentinel-3/OLCI product is the directional marine reflectance (i.e. not corrected for the BRDF effect), simply retrieved from L_w through:

$$\rho_w(\lambda_i) = \frac{\pi L_w(\lambda_i)}{t_{down}(\lambda_i) F_0(\lambda_i) \mu_s C_s} \quad (6)$$

Where F_0 is the mean extraterrestrial solar spectral irradiance.

Each radiometric quantity involved in Eq. (2) at band λ_i can be considered as the spectral integration of the actual quantity (continuous spectrum) with respect to the SRF of the sensor band; for instance the water-leaving radiance is computed as:

$$L_w(\lambda_i) = \frac{\int L_w(\lambda)\, SRF_i(\lambda) d\lambda}{\int SRF_i(\lambda) d\lambda} \tag{7}$$

In the Level-2 processor, the marine signal is retrieved after the so-called atmospheric correction (AC), which is formally the reverse writing of eq. (2):

$$L_w(\lambda_i) = \frac{\frac{L_t(\lambda_i)}{t_g(\lambda_i)} - L_{path}(\lambda_i)}{t_{up}(\lambda_i)} \tag{8}$$

where L_{path} merges the Rayleigh and the aerosol scattering:

$$L_{path}(\lambda_i) = L_R(\lambda_i) + L_a(\lambda_i) + L_{Ra}(\lambda_i) \tag{9}$$

In the standard AC (e.g. Gordon and Wang, 1994, for NASA sensors, Antoine and Morel, 1999, for MERIS and OLCI clear water branch), the unknown aerosol content involved in atmospheric radiance and transmittance is inferred from two bands in the NIR region, where it is assumed that the marine signal is either negligible (clear waters) or has been corrected (more turbid waters). Schematically, the aerosol optical thickness (AOT) and model which best match the radiometry in the NIR bands are selected from a database of aerosol IOPs computed for a well-defined climatology (e.g. Ahmad et al., 2010) and can be used with Eq. (8) to retrieve L_w in the visible (VIS) bands. For the OLCI ground segment this approach is referred to as the standard AC, in contrast to the Alternative Atmospheric Correction (AAC) which involves the whole spectrum inversion through artificial neural network technique (e.g. Doerffer and Schiller, 2007). This document focuses on the standard AC, since it is the baseline of the OLCI processing algorithm over open waters.

1.5. PURPOSE AND METHODOLOGY OF VICARIOUS CALIBRATION

1.5.1. PRINCIPLE OF VICARIOUS CALIBRATION

The decoupling between the NIR and VIS regions in the standard case is a fundamental aspect which means that the uncertainty at bottom of atmosphere (BOA) in one band depends on the uncertainty due to the TOA calibration in the same band only (i.e. no spectral dependence). Following Eq. (4) this can be quantified as:

$$\frac{\mathrm{u}(L_{wN})}{L_{wN}}(\lambda_i) = \frac{\frac{\mathrm{u}(L_t)}{L_t}(\lambda_i)}{\frac{t_g t \mu_s C_s C_q L_{wN}(\lambda_i)}{L_t(\lambda_i)}} \tag{10}$$

The denominator of Eq. (10) represents the contribution of marine radiance to the TOA signal. This equation justifies the well-known rules: "*If tL_w is 10% of L_t, and we want L_w with an uncertainty of*

±5%, one would expect that it would be necessary to know L_t with an uncertainty of no more than ±0.5% " (Gordon 1998). Such a TOA accuracy has not been achieved so far by the instrumental calibration alone, whose goal is about 2% in terms of reflectance for OLCI (Donlon et al., 2012).

This is exactly where OC-VCAL comes into play. Applied after the instrumental radiometric calibration (i.e. pre-launch as well as post-launch on-orbit), it consists in adjusting the TOA radiometry to meet the water-leaving radiance requirements. The adjustment is through the indirect use of high-quality ground-truth measurements, generally water-leaving radiance L_{wN}^t, concurrent with space acquisitions (e.g. Eplee et al., 2001). The signal reconstructed at TOA follows the very same physics as Eq. (4):

$$L_t^t(\lambda_i) = t_g^t(\lambda_i)\left(L_{path}^t(\lambda_i) + t^t(\lambda_i)\mu_s C_s C_Q^t(\lambda_i) L_{wN}^t(\lambda_i)\right) \tag{11}$$

where the superscript t refers to true (or targeted) quantities, defined at the same time and the same geometry as those of the acquisition of the spaceborne sensor (hence μ_s.and C_s do not need the superscript). Note that C_Q^t is the BRDF factor of the targeted seawater IOPs, which can be directly computed from L_{wN}^t. It is worth noting that Eq. (11) is expressed as a function of the fully normalised in situ water-leaving radiance L_{wN}^t, assumed to be an invariant apparent optical property accommodating for the slight difference in time between the sensor overpass and the in situ acquisition. The link with the actual water-leaving radiance L_w^{IS} measured in situ is:

$$L_{wN}^t(\lambda_i) = \frac{L_w^{IS}(\lambda_i)}{t_{g,down}^{IS}(\lambda_i) t_{down}^{IS}(\lambda_i) \mu_s^{IS} C_s^{IS} C_Q^{IS}(\lambda_i)} \tag{12}$$

where the superscript IS now refers to the in situ quantities, at the exact geometry and time of the in situ acquisition. Such a procedure is important to take into account the potential difference in the solar path length between the times of in situ and spaceborne observations. This normalisation follows Eq. (3) except that the downward gaseous transmittance at the in situ time, $t_{g,down}^{IS}$, has to be accounted for at this stage.

In practice, a vicarious calibration method produces gains $g(\lambda_i)$ for each validation point and each sensor band λ_i:

$$g(\lambda_i) = \frac{L_t^t(\lambda_i)}{L_t(\lambda_i)} \tag{13}$$

The pixel-per-pixel gains are then spatially averaged, providing a unique gain per match-up for each band (so called individual gain). Eventually, matchup-per-matchup gains are temporally averaged, yielding a unique set of gains $\bar{g}(\lambda_i)$ for each band λ_i, over the entire mission lifetime.

In the mission operation, OC-VCAL consists of applying the mission average gains $\bar{g}$ to the TOA radiometry. The resulting water-leaving radiance is thus computed as:

$$\overline{L_w^{cal}}(\lambda_i) = \frac{\bar{g}(\lambda_i)\dfrac{L_t(\lambda_i)}{t_g(\lambda_i)} - L_{path}(\lambda_i)}{t_{up}(\lambda_i)} \tag{14}$$

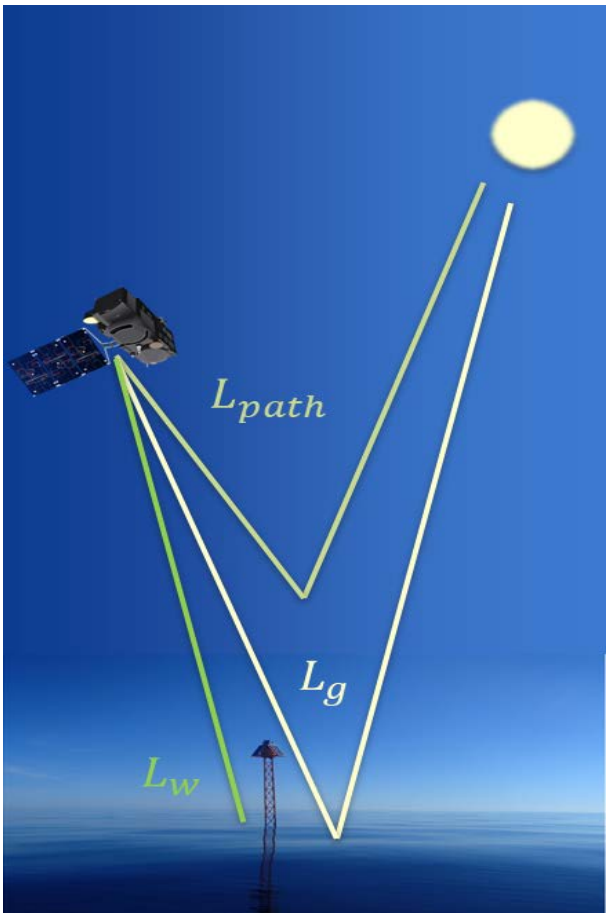

Figure 6. Schematic view of the vicarious calibration process

The targeted atmospheric functions involved in the reconstruction of the TOA signal (see Eq. (11)) must be recomputed with the same radiative transfer model (RTM) as the one implemented in the Level-2 processing chain, using as inputs in situ measurements collected at the time of the sensor overpass. The inputs required for the simulations are:

- The vertical profile of gaseous content in the atmosphere. By considering the spectral bands commonly used by OC sensors, three main absorbers are water vapour, ozone, oxygen and nitrogen dioxide;
- The aerosol IOPs (extinction coefficient, single scattering albedo (SSA) and phase function (APF)), the AOT, and the vertical distribution of the aerosols, if available, to compute the atmospheric path radiance and transmittance, combined with Rayleigh scattering and the aerosol-molecular coupling term;
- The barometric pressure to adjust the Rayleigh scattering functions;
- The sea surface state (wind speed just above the sea level) to account for the sky glint contribution in the atmospheric scattering functions;
- The IOP models required for the surface BRDF calculation of the C_Q factor.

1.5.2. SYSTEM VICARIOUS CALIBRATION

In this document, we shall narrow down the scope of OC-VCAL methods to System Vicarious Calibration (SVC), where the targeted atmospheric terms are exactly those retrieved by the Level-2 processing algorithm itself at pixel level (Gordon 1998). It means that Eq. (11) is applied with:

$$L_{path}^{t}(\lambda_i) = L_{path}(\lambda_i),\ t_g^t(\lambda_i) = t_g(\lambda_i) \text{ and } t^t(\lambda_i) = t(\lambda_i) \tag{15}$$

The intrinsic principle of SVC is that, at the match-up level or, more precisely, at the pixel level, applying the individual gain g computed through Eqs. (11)-(13)-(15) forces the system to exactly match the targeted in situ water-leaving radiance (i.e. L_w^t) in the sensor geometry at all bands.

The reason for this choice is that SVC is to date the only existing method able to minimise the uncertainty of vicarious gains due to the instrument calibration biases and the algorithms (atmosphere, BRDF and surface, see sections 3.3.3 and 3.5 for more details). SVC has been operationally implemented and exploited by NASA (Franz et al., 2007), ESA (Lerebourg et al., 2011) and NOAA (Wang et al., 2016). In the reminder of this document, we will only use the SVC terminology instead of OC-VCAL.

SVC must be understood as an adjustment of the full system comprising the spaceborne sensor and the Level-2 processing algorithm, in particular the AC. This means that SVC gains must be recomputed after any change is implemented in sensor calibration or in the algorithmic chain. For instance for OLCI, the clear water branch and the alternative complex water branch should have individual SVC gains.

The BRDF correction is computed from the marine spectrum itself (Morel al., 2002). In the SVC process, it is acquired from the in situ water-leaving radiance measurements L_{wN}^t and it requires optimization so that C_Q equates C_Q^t after SVC.

When applying mission average gains, it can be shown that the difference between $L_w^{\overline{cal}}$ and L_w^t is simply expressed as:

$$L_w^{\overline{cal}}(\lambda_i) - L_w^t(\lambda_i) = \left(\bar{g}(\lambda_i) - g(\lambda_i)\right)\frac{L_t(\lambda_i)}{t_g(\lambda_i)t_{up}(\lambda_i)} \tag{16}$$

This expression well explains the core concept of SVC, which is to cancel, on average, the discrepancy between the sensor observation and the calibration ground-truth data. This is referred to as a *systematic bias* removal. The actual bias removal depends on the individual gain averaging. For instance, summing Eq. (16) over all N match-ups demonstrates the need to weight the averaging of individual gains by the TOA radiance propagated at BOA in order to strictly remove the absolute bias, contrary to the usual practice in the ocean colour community where a simple average is taken:

$$\bar{g}(\lambda_i) = \frac{\sum_{n=1}^{N}\frac{L_t(\lambda_i)}{t_g(\lambda_i)t_{up}(\lambda_i)}g(\lambda_i)}{\sum_{n=1}^{N}\frac{L_t(\lambda_i)}{t_g(\lambda_i)t_{up}(\lambda_i)}} \tag{17}$$

Other choices, taking into account the gains uncertainty, may be more relevant and are discussed in more details in section 5.3.2.

Accuracy and robustness of the atmospheric correction over different atmospheric and water conditions plays a key role in the accuracy and precision of L_w. It directly impacts the consistency of individual vicarious gains and the applicability of SVC to regions other than that of the calibration site. Eq. (16) directly shows that any large dispersion in the vicarious gains would induce large uncertainty in the water-leaving radiance. Hence, any specified variability of L_w (standard deviation) can be translated into a specified variability in the gains. SVC itself can improve the accuracy in the water-leaving radiance (i.e. decrease the bias) but cannot improve its precision (i.e. scattering or dispersion).

As a reminder, the temporal evolution of the sensor calibration is handled by Level-1 (instrumental) calibration and not by SVC. But the stability of SVC gains can be monitored to verify the above assumption.

1.6. INTERNATIONAL BACKGROUND

The need for SVC has been acknowledged for a long time (e.g. Gordon, 1987, for a pioneering work) and has reached a global consensus between the main international coordinating groups, such as IOCCG and GCOS. GCOS recommends "*Continuation of support, by agencies, of bio-optical systems (e.g. MOBY, BOUSSOLE) for in situ data collection, to ensure appropriate vicarious calibration of spaceborne sensors*" (GCOS, 2011).

In practice, only two international SVC infrastructures are publicly accessible today to the OC community. In the USA, the Marine Optical BuoY (MOBY; Clark et al., 2001; Clark et al., 2003; Brown et al., 2007), initiated in 1985, has been used operationally since 1997 to calibrate most of space missions (SeaWiFS, MODIS, MERIS, VIIRS). In Europe, the "*BOUée pour l'acquiSition d'une Série Optique à Long termE"* (BOUSSOLE; Antoine et al., 2008a; Antoine et al. 2008b), initiated in 1998, has been operational since 2003 with two objectives: a scientific objective (research in bio-optic) and an objective for vicarious calibration, by providing data for the MERIS, OLCI and MSI missions in complement to MOBY data. The expertise and lessons gained through these two systems over the past two decades have to be considered in the present context.

Specifically focused on Copernicus, ESA has organised in February 2017 a workshop on "Options for future European satellite OCR vicarious adjustment infrastructure for the Sentinel-3/OLCI and Sentinel-2/MSI series". The workshop was in the frame of the programme Fiducial Reference Measurements for Satellite Ocean Colour (FRM4SOC). Requirements expressed during this workshop are taken into account in the present document.

In addition to the above, the European SVC effort is embedded in a broad international background with many lessons learnt and achievements (we refer the reader to section 9 for the acronyms definition):

- IOCCG: has a leading role and has issued recommendations about SVC in its report series (IOCCG, 2012; IOCCG, 2013a) as well as at the IOCS meeting in 2013. IOCCG also organised a dedicated workshop on SVC which detailed several requirements of most interest (IOCCG, 2013b).
- NASA: the work of Franz et al. (2007) and Bailey et al. (2008) is the baseline for the present study. This study also benefits of accomplishments of NASA's ROSES-14 Ocean Biology and Biogeochemistry call for ocean colour remote sensing vicarious (in situ) calibration instruments (2014).
- ESA MERIS: lessons learned from MERIS (e.g. Lerebourg et al., 2011) are particularly relevant for OLCI in the Copernicus context.

- ESA OC-CCI: the recent and on-going work on SVC for non-standard AC is part of the picture for Copernicus (Mazeran et al., 2017).
- JRC: the recent report of Zibordi et al. (2017a), summarising the JRC peer reviewed SVC findings (Zibordi et al., 2015; Zibordi and Mélin, 2017; Zibordi et al., 2017b) is of particular interest for defining requirements and recommendations for a European SVC infrastructure.
- INSITU-OCR White paper (2012): Both this document and the mapping exercise include recommendations on SVC that should be followed on an inter-agency basis.
- NOAA: MOBY technology refreshment, including capabilities allowing further decrease of MOBY's uncertainty budget.
- MOBY-Net (Voss et al,. 2015): future system under-development for MOBY to support multiple SVC remote sites.
- AERONET-OC (Zibordi et al., 2009b): although not designed to meet the SVC uncertainty requirements, this network experience is important for its strong calibration effort, uncertainty assessment and operational structure.
- Copernicus S3VT activities (Casal et al., 2014): it includes projects such as the future MOBY-Net buoy off Perth.
- CEOS, in particular its Working Group on Calibration & Validation (WGCV): although SVC is not explicitly in its scope, this group offers important expertise in SI-traceability of EO measurements and instrument calibration that is relevant to SVC.
- QA4EO (Fox, 2010): this is a highly relevant formalism for the EO uncertainty budget specification. This SVC document is a pertinent input to the QA4EO guides that include other procedures, such as Moon in-flight calibration, and Rayleigh scattering calibration.
- FIDUCEO H2020: this project systematically applies the insights and techniques of metrology to EO, demonstrating the traceability of uncertainties of satellite-derived CDR.

2. SVC TRACEABILITY CHAIN AND UNCERTAINTY APPROACH

2.1. CONCEPTS OF METROLOGY

The formalism of uncertainty used in this document relies on the Guide to the expression of Uncertainty in Measurement (GUM; JCGM, 2008 and JCGM, 2011) and the International Vocabulary of Metrology (VIM, JCGM 2012). In Europe, application of these concepts to ocean colour has been largely eased thanks to the recent collaboration between EO and metrology fields, led by the National Physics Laboratory (NPL; see e.g. Fox, 2001 for the QA4EO framework) and studied more specifically in projects such as MetEOC (Woolliams et al. 2015) and FIDUCEO (Merchant et al. 2016). A comprehensive example showing the application of GUM to in situ ocean colour radiometry measurements was recently presented for AERONET-OC data (Gergely and Zibordi, 2014).

First, metrology defines the *measurand* as *the quantity that is intended to be measured*; in the SVC context this is typically the ground-truth water-leaving radiance. Then the *uncertainty of measurement* is defined as a *non-negative parameter characterising the dispersion of the quantity values being attributed to a measurand, based on the information used*. For example, this parameter can be the standard deviation when the probability density function characterising the uncertainty follows a normal law. Finally, the *uncertainty budget* provides the *components of the uncertainty of a measurand that comes from measurement, and their calculation and combination*.

Traceability is another key concept in metrology for accurately developing an uncertainty budget when the final measurand comes from several steps. CEOS defines it as the *property of a measurement result relating the result to a stated metrological reference through an unbroken chain of calibrations of a measuring system or comparisons, each contributing to the stated measurement uncertainty*. Traceability should, ideally, be to the International System of Units (SI), that is the "stated metrological reference" should be formally calibrated in SI unit through a National Metrology Institute (NMI). The unbroken chain of calibration or comparison is called a *traceability chain*.

Although SVC vicarious gains are not a *measurand* per se, we shall apply same principle of metrology to rigorously derive their uncertainty budget and get in turn SI traceability of the calibrated water-leaving reflectance. In this way, this document applies the methodology of Woolliams et al. (2015) to the SVC problem, comprising these eight steps:

1. **Describe the traceability chain**: A diagram in section 2.2 hereafter describes the traceability route of the SVC process estimating backward from the final quantities, which are mission-averaged SVC gains, to input sources which are ideally SI traceable (e.g. a FEL lamp calibrated by a NMI). All steps in the process may not however be SI traceable, although they do have an associated uncertainty (e.g. the steps using radiative transfer computations).

2. **Write down the calculation equations**: Many components of the diagram are modelled by an equation. The respective equations are included in the sections where the individual components are described. An example is section 4.1.1.2 which includes the equations determining the spectral and radiometric response of radiometers.

3. **Consider the sources of uncertainties**: Each step in the SVC process is associated with some uncertainties. The uncertainties are associated with quantities involved in the measurement equations, like the SI-traceable uncertainty of a calibration lamp. Thanks to some a priori knowledge on the process, it may be wise to neglect some sources. For instance, the refractive index of seawater has its own uncertainty, due to its variation with temperature and salinity. However, the literature tells us that less than 0.1% variation is expected on the index for 10° C variation (e.g. Quan and Fry, 1995), so that it may not be necessary to go to such level of

uncertainty if a temperature correction is already implemented. The sources of uncertainties are identified in the traceability chain (see section 2.2).

4. **Create the measurement equations**: The equations consist of an extended version of the radiative process equations, for instance combining all calculations into one measurement equation for each main subsection of the traceability chain. For SVC, we have the main ocean colour retrieval equation related to L_w, and another equations related to the mission-average gain. Measurement equations can include uncertainties not previously taken into account (e.g. ageing of the sensor's diffuser, effect of geometry on the field measurement). At the end the desired quantity should be written as a function of all input parameters: $f(x_1, \cdots, x_i \cdots, x_n)$. The key quantities in the SVC process are the SVC gains and, eventually, the water-leaving radiance after SVC. Section 2.3 includes the complete set of equations to derive these quantities for the standard AC.

5. **Determine the sensitivity coefficients**: The coefficients express how much a source of uncertainty impacts the quantity we wish to measure. Mathematically speaking, this is the partial derivative of the (output) quantity with respect to the input variables:

$$c_i = \frac{\partial f(x_1, \cdots, x_i \cdots, x_n)}{\partial x_i} \tag{18}$$

   The absolute uncertainty of f, due to the input uncertainty $u(x_i)$ only, is computed as:

$$u_i(f) = c_i \, u(x_i) \tag{19}$$

   It can also be formulated in relative term $\tilde{c}_i = \frac{\partial f}{\partial x_i}\frac{x_i}{f}$ so that $\frac{u_i(f)}{f} = \tilde{c}_i \frac{u(x_i)}{x_i}$.

6. **Assign uncertainties**: A table produced with this document lists all identified uncertainty components and provides their associated uncertainties $u(x_i)$. The quantified uncertainty can be, in general, a unique number like the standard-deviation for random uncertainty. Care must be taken to define the confidence level for each uncertainty (e.g. the confidence level associated with the uncertainty of an irradiance lamp is often 95%, i.e. *k=2*). There may also be systematic uncertainty (e.g. the stray light effect, if not corrected). The full description of the uncertainty should be given by the probability density function (PDF). Finally the covariance $u(x_i, x_j)$ between different sources of uncertainty must be assessed. It expresses the correlation between the random variables x_i and x_j and is related to their correlation coefficient $r(x_i, x_j)$:

$$u(x_i, x_j) = r(x_i, x_j) u(x_i) u(x_j) \tag{20}$$

   The uncertainty table for SVC is introduced in section 2.3.4 and the full table is available as an Excel spread sheet.

7. **Combine and propagate uncertainties**: This is done following the law of propagation of uncertainty of the GUM (JCGM, 2008). In the case where correlations exist, the general formulation is:

$$u^2(f) = \sum_{i=1}^{n} {c_i}^2 \, u^2(x_i) + 2 \sum_{i=1}^{n-1} \sum_{j=i+1}^{n} c_i c_j u(x_i, x_j) \quad (21)$$

This provides the standard uncertainty. Some steps in the traceability diagram may not be processed so easily and rely on either numerical methods (numerical differentiation or Monte-Carlo simulation) or experimental measurements. Also the first order law of Eq. (21) has its limitations in case of non-linear models, and may require either adding higher orders or using a Monte-Carlo approach (JCGM, 2011).This calculation is done for the SVC gains, in sections 2.3.3 (individual gains) and 2.3.2 (mission wide gain), using the values of the Excel spread sheet.

8. **Expanded uncertainties**: This last step converts the standard uncertainty to the expanded uncertainty with respect to the desired level of confidence. This is achieved by multiplication by a coverage factor *k*. For instance, if we deal with the Gaussian distribution, the coverage factor *k=2* will provide an uncertainty estimate in the 95.45% confidence interval. In this document, the coverage factor is *k=1* unless otherwise stated.

In step 6, we highlight the importance of taking into account correlations of uncertainties: if they exist and are neglected, the calculated uncertainty can be quite significantly wrong. We refer the reader to Johnson et al. (2014) for an example of covariance computation, in the case of calibration factors of an irradiance sensor and a radiance sensor calibrated with the same FEL lamp. Importantly, the uncertainty budget should be validated by comparison with measurements or additional evaluations.

2.2. SVC TRACEABILITY CHAIN

The SVC traceability chain is the underlying principle of the infrastructure requirements to ensure SI-traceable vicarious gains and, in turn, ensure traceability in the accuracy of the Copernicus OCR and downstream services. In strict logic, SI-traceability of the in situ radiometer alone does not insure full traceability: the spaceborne sensor should also demonstrate SI-traceability, what is out of the scope of the present document. The overall chain for SVC is sketched on Figure 7. Then each element of the overall process is detailed from Figure 8 to Figure 9. For each element (e.g. “Field Lw radiometer” in Figure 8), the individual components are indicated (e.g. “Radiometer”), and for each component the contributors are listed (e.g. “SRF”). These latter, which all contribute to the final gain calculations and uncertainty, are classified according to the frequency of change (or stability during deployment). This classification is indicated by different colours in the diagram:

- Temporally stable (black colour): these contributors need to be carefully characterised, often in a laboratory. This characterisation does not change frequently, if at all. An example is the relative spectral response of the field radiometer, or the bathymetry at the location of a measurement platform.
- Temporally changing with low frequency (orange colour): these contributors require characterisation in regular intervals, such as the absolute calibration of a field radiometer in the laboratory.
- Changing concurrently with the measurement itself (purple colour): these contributors change concurrent with the field radiometer measurement and need to be recorded for every acquisition. The random component of the uncertainties is typically derived by replicate measurements (but not the systematic component). Some examples are the wind speed and other environmental conditions, or the dark current of a radiometer.

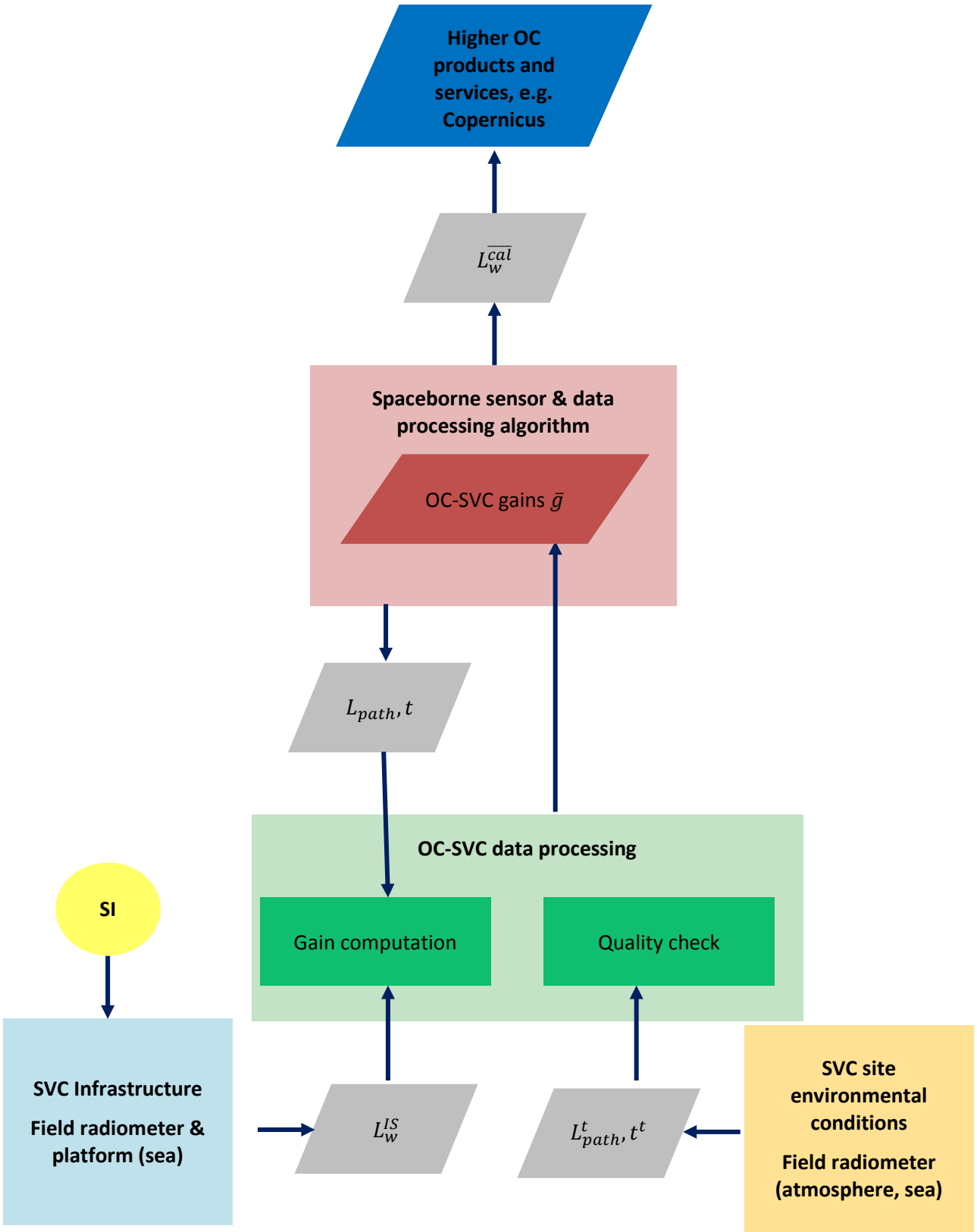

Figure 7. Main steps (rectangles) and data (parallelogram) of the SVC process, with SI-traceability (yellow circle)

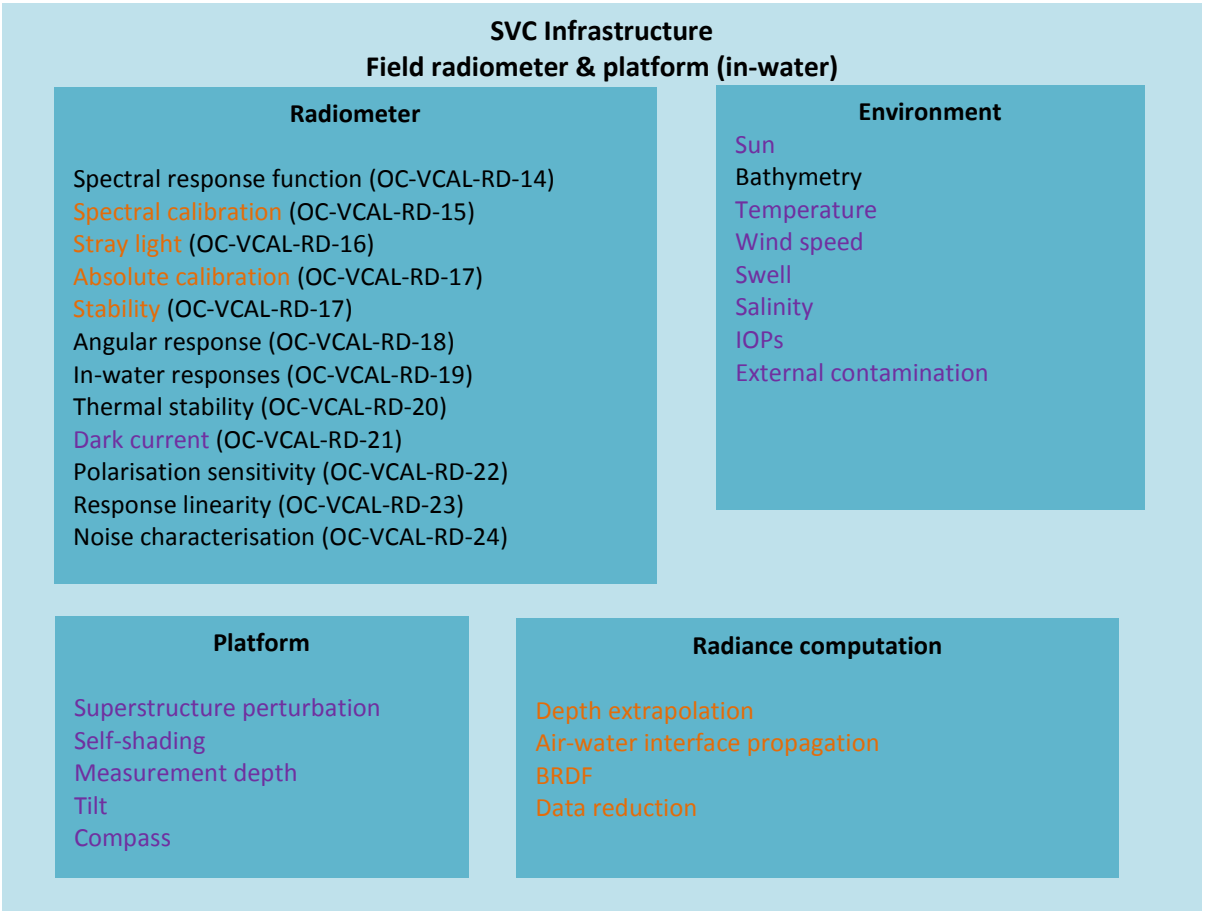

Figure 8. Components of the SVC field infrastructure (in-water); see text for colour code.

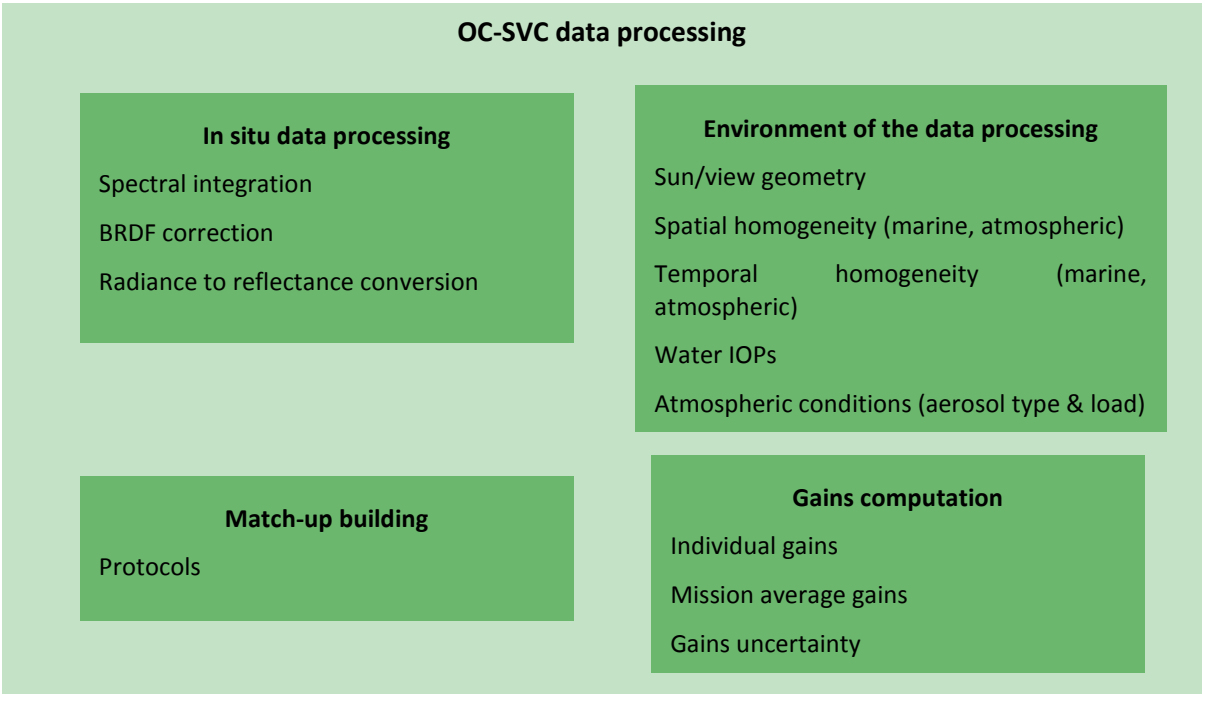

Figure 9. Components of the SVC data processing

2.3. SVC UNCERTAINTY BUDGET

In the following it should be remembered that uncertainty refers to standard uncertainty (i.e. coverage factor *k=1*). The distinction between the random and systematic components of the uncertainty is only done in the companion Excel file introduced in section 2.3.4.

2.3.1. UNCERTAINTY ON WATER-LEAVING RADIANCE

The goal of the SVC uncertainty budget is to link the uncertainty of the Level-2 water-leaving radiance after SVC, $L_w^{\overline{cal}}$, see Eq. (14), to the uncertainties of the SVC system. By definition, SVC removes the bias in $L_w^{\overline{cal}}$ but leaves residual uncertainties due to the uncertainty $u(\bar{g})$ on the mission average vicarious gain. Assuming standard AC and SVC, this link at each band λ_i can be made explicit by:

$$\frac{u\left(L_w^{\overline{cal}}(\lambda_i)\right)}{L_w^{\overline{cal}}(\lambda_i)} = u\left(\bar{g}(\lambda_i)\right) \Big/ \frac{t_g(\lambda_i)t_{up}(\lambda_i)L_w^{\overline{cal}}(\lambda_i)}{L_t(\lambda_i)} \tag{22}$$

This link would differ in the case of non-standard ACs for which the covariances of uncertainties have to be accounted for.

Note that this equation includes only the impact of SVC and does not deal with other sources of uncertainties in the Level-2 processing algorithm, such as gaseous, sun glint and atmospheric corrections, which are out of the scope of the present work. In other words, Eq. (22) is true for the specific calibration site (atmosphere, marine conditions, and geometries of observation) but should include other terms in other conditions. This fundamental link, written here in terms of relative uncertainty, shall be considered for:

1. Defining the requirement on the SVC system uncertainty. Similarly to Eq.(10), Eq. (22) shows that reaching 5% uncertainty on L_w requires an $u(\bar{g})$ of about 0.5% when the relative contribution of the marine surface to TOA signal is about 10%. This corresponds to the required 0.5% uncertainty on TOA radiance in the blue and green bands after vicarious calibration which was recommended by IOCCG (2012) and has been recently revised downward to a target value of 0.3% (NASA, 2014). In fact, the exact requirement is wavelength dependent and strongly varies with this relative contribution; for instance it can be as low as about 0.25% at 412 nm to meet the same performance over mesotrophic and coastal waters (see Zibordi et al., 2015).
2. Computing, in operation, the actual uncertainty of $L_w^{\overline{cal}}$ on a pixel-by-pixel basis, given the actual estimate on $u(\bar{g})$.

2.3.2. UNCERTAINTY ON THE MISSION AVERAGE GAIN

Uncertainty of $\bar{g}$ relates to the uncertainty of each individual gain g and on the averaging process itself (i.e. scattering of individual gains and number of match-ups). In all generality, the averaging can be written as:

$$\bar{g}(\lambda_i) = \frac{\sum_{n=1}^{N} w(\lambda_i) g(\lambda_i)}{\sum_{n=1}^{N} w(\lambda_i)} \tag{23}$$

where $w(\lambda_i)$ is a weighting coefficient for match-ups, either fixed to unity or dependent on the actual match-up (see Eq. (17) for an example and section 5.3.2 for detailed discussion); in the latter case we assume for the sake of simplicity that the weights have a negligible uncertainty. It follows that the squared uncertainty in the average gain is defined as:

$$u^2\big(\bar{g}(\lambda_i)\big) = \frac{\sum_{n=1}^{N} w^2(\lambda_i) {u_r}^2\big(g(\lambda_i)\big)}{\left(\sum_{n=1}^{N} w(\lambda_i)\right)^2} + {u_s}^2\big(g(\lambda_i)\big) \tag{24}$$

Where $u_r\big(g(\lambda_i)\big)$ and $u_s\big(g(\lambda_i)\big)$ are respectively the random and systematic component of $g(\lambda_i)$. If $w(\lambda_i)$ is set to unity and individual gains are assumed to have all the same purely random uncertainty $u(g)$, this yields $u(\bar{g}) = u(g)/\sqrt{N}$. However, such assumptions are not necessary true and the general form of Eq. (24) shall be favoured.

2.3.3. UNCERTAINTY OF INDIVIDUAL GAINS

At this stage, uncertainty of the individual gains is thus the main objective of the uncertainty budget. In the following, we do not explicitly include the uncertainty of the satellite radiometry L_t, because it is already accounted for in the spatial variability of the gains within the macro-pixel; for instance instruments with lower signal-to-noise ratio (SNR) yield larger noise in the gains.

From basic Eqs. (11)-(13), and removing wavelength for a better clarity, the squared uncertainty is:

$$u^2(g) = \left(\frac{t_g^t t^t\, \mu_s C_s C_Q^t L_{wN}^t}{L_t}\right)^2 \left[\left(\frac{u(L_{wN}^t)}{L_{wN}^t}\right)^2 + \left(\frac{u\big(C_Q^t\big)}{C_Q^t}\right)^2 + \left(\frac{u(t^t)}{t^t}\right)^2 + \left(\frac{u\big(L_{path}^t\big)}{L_{path}^t}\right)^2 \left(\frac{L_{path}^t}{t^t\, \mu_s C_s C_Q^t L_{wN}^t}\right)^2 + 2\frac{u\big(L_{path}^t, t^t\big)}{t^t L_{path}^t} \frac{L_{path}^t}{t^t\, \mu_s C_s C_Q^t L_{wN}^t}\right] \tag{25}$$

In contrast to Eq. (22), the multiplicative component in the vicarious gain uncertainty decreases a priori in mesotrophic and coastal complex absorbing waters, where the $t_g^t t^t C_Q^t L_{wN}^t / L_t$ ratio becomes small. However, complex waters in practice counterbalance this decrease by an increased uncertainty of the additive components in the square brackets, including the atmospheric path uncertainty and its temporal variability $L_{path}^t \; and \; t^t$, the in situ measurement and its temporal variability, i.e. $u(L_{wN}^t)/L_{wN}^t$, or the BRDF correction $u\big(C_Q^t\big)/C_Q^t$. Also, a lower ratio gives more importance to the atmospheric uncertainty. Hence, the complete formulation is required to get the realistic uncertainty estimate.

Eq. (25) includes the uncertainty component due to the targeted atmospheric quantities used in the gain computation, i.e. t^t and L_{path}^t. These terms disappear when calculating individual SVC gains. By construction, SVC allows the exact retrieval of the targeted marine signal, on a matchup-per-matchup basis, by formally setting $t^t = t$ and $L_{path}^t = L_{path}$, see section 3.3.3 and Zibordi et al.

(2015). To account for this, we simplify the formulation used in the uncertainty budget in the appendix:

$$u(g) = \frac{t_g t\, \mu_s C_s C_Q^t L_{wN}^t}{L_t} \sqrt{\left(\frac{u(L_{wN}^t)}{L_{wN}^t}\right)^2 + \left(\frac{u(C_Q^t)}{C_Q^t}\right)^2} \quad (26)$$

Nevertheless, this perfect retrieval is artificial and does not mean that the individual gains are not affected by the uncertainty related to the atmosphere. The atmosphere has a large contribution to the total uncertainty of the SVC process because of its large contribution to the TOA signal. In fact, if the atmospheric correction happens to be largely wrong over a given pixel, the computed gain contains intrinsic uncertainty which impacts the final averaged gains and the relevance of the SVC over other pixels or other conditions than these of the calibration site.

Uncertainty on transmittance and path radiance shall be assessed at least when selecting the site, as discussed in section 3.5. The location of the site shall purposely minimize these uncertainties due to its inherent atmospheric conditions that produce the lowest modelling uncertainties.

The relative uncertainty on the in situ normalised water-leaving radiance, $u(L_{wN}^t)/L_{wN}^t$, is the last and most difficult component to be estimated. The sources of uncertainty are listed in the previous traceability chain and detailed hereafter in sections 4 and 5. The combination and propagation of these uncertainties can be achieved in two different ways:

- Either by providing a unique uncertainty estimate to each component, based on experimental validation or overall uncertainty computation. This is the approach proposed so far at MOBY (Brown et al., 2007). The total square uncertainty on L_{wN}^t is then simply computed by the quadratic sum of all components. This approach is interesting for quickly identifying the most problematic source of uncertainty and providing a unique uncertainty (at each band), easily transferable to gain level by Eq. (25).
- Or by associating a PDF with each input parameter of the in situ data processing (e.g. environmental and geometrical conditions) and running a Monte-Carlo method to get the uncertainty distribution on resulting L_{wN}^t. This approach is currently investigated at BOUSSOLE (Bialek et al., 2016). A potential interest of this method is to provide the actual uncertainty of a measurement considering the exact conditions at that time (e.g. solar zenith angle, temperature, angle of the sensor tilt,…), and derive a match-up per match-up uncertainty. This should allow a better screening (or weighting) of the gains.

While the latter approach is theoretically more accurate (no first order approximation in the uncertainty propagation), it is quite idealised, requires a large effort and can only be implemented when a specific SVC infrastructure has been chosen. Hence, in the present context we shall only study the former method.

2.3.4. EXAMPLE OF QUANTIFIED UNCERTAINTY BUDGET

The exercise is conducted in the Excel companion provided in the annex of this document for an in-water system (see Figure 10 below). In this file, the final uncertainty of the vicarious gains is based on Eqs. (24)-(25) assuming the same uncertainty for all the match-ups and a simple average ($w(\lambda_i) = 1$). Two major input parameters in the computation are the ratio $t_g^t t^t L_{wN}^t / L_t$ and the number of match-ups N, which can be specified by the reader. We emphasise that this detailed uncertainty

budget is only an example: the detailed numbers are indicative and allow one to reach the overall targeted uncertainty of the mission average gains. This Excel file should be filled with the actual numbers of any system to check that this system meets the expected overall uncertainty in the SVC process.

OC-VCAL ID	Uncertainty source	rel_unc(400) rand.	rel_unc(400) syst
In situ Lw measurement			
OC-VCAL-RD-14	Spectral resolution		0.50%
OC-VCAL-RD-15	Spectral calibration		0.10%
OC-VCAL-RD-16	Stray-light		0.75%
OC-VCAL-RD-17	Radiometric calibration & stability		2.00%
OC-VCAL-RD-18	Angular response		
OC-VCAL-RD-19	Immersion factor	0.25%	
OC-VCAL-RD-20	Thermal stability	0.30%	
OC-VCAL-RD-21	Dark current		
OC-VCAL-RD-22	Polarisation sensivity	0.20%	
OC-VCAL-RD-23	Non-linearity response		0.10%
OC-VCAL-RD-24	Noise characterisation		
OC-VCAL-RD-25	Environ. conditions (like-to-like rule)	0.50%	
OC-VCAL-RD-26	Shading		0.25%
OC-VCAL-RD-27	Tilting & BRDF	0.30%	
OC-VCAL-RD-28	Depth-extrapolation	1.00%	1.00%
OC-VCAL-RD-29	Surface propagation	0.25%	
OC-VCAL-RD-30	Data reduction	2.10%	
	Spare line for other effects		
Total uncertainty on in situ Lw		2.45%	2.43%
Total uncertainty on in situ Lw (rand. + syst)		3.45%	
In situ Lw post-processing and match-up			
OC-VCAL-RD-35-36	Environmental variability against satellite	5.00%	
OC-VCAL-RD-41	Spectral integration to satellite SRF		0.20%
OC-VCAL-RD-42	Normalisation & BRDF corr. to satellite geometry	1.00%	1.00%
OC-VCAL-RD-43-44-45	Match-up process	5.00%	
Total uncertainty on targeted LwN		7.55%	2.63%
Total uncertainty on targeted LwN (rand. + syst.)		8.00%	
SVC gains			
OC-VCAL-RD-46	Individual gains (Eq. 26)	0.38%	0.13%
OC-VCAL-RD-47	Averaging (Eq. 24)	0.05%	0.13%
Total uncertainty on mission average gain (rand. + syst.)		**0.14%**	

Input parameters at the OC-VCAL site	400
tg*t*LwN/Lt	5.00%
Cq (BRDF correction)	1
Number of match-ups	50

Figure 10. Excerpt from the Excel annex file (here limited to band 400 nm) listing the uncertainty sources and providing an example of quantified uncertainty for each component and resulting uncertainty on the mission-average gains. Note that the contribution of marine signal to total TOA signal has been set to 5% (mesotrophic waters).

3. REQUIREMENTS ON THE SVC PROCESS

3.1. SPECIFICITIES RELATED TO SPACE SENSORS

3.1.1. SPECTRAL RANGE AND SRF

Characterisation of the spaceborne sensor spectral bands is essential to ensure a perfect consistency with the radiometry measured by the field radiometer.

OC-VCAL-RD-1. The spectral response function (SRF) of the satellite shall be characterised; this includes the out-of-band response. It shall be monitored along the mission lifetime of the spaceborne sensor.

OC-VCAL-RU-1. Any uncertainty in this characterisation may affect the vicarious gains; if meaningful, it should be propagated in the Level-1 chain and contribute to the uncertainty of the TOA spectral reflectance $L_t(\lambda_i)$.

OC-VCAL-RV-1. N/A

3.1.2. TEMPORAL DEGRADATION

By essence, a unique SVC gain applied throughout the mission lifetime cannot correct for temporal degradation of the spaceborne radiometer. Hence, the radiometric calibration shall correct for any temporal changes in the sensor response. For OLCI, solar diffusers are the radiometric standard for the instrument. The primary diffuser is used about every two weeks for monitoring the temporal degradation of the sensor performance. The use of a second diffuser, deployed only every three months, allows monitoring ageing of the primary diffuser (Delwart and Bourg, 2011). Alternatively, temporal degradation can be monitored and corrected with stable targets like the Moon, which have been the practice for a number of missions, including SeaWiFS, MODIS and VIIRS. According to Ohring et al. (2007), “the Moon can be used for stability monitoring that meets climate-level requirements, but uncertainty in the absolute accuracy limits its use as an absolute standard”. Inspecting the time-series of individual gains can be used to check the correction for the sensor degradation.

OC-VCAL-RD-2. The justification for one unique average gain over the mission lifetime shall rely on a correction for temporal degradation, computed as part of the Level-1 instrumental calibration.

OC-VCAL-RU-2. The uncertainty of the temporal degradation correction shall be assessed a posteriori, by investigating the instrument degradation model with the observed raw SVC gain time series.

OC-VCAL-RV-2. Stability of individual SVC gain time series must be monitored to verify the temporal Level-1 calibration.

3.1.3. OPTICAL SYSTEM

SVC relies on thorough characterization of the ocean colour sensor where all efforts are taken to quantify the elements impacting the quality of radiometric data and correct for their evolution. To date, the principles developed originally for NASA whisk-broom scanning radiometers (such as SeaWiFS and MODIS) have been directly transferred to push-broom sensors with several cameras (MERIS, OLCI). It has, however, not been demonstrated that a unique gain can complement (i.e. correct for any systematic bias) the radiometric instrumental calibration of all cameras. In fact, following the logic of SVC, one could expect to derive one mission average gain per camera or even per detector element, what is unachievable with a limited number of vicarious site matchups. Another related concern is that, because of the cyclic overpass of the satellite over a given target, gains are generally computed for a limited range of camera and detector index. This is illustrated on Figure 11 for MERIS gains computed at MOBY: while the time-series (left) seems to provide overall consistent values (N=91), the distribution as function of detector index (right) shows how badly these gains actually represent the full MERIS optical system (gains mainly computed for camera 1 and camera 2). It is impossible to ensure that these gains have a positive impact, as an example on cameras 3 and 5, unless an on-board relative calibration device is available, like the diffusers on MERIS or OLCI. The BRDF of the diffuser shall be characterised. Complementarily, the Level-1 calibration can be harmonised across the swath using stable homogeneous marine targets (e.g. oligotrophic open waters, as done for MODIS, Kwiatkowska et al. 2008) or equalisation technique over bright targets (Bouvet and Manino 2010).

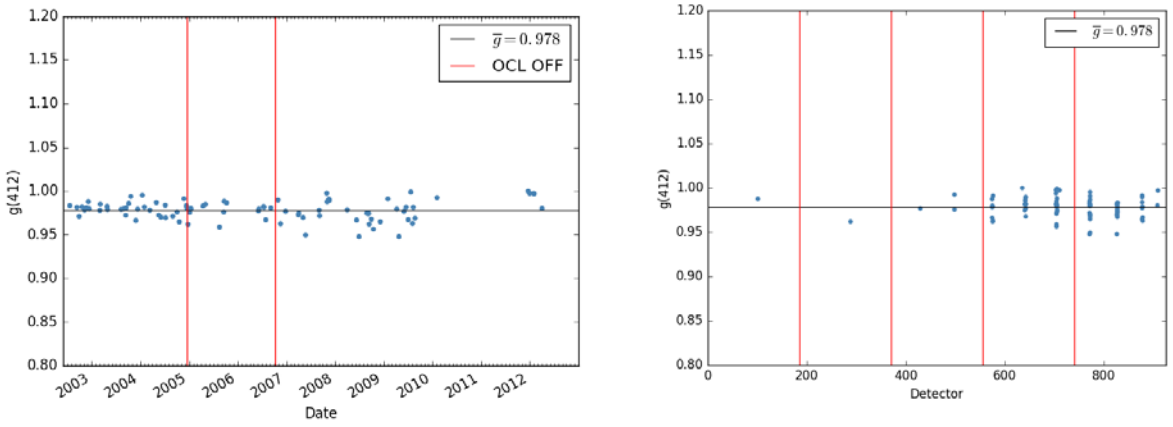

Figure 11. MERIS SVC gains at MOBY from preliminary MERIS 4th reprocessing. Left: as a function of time. Right: as a function of detector index

OC-VCAL-RD-3. The justification for one unique average gain across track (i.e. for all cameras and/or all pixels) shall rely on the Level-1 relative calibration. For OLCI, these are the on-board diffusers which shall be characterised at all relevant geometries. Harmonisation of the across-track calibration can be complemented using homogeneous targets.

OC-VCAL-RU-3. Uncertainty of the on-board diffusers is not part of the uncertainty of the individual SVC gains. However, when the gains do not cover the full range of detectors, and if there is a residual uncertainty in the across-swath harmonisation, this uncertainty shall be included in the mission average gain.

OC-VCAL-RV-3. When a statistically significant number of match-ups can be achieved for various locations across track (detectors in OLCI), individual SVC gains shall be monitored to detect any cross-track residual dependence. On-board diffuser data can also be used to check the inter-band relative SVC gains.

3.1.4. SATELLITE SENSOR RESPONSE

OC-VCAL-RD-4. Vicarious calibration, based on a narrow range of radiance, shall rely on a Level-1 non-linearity correction.

OC-VCAL-RU-4. N/A

OC-VCAL-RV-4. N/A

3.1.5. DETECTOR DEPENDENT WAVELENGTH

For sensors such as OLCI and MERIS, there is a cross-track variation in wavelength. To deal with a unique theoretical wavelength per band, the processing algorithm requires an upstream correction (the so-called smile correction). Computation and application of vicarious gains shall be done consistently with this correction, i.e. either before the smile correction (considering the SRF of the exact pixels imaging the in-situ target) or after the smile correction. Application after the smile correction simplifies the process (Lerebourg et al., 2011), however vicarious gains are then applied within the Level-2 processing algorithm, and not directly on the input TOA radiances provided in the Level-1 data.

3.1.6. SPECTRAL ALIGNMENT

Some radiometers have their detectors on different focal planes which need to be properly adjusted during resampling of the spectrum. This is, for example, an important issue for Sentinel-2. SVC should be applied after this correction.

3.2. CHARACTERISATION OF THE LEVEL-2 PROCESSING CHAIN

It is demonstrated in Mazeran et al. (2017) that the concept of SVC can be formalised as a sensitivity problem between TOA and BOA and that the approach defined for standard AC (Franz et al., 2007) is a very advantageous case where the linearity and decoupling between all bands ensure the relevance of the SVC (i.e. a removal, on average, of systematic bias at BOA) as well as the forward computation of gains. For other types of processors, which are either already in use in Copernicus services (Steinmetz et al., 2012) or potentially expected to be implemented in the next years, there is a strong need for characterising this TOA to BOA sensitivity: linearity or non-linearity of the water-leaving reflectance with respect to the TOA radiometry, the level of sensitivity, the spectral coupling or not, the necessity for calibrating the NIR bands. A generic method is to rely on numerical differentiation and compute the Jacobian matrix of the Level-2 chain. Another key point in the Level-2 chain characterisation is to get an understanding (or at least a description) of uncertainties of water-leaving reflectance in relation with environmental conditions: for instance, how does the processor perform on some types of aerosols, or over some types of complex waters affecting the AC. Indeed,

the approach adopted by Franz et al. (2007) was successful thanks to the robustness of the standard AC processor. Characterising the processor performance and its variability (Zibordi et al., 2009a) is a requirement which should contribute when choosing the optimal environmental condition of the SVC site.

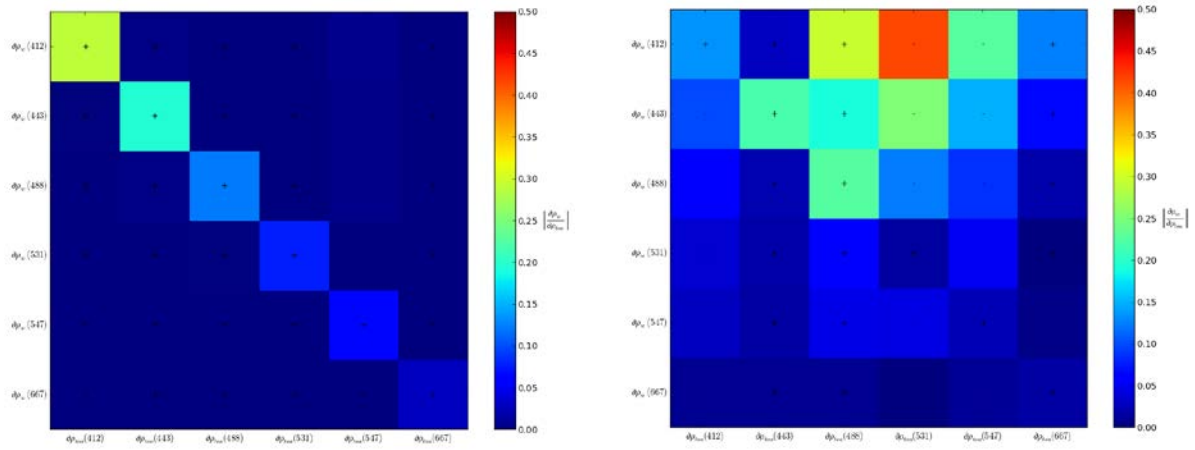

Figure 12. Jacobian matrix over a clear water pixel acquired by MODIS for SeaDAS processor (left) and POLYMER (right). Colours give the amplitude of $\frac{\partial L_w(\lambda_i)}{\partial L_t(\lambda_j)}$ and the sign is printed in the cell.

OC-VCAL-RD-5. The Level-2 processing chain shall be characterised through computation of the Jacobian matrix to conclude on the bands to calibrate and effects of TOA gains on the marine reflectance.

OC-VCAL-RU-5. N/A

OC-VCAL-RV-5. N/A

3.3. SVC METHODOLOGY

3.3.1. RADIOMETRIC REFERENCE MEASUREMENT

The Level-2 processing algorithms of OLCI, VIIRS and other instruments, deal mainly with radiometric quantities expressed in reflectance instead of spectral radiance, and for OLCI provide directional marine reflectance. However the primary quantity measured both at sea level (in situ) and by the satellite is in units of spectral radiance (i.e. a radiant energy per unit area, per unit solid angle, per unit wavelength, in $mW.m^{-2}.sr^{-1}.nm^{-1}$). Furthermore, because the OLCI instrumental calibration is done in terms of reflectance (through the on-board diffusers), SVC is the unique means to ensure SI-traceability of the TOA measured radiance. Therefore SVC should, intrinsically, be expressed in units of radiance. Dealing with reflectance in the processing algorithm is a matter of conversion, which however should be done carefully by using the very same solar irradiance model (at sea level). This explains why it is more straightforward to establish traceability to the SI using in situ spectral radiance rather than reflectance values: the in situ solar irradiance might not be compatible with the

EO's one. Additionally, it is required to convert all downward transmittance (from Sun to target) from the satellite to the in situ geometry to take into account the real solar-path length at the time of the in situ measurement (Franz et al. 2007).

OC-VCAL-RD-6. The in situ quantity used in the SVC shall be the fully normalised water-leaving radiance L_{wN}^{t} (including BRDF effects, Morel et al., 2002). In situ solar irradiance may be measured for quality control or other purposes, but not used in the SVC process. Conversion to marine reflectance, if necessary, shall use the solar irradiance model of the Level-2 processing algorithm.

OC-VCAL-RU-6. N/A

OC-VCAL-RV-6. N/A

3.3.2. NIR BANDS

In the NIR, the unique SVC approach existing to date is based on very oligotrophic waters where the water-leaving radiance can be assumed negligible. This is not a strict requirement but a practical solution to avoid complex and unreliable in situ measurements in this spectral domain and to assure clear marine atmospheric properties for reducing algorithmic uncertainties. The sites considered for NIR SVC are usually different from those for the VIS bands, and typically encompass the South Pacific Gyre (SPG) or South Indian Ocean (SIO). This is the baseline considered so far for the reference signal at sea level.

The exact methodology for NIR gain computations may vary, like fixing gain to unity for one (or a few) band(s) and assuming (or not) a given aerosol model over the site; or like free aerosol shape fitting across many NIR bands. This actually depends on the sensor considered. For instance, Wang and Gordon (2002) have demonstrated that TOA uncertainty of up to 10% in the NIR region does not significantly affect the SVC process in the VIS (the vicarious gains in the VIS domain are able to adjust for any gains in the NIR), given the robustness of the SeaWiFS AC. This has allowed the SeaWiFS band at 865 nm not to be vicariously calibrated, despite an acknowledged radiometric issue (Franz et al., 2001; Wang et al., 2005). This principle has been successfully extended to the SVC of VIIRS processed with the SWIR and NIR-SWIR AC (Wang et al. 2016).

OC-VCAL-RD-7. SVC in the NIR region shall rely on one (or several) very clear water site(s) with negligible signal starting from 700 nm and with very clear maritime atmosphere. The site(s) may be possibly different than that (those) of the VIS SVC, in order to effectively minimize algorithmic uncertainties in the NIR.

OC-VCAL-RU-7. In the SVC process, it shall be demonstrated that uncertainties on the NIR TOA reconstructed signal, $L_t(\lambda_{NIR})$, do not impact the individual gains accuracy and stability in the VIS domain (robustness of AC).

OC-VCAL-RV-7. N/A

3.3.3. VISIBLE BANDS

The principle of SVC in the VIS domain has been covered in section 1.5. Essentially, it requires highly accurate in situ measurements and the exact atmospheric path radiance and transmittance as retrieved by the processing algorithm for the in situ matchup pixels. Thus, VIS SVC is a relative adjustment to the NIR bands (Wang and Gordon, 2002; Wang et al., 2016) and is highly dependent on the AC. Robustness of the AC is crucial to ensure that SVC gains computed in some very particular conditions do not degrade the performance of OCR in other conditions. For instance, Ahmed et al. (2013) have detected more frequent occurrences of VIIRS negative water-leaving radiance at the Long Island Sound Coastal Observatory (LISCO) when using vicarious gains computed at MOBY. IOCCG (2012) also states that "since the primary vicarious calibration site is usually in an open ocean environment, care should be taken to obtain sufficient in situ data from turbid waters for validation purposes". In-depth validation and improvement of the AC should be a continuous concern in parallel with any SVC programme.

OC-VCAL-RD-8. When based on a SVC approach, the targeted TOA signal constructed to derive individual gains in the VIS region, L_t^t, shall rely on exactly the same RTM as that used in the Level-2 processor, with aerosol, ancillary data and auxiliary data matching exactly those of the considered pixel. Any update in the processing algorithm requires an update of the SVC gains.

OC-VCAL-RU-8. When Space Agencies use the SVC derived over very clear waters for the operational processing of their missions at global scale, the impact over more turbid and complex waters shall be assessed to detect any degradation for coastal applications. This means a high quality validation dataset (Fiducial Reference Measurements, FRM) over various water types is required in parallel of the SVC infrastructure. Any degradation of the Level-2 performance over complex waters shall question the robustness of the algorithms, primarily the AC. This does not question the SVC itself, but its applicability to operational processing at global scales. The FRM dataset could also be used to evaluate various SVC gain computation methodologies and select the optimal one(s). Note that the requirements on the uncertainty of the targeted TOA signal are given in OC-VCAL-RU-12.

OC-VCAL-RV-8. To check the proper implementation of the SVC in the Level-2 processing algorithm, the derived pixel-by-pixel vicarious gains shall be applied and they shall result in the exact L_w retrieval as the SVC in situ measurements used in the construction of L_t^t.

3.4. SEA-TRUTH SIGNAL

3.4.1. RANGE OF RADIOMETRY

Although vicarious gains computed through the SVC approach are relative to the AC, and theoretically adjust any bias of the processor itself, their suitability over the whole range of environmental conditions encountered by the space mission is not automatically ensured: "the calibration adjustments, which are dependent on atmospheric correction, are not expected to offset algorithm deficiencies over the entire range of oceanic and atmospheric conditions, especially in coastal regions and inland waters, since they are performed over open-ocean sites with typical maritime aerosols" (IOCCG, 2013a). This is essentially due to acknowledged heterogeneous performance of the algorithms over different marine/atmospheric optical properties or observation/illumination geometries (Mélin et al., 2016). It follows that a unique set of spectral

gains, averaged over the mission lifetime, does not prevent (and may even amplify) a bias in various water types, as demonstrated in Eq. (16). Thus, the selection of the SVC site contains unavoidable limitations in terms of applicability.

The location of the site should be justified by minimising the uncertainties in the vicarious gains, rather than being based on the application. Taking the example of MOBY, the choice of Hawaii came from the higher confidence in measurement over the oligotrophic water type, as well as low aerosol loading and stable aerosol type to minimise uncertainties of the AC in the SVC process (see section 3.5).

OC-VCAL-RD-9. The choice of the SVC site shall not be driven by the application ("Case-1" or "Case-2") but by the total uncertainty budget of the site and the final vicarious gains. Using Eq. (25), the total uncertainty budget at the proposed site shall be derived. It is understood that mesotrophic waters may better minimise the uncertainty of gains due to lower L_{wN}^{t}, compared to oligotrophic waters (see Zibordi and Mélin, 2017), however the uncertainty of all components shall be quantified, including the atmosphere, BRDF correction and spatial variability.

OC-VCAL-RU-9. The complete uncertainty budget shall be derived to demonstrate the relevance of any SVC site following Eq. (25). A key parameter is the relative uncertainty on L_{wN}^{t} scaled by its ratio to the total signal, i.e. $(u(L_{wN}^{t})/L_{wN}^{t}) * \left(t_g^t t^t L_{wN}^{t}/L_t\right)$.

OC-VCAL-RV-9. N/A

3.4.2. ABSOLUTE ACCURACY

According to the uncertainty budget of section 2.3, based on standard AC, an uncertainty of less than 5% in the sea-truth measurement is required. This uncertainty combines all in situ contributions: "from instrument absolute calibration, characterisation (including at least spectral calibration, nonlinearity, stray light perturbation and polarisation sensitivity, temperature dependence and, if applicable, geometrical and in-water response), environmental perturbation, and data processing" (NASA, 2014; Zibordi and Voss, 2014a).

OC-VCAL-RD-10. The uncertainty of less than 5% in the blue-green spectral region is required. This uncertainty is constrained by the space mission requirements (see section 1.3). Specifically, the allowable uncertainty of the sea-truth signal shall be quantified through the full uncertainty budget (section 2.3) to achieve an uncertainty on the mission average gain of no more than 0.5% (threshold) and ideally of 0.3% (goal) in the blue-green spectral regions (between 400 nm and 560 nm). The translation in terms of uncertainty at the match-up level depends on the systematic and random component of the uncertainty, as well as the number of matchups (mission specific); for instance, under conditions as those at MOBY, considering only the systematic component (simplistic assumption), this implies the uncertainty at sea level of less than 5% in this spectral domain.

OC-VCAL-RU-10. Coming either from in-house development or a commercial manufacturer, there shall be evidence that the uncertainty estimate is reliable. A complete characterisation,

including full uncertainty budget of the instrument, shall be provided following a standardised uncertainty budget definition.

OC-VCAL-RV-10. N/A

3.4.3. INTER-BAND ACCURACY

Requirements on inter-band accuracy likely depend on atmospheric correction and applications. This has still to be defined.

3.4.4. NUMBER OF SVC SITES

While a single site is in principle enough in the process of SVC, dealing with multiple sites may be, in practice, a way to increase the number of data and decrease the global uncertainty, assuming the full equivalence between the sites and the derived gains. This has motivated the use of both BOUSSOLE and MOBY to derive the MERIS gains.

Statistical test, such as χ^2test of homogeneity, can demonstrate the equivalence in the gains derived by two infrastructures (subscript 1 and 2 below):

$$\chi^2 = \frac{|\bar{g}_1 - \bar{g}_2|}{\sqrt{\sigma_1^2/N_1 + \sigma_2^2/N_2}} \quad (27)$$

When χ^2 is below 1.96, there is 95% probability that both sets of gains belong to the same distribution. This estimator depends not only on the in situ measurements, but also on the whole SVC process, in particular on the AC. This equivalence has been reached between MOBY and BOUSSOLE for the MERIS 4th reprocessing, at several bands, thanks to an improved robustness of the AC (Figure 13).

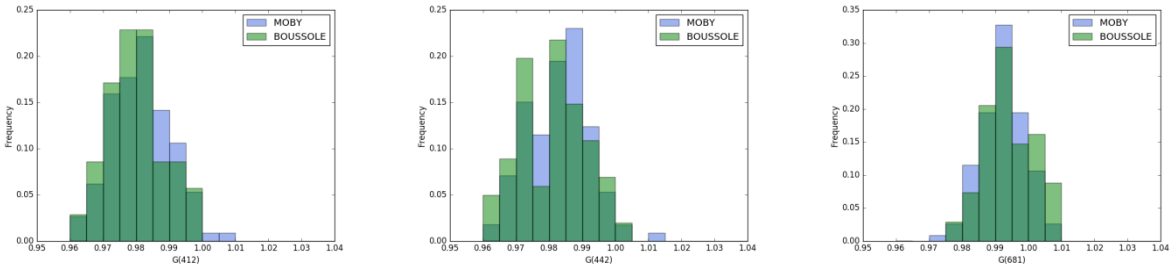

Figure 13. MOBY (blue) and BOUSSOLE (green) histograms of SVC gains computed for MERIS 4th reprocessing at 412 (left), 443 (middle) and 681 nm (right). From Antoine and Mazeran 2017. Values of χ^2 at these bands are respectively 0.46, 1.72 and 1.59, i.e. lower than 1.96.

OC-VCAL-RD-11. In terms of physics, there is no requirement for using multiple SVC sites if the selected site meets or exceeds SVC uncertainty requirements. From a metrology point of view, several sites are preferred. Site uncertainties could weigh the average SVC gains; for instance, three equivalent sites would allow checking to see if one of them is drifting (yet other less expensive solutions may exist for such a purpose). Redundancy of sites is recommended to ensure the long-term operational objective of vicarious calibration and to avoid any data gap due to failure of one instrument (IOCCG, 2012; IOCCG, 2013b). Using several sites may be justified for some operational applications in order to reach more quickly the required number of match-ups (see section 5.3.2); for instance, removing the bias in L_w in a just launched space mission needs match-ups in its early phase, while climate change investigations need only a sufficient number of match-ups after several years. The exact location of the site(s) shall take into account the real orbit of the considered OC satellites, to optimise the number of imaging cameras/detectors and the number of match-ups (orbit overlap); option for multiple sites at different latitudes shall be investigated.

OC-VCAL-RU-11. In the case where multiple sites are implemented, they shall be strictly equivalent in terms of the complete uncertainty budget as in Eq. (25), precision, traceability, observation conditions (NASA, 2014; Zibordi and Mélin, 2017) and shall use harmonised protocols.

OC-VCAL-RV-11. Equivalence in the vicarious gains computed over various sites shall be demonstrated in terms of absolute level, uncertainty and stability. Statistical tests (e.g. test of homogeneity, Eq. 27) shall demonstrate that gains computed over different sites belong to the same distribution and can be weight-averaged.

3.5. AEROSOL CHARACTERISATION

Quantifying the uncertainty related to the atmospheric component is mandatory for selecting the optimal SVC site(s). The experience has shown that atmospheres characterized by maritime aerosols, generally stable over time, predictable, and with low optical thickness, are the most appropriate because they are modelled in the AC process with the lowest uncertainties (Franz et al., 2007).

Atmospheric measurements are not used in the current vicarious calibration operated by NASA and ESA, essentially for methodological reasons which have led to move from radiometric vicarious calibration to SVC (Franz et al., 2007). However such measurements are now advised by NASA at least for characterising the site and selecting the match-ups (NASA, 2014). We have shown in section 2.3 that SVC gains depend on the atmospheric scattering functions (L_{path}^{t} and t^{t}), directly estimated in a SVC approach by the Level-2 AC, which obviously performs with some uncertainties. The variability observed in the time-series of individual gains might be partly due to these components that a priori vary with the Sun/view angular geometry, the IOPs of the atmosphere, and the water surface conditions (i.e. the level of roughness induced by the wind speed, the barometric pressure, and BRDF). Furthermore the applicability of the SVC gains established at one site to other regions characterised by different atmosphere may be questioned depending on the robustness of the AC.

To provide estimates on these scattering atmospheric functions, we have applied the approach of Aznay et al. (2014) to the Lanai site equipped with an AERONET station close to the MOBY buoy. In short, the method consists in using the AOT and IOPs of aerosols (i.e. the SSA and APF) derived from solar extinction measurements and sky radiance acquisitions, as inputs to a RTM, here the successive orders (SO) of the scattering code (Lenoble et al., 2007). These calculations were conducted at exact angular geometries and same surface conditions (wind speed and barometric pressure) as MERIS

pixels matching the ground measurements. They provided then reference values of L_{path}^{t} and t^{t} that could be directly compared to their MERIS counterpart, L_{path} and t. Histograms of relative uncertainties $u(L_{path})/L_{path}$ and $u(t)/t$, displayed in Figure 14, were computed on a sub-set of very clear matchups (no cloud, no medium and high glint in about 6x6 km^2 around the site) and for every pixel, for allowing the analysis of the spatial variability within the match-ups. A positive bias of about 2.5% in relative value can be observed in L_{path} and would require more inspection of the MERIS AC. Overall relative uncertainty of 3% and 1% (1-sigma) are found on the atmospheric path radiance and total (i.e. along the downward and upward paths) transmittance, respectively.

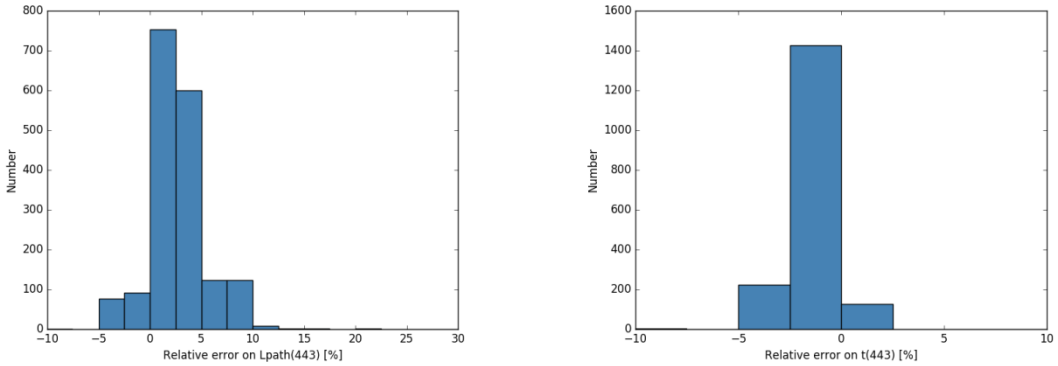

Figure 14. Histogram of $\sigma_{L_{path}}/L_{path}\,(443)$ (left) and $\sigma_t/t\,(443)$ (right) estimated for MERIS (3rd reprocessing) at the Lanai site against AERONET data.

OC-VCAL-RD-12. Atmosphere above the SVC site shall be characterised in situ in terms of AOT, aerosol type and variability of gaseous absorption. At least one year of continuous data is required to describe the seasonal cycle at the site and, ideally, a longer history record. Maritime aerosols, generally stable over time, predictable, and with low optical thickness are the target. The molecular and aerosol quantities used to compute gains in a SVC approach, that is L_{path} and t derived by the satellite, shall be compared to these ground-truth measurements using the same RTM as that used in the Level-2 processing algorithm.

OC-VCAL-RU-12. Uncertainty in L_{path} and t shall be estimated to compare performance of the AC over various sites and help selecting the site which minimises this uncertainty and provides the best conditions. Analysis with respect to scattering angles should be done to detect any trends (e.g. backscattering geometry of OLCI). Uncertainties assessed for MERIS at Lanai near MOBY of about 3% and 1% in these two terms contribute to about 3% in the total gain uncertainty, which is acceptable at the match-up level, and can be then considered as a recommendation.

OC-VCAL-RV-12. N/A

4. REQUIREMENTS ON THE SVC FIELD INFRASTRUCTURE

4.1. RADIOMETER CHARACTERISATION AND CALIBRATION

4.1.1. SPECTRAL ASPECTS

4.1.1.1. SPECTRAL COVERAGE

The spectral bands of S3/OLCI are listed in Table 1, together with spectral bands of S3/SLSTR and S2/MSI. For the vicarious calibration of all OLCI bands except 940 and 1020 nm, it is necessary to cover the spectral range 380-900 nm. Ideally starting at 340 nm would also allow handling the future NASA/PACE mission. For waters with low particulate backscatter, as it is the case for many open sea locations, it is possible to simply assume negligible water-leaving radiance for the spectral bands at wavelengths larger than 700 nm for the purpose of vicarious calibration. In such case, it is required to effectively demonstrate that the NIR signal is negligible at the site and to quantify the uncertainty due to this assumption. NIR measurements can then be done with relaxed criteria, e.g. by a single multispectral radiometer, still associated with a rigorous uncertainty budget. At the same time, SVC for these bands is reliably accomplished using the NIR SVC method described in section 3.3.2.

If operating in locations with non-negligible water-leaving radiance at wavelengths longer than 700 nm, it is necessary to either collect measurements for such wavelengths, e.g. with above-water systems, or model the water-leaving radiance at these wavelengths from measurements in the VIS/NIR spectral domain and estimate the associated modelling uncertainties. For OLCI 1020 nm band, water-leaving radiance is measurable in the world's most turbid waters (Knaeps et al., 2012). However, such waters, typically turbid estuaries and river plumes, have generally high spatial and temporal variability and are hence unsuitable for vicarious calibration.

The S3/OLCI, S2/MSI and S3/SLSTR SWIR bands at 1.02 µm, 1.6 µm and 2.2 µm are very useful for the AC over turbid waters (Wang and Shi, 2016; Vanhellemont and Ruddick, 2015) and, consequently, should be vicariously calibrated (see section 3.3.2). For these bands, the water-leaving radiance can be neglected in open waters and the uncertainty for such an assumption quantified (Wang et al., 2016).

The spectral coverage 380-900nm discussed above for OLCI is suitable for all current OC sensors including HY-1B/COCTS, HY-1B/CZI, COMS/GOCI, Terra/MODIS, -Aqua/ MODIS, OceanSat-2/OCM-2 and SNPP/VIIRS. This spectral coverage is also suitable for SVC of the vast majority of sensors designed originally for land applications including LANDSAT-8 (and follow-ons), S2/MSI and PROBA-V.

For a few future OC sensors, notably NASA/PACE, NASA/GEO-CAPE and NASA/HyspIRI missions, the spectral coverage 380-900 nm would need to be extended towards shorter wavelengths, e.g. 340-350 nm or even shorter to account for out of band response.

Table 1. Central wavelength and width of OLCI spectral channels. OLCI bands marked in grey are not available as Level-2 radiometric products. OLCI bands in red are new with respect to previous bands on MERIS. Sentinel-3/SLSTR and Sentinel-2 (S2) wavelengths are given, although it is noted that these have much lower signal to noise. Source: https://sentinel.esa.int/web/sentinel/user-guides/

	OLCI band	OLCI centre (nm)	OLCI width (nm)	SLSTR centre/ width (nm)	MSI centre/ width (nm)
VIS	Oa1	**400**	15	-	-
	Oa2	412.5	10	-	-
	Oa3	442.5	10	-	443/20
	Oa4	490	10	-	490/65
	Oa5	510	10	-	-
	Oa6	560	10	555 / 20	560/35
	Oa7	620	10	-	-
	Oa8	665	10	*659 / 20*	665/30
	Oa9	**673.75**	7.5	-	-
	Oa10	681.25	7.5	-	-
NIR	Oa11	708.75	10	-	705/15
	Oa12	753.75	7.5	-	740/15
	Oa13	761.25	2.5	-	-
	Oa14	764.375	3.75	-	-
	Oa15	767.5	2.5	-	-
	Oa16	778.75	15	-	783/20
	Oa17	865	20	865 / 20	865/20
	Oa18	885	10	-	-
	Oa19	900	10	-	-
	Oa20	940	20	-	945/20
SWIR	Oa21	**1 020**	40	-	-
				1 375 / 15	1 375/30
				1 610 / 60	1 610/90
				2 250 / 50	2 190/180

OC-VCAL-RD-13. Spectral coverage should be sufficient to cover both the in-band and full band spectral characteristics of the satellite sensor, specifically 380-900 nm for S3/OLCI, S2/MSI and all current OC. Ideally it should start at 340 nm for the future NASA/PACE mission.

OC-VCAL-RU-13. If part of the spectral coverage is achieved by modelling the water-leaving radiance from other wavelengths (e.g. for the range 700-900nm in low reflectance waters) the residual uncertainty due to limited spectral coverage of the SVC instrumentation must be determined. This can be achieved with a NIR measurement with relaxed criteria (e.g. a single multispectral radiometer, in contrast to a hyperspectral radiometer for the VIS bands, see section 4.1.1.2).

OC-VCAL-RV-13. The spectral coverage of each individual instrument should be provided via a report describing laboratory tests. If part of the spectral coverage is achieved by modelling the water-leaving radiance (e.g. for the range 700-900 nm in low reflectance waters) then a report describing RTM simulations with varying IOPs at the measurement site should be provided as a basis for the uncertainty estimate.

4.1.1.2. SPECTRAL RESOLUTION AND RESPONSE FUNCTION

To properly derive an in situ water-leaving radiance comparable to that measured by the spaceborne sensor (see Eq. 7), the following spectral integration has to be performed for each sensor band λ_i:

$$L_w^t(\lambda_i) = \frac{\int L_w^{IS}(\lambda_j) SRF_i(\lambda_j) d\lambda_j}{\int SRF_i(\lambda_j) d\lambda_j} \tag{28}$$

where $L_w^{IS}(\lambda_j)$ is the water-leaving radiance determined at any wavelength λ_j with the field instrument and SRF_i is the spectral response function of the appropriate spaceborne sensor band λ_i. In fact, $L_w^{IS}(\lambda_j)$ depends itself on the SRF of the field radiometer, SRF_j^{IS}:

$$L_w^{IS}(\lambda_j) = \frac{\int L_w^{IS}(\lambda) SRF_j^{IS}(\lambda) d\lambda}{\int SRF_j^{IS}(\lambda) d\lambda} \tag{29}$$

Because SRF_j^{IS} is neither perfect nor equal to SRF_i, the spectral resolution (defined by the sensor bandwidth) and the spectral sampling interval (i.e., the distance between center-wavelengths of adjacent bands) of the field radiometer must be sufficient to properly resolve the SRF of any spaceborne sensor channel. Obviously, some errors are introduced when the spectral resolution is not sufficient to correctly model the satellite bandpass. The current MOBY system has approximately 0.5 nm/pixel as the spectral spacing between channels and approximately 1 nm spectral bandpass for each of them. Two studies (Flora et al., 2006; Zibordi et al., 2017b) have shown that when these specifications are relaxed additional errors are incurred in deriving the appropriate water-leaving radiance for the spaceborne sensor channels. Flora et al. (2006) found that the spectral resolution of the in situ measurements must be a factor of 2-5 times higher than the spaceborne sensor bandwidth in order to reduce biases in the derived water-leaving radiances to less than 1%. For example, an in situ instrument with a 10 nm full-width-at-half-maximum (FWHM) and a 3.3 nm

spectral spacing (which is typically the case of a commercial hyperspectral instrument) will introduce biases up to +/-1% in the MODIS type band averaged radiances.

In the case of multispectral radiometers the non-continuous/irregular sampling of the L_w^t spectrum may be mitigated by modelling the water-leaving radiance for wavelengths between measurements ("band-shifting" method), but with generally larger uncertainties. If a single multispectral radiometer needs to be chosen, the priority shall be given to the S3/OLCI bands.

OC-VCAL-RD-14. When a unique in situ radiometer is intended to be used for the SVC of multiple Copernicus instruments, hyperspectral resolution shall be required. Spectral resolution shall be sufficient to resolve the full spectral SRF of each satellite sensor. To limit the bias to less than 0.5% in L_w^t (after integration on the sensor SRF), a spectral resolution better than 3 nm, with a sampling interval of about 1 nm, is required for a multispectral sensor such as OLCI (NASA 2014, Zibordi et al. 2017b), and a sub-nanometer resolution is required when dealing with hyperspectral satellite sensor such as PACE. Note that for a hyperspectral in situ radiometer, the resolution can be relaxed from 3 nm to 1 nm when using remote-sensing reflectance (see Eq. 34) instead of water-leaving radiance in the SVC process.

OC-VCAL-RU-14. Residual uncertainty due to spectral convolution of SVC measurements over the SRF of the spaceborne sensor spectral band must be determined, following for example the approach proposed by Zibordi et al. (2017b).

OC-VCAL-RV-14. The SRF of the SVC field instrument should be documented on the basis of laboratory characterisations. The estimation of uncertainty due to the difference in SRF between the SVC field instrument and the spaceborne sensor should be provided via a report describing tests; e.g. applying Eq. (29) to the sensor SRF for a variety of L_w spectra representative of the water type at the SVC site and derived from, either acquisition at finer spectral resolution (e.g. 1 nm) than that of the SVC field instrument, or radiative transfer simulations at finer spectral resolution with varying IOPs typical of the calibration site and including inelastic processes.

4.1.1.3. SPECTRAL CALIBRATION

The specific spectral resolution and the centre wavelength of each channel must be understood for both hyperspectral and multispectral field instruments. Because the surface irradiance spectrum presents the effects of many narrow absorption/emission lines included in the extraterrestrial solar irradiance spectrum (due to variations of temperature in the Sun and its chemical compounds), any small change in wavelength of the field instrument may induce variations in the retrieved radiance (see Figure 15). For both hyperspectral and multi-channel instruments, these characterisations can be done in the laboratory by either measuring the full SRF of a multichannel instrument, or illuminating the hyperspectral instrument with gas discharge lamps or laser lines. One advantage of hyperspectral instruments is that this calibration, and the stability of this calibration, can be maintained in the field by the use of Fraunhofer lines in the solar spectrum (Meroni et al., 2010). A reasonable goal is for the spectral position of each channel of the in-situ instrument to vary by less than 0.2 nm during field deployment; this number actually depends on the spectral resolution and would need to go below 0.1 nm for a 1 nm resolution.

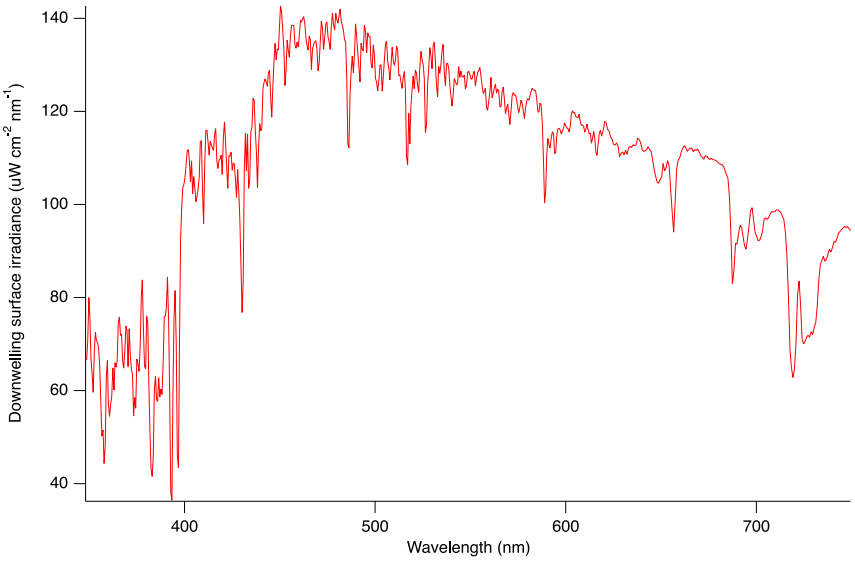

Figure 15. Example of surface irradiance spectrum, measured with MOBY, showing its spectral complexity.

OC-VCAL-RD-15. Spectral calibration and its stability during deployment must be sufficient to maintain the radiometric accuracy of the retrieved L_w^{IS}. A reasonable goal is 0.2 nm for each channel of the field spectrometer.

OC-VCAL-RU-15. Residual uncertainty due to the temporal variability of SRF of the SVC field instrumentation must be determined.

OC-VCAL-RV-15. A report should be provided quantifying the impact of the temporal variability of the in situ SRF (SRF^{IS}) on the spaceborne sensor band-weighted water-leaving radiance L_w^t using measured SVC SRF and typical L_w spectra for the measurement location.

4.1.1.4. STRAY LIGHT

Stray light is a problem for hyperspectral radiometers, in which a monochromatic source of radiance at one wavelength causes a signal at other wavelengths due to internal scattering in the radiometer. The resulting error is systematic and may reach almost 10% on the water-leaving radiance for bands near 400 nm if not corrected (MOBY case; Feinholz et al., 2009). This effect can be even larger in the red wavelengths if one spectrometer is used for the entire spectral range. Hence, stray light needs to be characterised and systematically corrected for all measurements, due to the wide range of existing marine radiance spectra. This correction should take into account the difference between the spectral composition of the calibration light source and of the water-leaving radiance (e.g. Talone et al., 2016).

Laboratory characterisation of the stray light distribution function (SDF) is particularly time-consuming. Analysis of the TriOS/RAMSES instrument suggests that a single SDF of spectrographs from the same production batch may have about 0.7-1% uncertainty (Talone et al., 2016). Reducing this uncertainty requires a characterisation of the SDF for each instrument at least once, and then re-checking it during routine calibration at several wavelengths.

OC-VCAL-RD-16. Stray light shall be characterised for each individual radiometer through the stray light distribution function (SDF). Characterisation at series level may be sufficient as far as this supplementary source of uncertainty is included in the uncertainty budget. A temporal monitoring to detect sudden changes is required (e.g. internal sources). Measurements shall be corrected systematically for stray light with quality-controlled algorithms taking into account the spectral composition of both calibration light source and in situ measurement. Residual uncertainty of the correction shall be documented.

OC-VCAL-RU-16. Uncertainty associated with stray light correction shall be reassessed for each set of measurements after any stray light characterisation. This can be achieved using calibrated blue sources as validation sources.

OC-VCAL-RV-16. Laboratory tests should be reported, following best existing practices as documented by Feinholz et al. (2009), providing the SDF for each radiometer or each class of radiometer together with an estimate of the inter-instrument variability of the SDF. Residual uncertainty after correction shall be verified; e.g. by taking a variety of L_w spectra typical of the measurement location, convoluting with the instrument SDF (and its variability) and applying the stray light correction scheme to estimate the original L_w spectra. Test measurements should be done during routine recalibrations to verify the stability of the SDF.

4.1.2. RADIOMETRIC ASPECTS

4.1.2.1. ABSOLUTE RADIOMETER CALIBRATION AND STABILITY (IN AIR)

To be useful in the SVC process the in situ instrument must maintain a level of absolute radiometric calibration and stability of this calibration during deployment. The recent NASA vicarious calibration Request For Proposals (NASA, 2014; Zibordi and Voss, 2014b) specified absolute spectral radiometric uncertainty less than 4% in the blue-green region of the solar spectrum (above 400 nm) and approximately 5% at the red wavelengths. This included all sources of uncertainty, from laboratory measurements, through deployment, and data reduction. In addition the NASA Request For Proposals specified that this uncertainty must be maintained to within 1% during the deployment. To achieve it, the fundamental radiometric calibration (in air) must be much more accurate, on the order of 1-2% to accommodate the additional uncertainties that will occur along the acquisition and processing stages. This radiometric calibration is typically achieved by laboratory calibration using FEL lamps, or calibrated integration spheres, which are in turn traceable to a primary optical calibration source, typically a cryogenic radiometer maintained by a NMI (e.g. NIST, NPL).

Regarding the UV domain, which is of interest for missions such as PACE, new types of sources with higher SNR than standard Quartz Tungsten Halogen lamp could be developed.

Stability of the radiometric calibration should be monitored in the field either continuously (preferably at “system” level, e.g. through the entrance optics) or during regular field visits. Redundancy and overlap of instrumentation also facilitates continuous monitoring of radiometric sensitivity during deployments.

OC-VCAL-RD-17. Radiometric calibration of the instrument (in air) must be held to 1-2% uncertainty in the VIS domain (above 400 nm) and traceable to SI unit via a NMI. This calibration

must be maintained to within 1% during each deployment. Stability of the radiometric calibration during deployments must be monitored.

OC-VCAL-RU-17. The residual uncertainties in the laboratory radiometric calibration and the radiometric stability of instruments during deployments must be understood and quantified.

OC-VCAL-RV-17. A full radiometric calibration history shall be supplied for each OC SVC instrument including both the laboratory calibration and the field stability monitoring. The impact of uncertainties in the radiometric calibration, both during the laboratory calibrations and because of temporal variability during deployments, shall be propagated to give uncertainties in the L_w^{IS} measurement.

4.1.2.2. ANGULAR RESPONSE

For in-water instrumentation the upwelling radiance field is relatively smooth when viewed in the nadir direction. Because of this the angular acceptance of the radiance detector is not critical and can be as large as 10° (half-angle) field of view (FOV) (Ocean Optics Protocols, Rev 4, Vol II). Radiometers with large FOV are often difficult to calibrate in the laboratory, because a large extended source of radiance is required. A smaller FOV (e.g. such as MOBY with 1.73° full-angle) can be used, but care must be taken to either increase the number of samples to be averaged or increase the integration time to account for the decreased solid angle that has been viewed by the sensor.

OC-VCAL-RD-18. For underwater instrumentation, the half-angle FOV of the radiance detector must be less than 10°; in open waters this is not a strict limit because the radiance field is very homogeneous, the only limit in practice being to avoid imaging the deployment platform.

OC-VCAL-RU-18. The uncertainty associated with finite FOV should be quantified.

OC-VCAL-RV-18. The FOV of each instrument should be reported on the basis of laboratory tests. For nadir-viewing underwater measurements the uncertainty associated with this FOV should be estimated for typical angular distributions of upwelling radiance for the measurement location.

4.1.2.3. IN-WATER RESPONSE (RADIANCE SENSOR)

Radiometers will have a different response in water than in air, and since most radiometers are calibrated in air, this difference must be determined. The immersion factor accounts for this difference (Mueller and Austin, 2003), and must be determined for each class of radiometer (Zibordi, 2006). The immersion factor is caused by the difference in the refractive index of air and water, and hence varies with the refractive index of seawater, which itself varies with wavelength, temperature and salinity. Thus, the immersion factor must be estimated for the instrument, and the effect of variation of the refractive index with a range of salinities and temperatures (Austin and Halikas, 1976; Quan and Fry, 1995) relevant to the SVC site must be determined. For many simple radiometers, the immersion factor can be calculated from theoretical first principals to ensure a very

low uncertainty, but it must be experimentally verified. The uncertainty estimate for this factor in MOBY is 0.05% (Feinholz et al., 2017).

OC-VCAL-RD-19. The immersion factor for the field radiance sensor, or series of sensors, must be measured.

OC-VCAL-RU-19. The uncertainty of the immersion coefficient of the radiance sensor should be targeted to 0.05% (reference used at MOBY) and shall, in any case, not be higher than 0.25% as it then starts to affect the total uncertainty budget. The range of uncertainty in the immersion factor due to temperature and salinity in the operational area of the SVC site must be included.

OC-VCAL-RV-19. It should be verified that the estimated immersion factor agrees with the simple theoretical model (Mueller and Austin, 2003), within the uncertainty of the model.

4.1.2.4. THERMAL STABILITY

One source of variability of the instrument sensitivity relates to its thermal stability. Depending on the environment, an in situ radiometer could be expected to operate in the range from 10°C to 30°C. Hence a difference between the in temperature during operation in the field and the calibration temperature introduces systematic error. The temperature response of the radiometer must be characterised for the range of temperatures relevant to its operational environment. It is recommended that the residual uncertainty after temperature correction is less than 0.3% over the above-mentioned range. For the MOBY optical system, located in a tropical site but also held at 10 m below the surface, the range of temperatures in which the instrument will be exposed, while in the field, is much smaller than that of free-floating systems or of any instrument operated in marine regions affected by significant seasonal changes in water temperature.

Laboratory characterisation of the thermal sensitivity of each instrument is definitely time-consuming (Zibordi et al., 2017c). Still, the determination of the thermal response for specific groups of instruments, albeit with higher uncertainty, should be a requirement. Knowledge of the internal detector temperature is essential to facilitate the application of thermal corrections for instruments without thermal regulation. For some instruments it may be possible to estimate detector temperature from dark current (see section 4.1.2.5) or apply a thermal correction based on dark current instead of detector temperature.

OC-VCAL-RD-20. The OC-SVC instrument temperature shall be determined continuously, e.g. thanks to redundant inclusion of thermistors and the uncertainty associated with temperature effects shall be quantified.

OC-VCAL-RU-20. The uncertainty in the temperature characterisation must be understood and held to less than 0.3%.

OC-VCAL-RV-20. The thermal sensitivity of OC SVC instrument will be characterised on the basis of laboratory tests. The operating and/or ambient temperature of OC SVC instruments will be

monitored during deployments and used to correct for temperature effects. The uncertainty associated with thermal effects will be estimated, after application of any correction method, for typical measurements and typical operating conditions of the measurement location.

4.1.2.5. DARK CURRENT

Electric signals ("dark current") are generated within optical instruments giving a raw non-zero measurement even in absence of incoming light. Dark signal will depend on various factors including integration time and operating temperature, and may be highly variable in time giving instrument "noise". The dark signal can be measured by blocking the incoming light source, e.g. via a mechanical shutter or by light-blocked pixels of a CCD array, and subtracted from measurements (dark correction).

OC-VCAL-RD-21. The dark signal shall be measured and corrected. Measurements will be made with sufficient replicates or integration time to minimise dark current effects.

OC-VCAL-RU-21. The uncertainty associated with dark signal, after correction, shall be quantified.

OC-VCAL-RV-21. The methodology adopted for the dark signal measurement and its correction shall be reported and the uncertainty estimates shall be validated taking into account possible time or signal-related variation of dark current.

4.1.2.6. POLARISATION SENSITIVITY

If the radiometer has a polarisation sensitivity, then the polarised light intensity will interact with the instrument and cause variability in response that will vary with solar zenith angle, instrument orientation, and IOPs of water and atmospheric constituents. For in-water instruments, the upwelling radiance can be polarised, with up to a 60% degree of polarisation (DOP) that mainly depends on the wavelength, IOPs of water, and the solar zenith angle (e.g. Voss and Souaidia, 2010), although the DOP is rarely so high at nadir. If the polarisation sensitivity of the instrument is kept below 1%, this will be less than a 0.6% effect at most, but more commonly less than 0.2% in most cases for the nadir view direction.

If the polarisation sensitivity of the instrument is kept below 2%, this will be less than a 1% effect at most, but more commonly less than 0.2% in most cases for the in-water case and the nadir view direction.

OC-VCAL-RD-22. The polarisation sensitivity of the field instrument must be less than 1% and fully characterised.

OC-VCAL-RU-22. The uncertainty of L_w^{IS} due to the polarisation sensitivity must be determined for the specific operating conditions at the time of the measurement.

OC-VCAL-RV-22. The wavelength dependent polarisation sensitivity of each instrument shall be documented based on laboratory tests; e.g. by azimuthal rotation of the instrument illuminated by a strongly polarised light intensity source of a known DOP. The polarisation sensitivity of each instrument shall be applied to radiance field vector (Stokes parameters), e.g. simulated and typical of conditions at the measurement location to validate the uncertainty estimate.

4.1.2.7. NON-LINEARITY RESPONSE

Radiometric sensors may exhibit a non-linearity in their response. This can cause a problem with hyperspectral sensors, where the spectral variation in received irradiance can be very large. In addition, it is likely that there will be variations in the source spectral intensity between measurements performed in the laboratory for calibration purposes and those performed in the field. It is possible for this instrument linearity to be accurately characterised and corrected. In this case, it is important to do this correction to within 0.1%.

OC-VCAL-RD-23. The linearity of the instrument must be characterised and corrected to have an uncertainty of less than 0.1%. Achieving such an uncertainty in the correction requires “absolute” methods, most commonly the flux-doubling method and its improved variants (Yoon et al. 2003, White et al. 2008).

OC-VCAL-RU-23. The residual uncertainty due to the linearity correction must be determined.

OC-VCAL-RV-23. The non-linearity of instrument response and its variability shall be documented on the basis of laboratory tests with different incident light intensities and integration times. The impact of non-linear response will be estimated, after the application of any correction method, with radiance fields typical of the measurement location.

4.1.2.8. NOISE CHARACTERISATION

In addition to the dark current reported in section 4.1.2.5, other factors relating to the instrument design and/or the discrete photon nature of light may give very fast fluctuations in the measured signal that cannot be characterised, termed here “noise”. As an example this may be encountered in a CCD-based hyperspectral systems operating with an integration time too short for dark targets. It is especially the case of instruments with a single integration for the entire spectrum but with very different light levels across the spectrum, e.g. comparing VIS with NIR wavelengths. In general, this noise can be reduced by increasing the integration time and/or by averaging over many replicate measurements, although this may be subject to other constraints such as avoiding saturation at wavelengths with high light levels and time restrictions for fast profiling with vertically profiling systems.

Here, the noise refers only to instrument-related variability of the signal – other sources of high frequency variability of the measured signal may arise from “environmental effects” such as wave-focusing for underwater measurements.

OC-VCAL-RD-24. Instrument noise shall be kept at levels that do not impact the total uncertainty of a measurement.

OC-VCAL-RU-24. The uncertainty due to the instrument noise shall be quantified.

OC-VCAL-RV-24. The minimisation of instrument noise shall be demonstrated by quantifying instrument-related temporal variability for replicate measurements.

4.1.3. *LIKE-TO-LIKE* RULE

A general issue in the radiometer characterisation and calibration described above is that biases might be introduced because of different parameters and environmental conditions between the target we want to measure and the calibration target. Figure 16 gives an example for the relative spectral distribution, where a lamp-based calibration source produces a higher radiometry in the red and NIR region compared to an actual marine signal. Other influencing parameters may be the spatial difference (near field versus far field), polarisation, temperature, etc. According to Johnson et al. (2003), the *like-to-like* rule should be followed as much as possible to avoid introducing systematic bias.

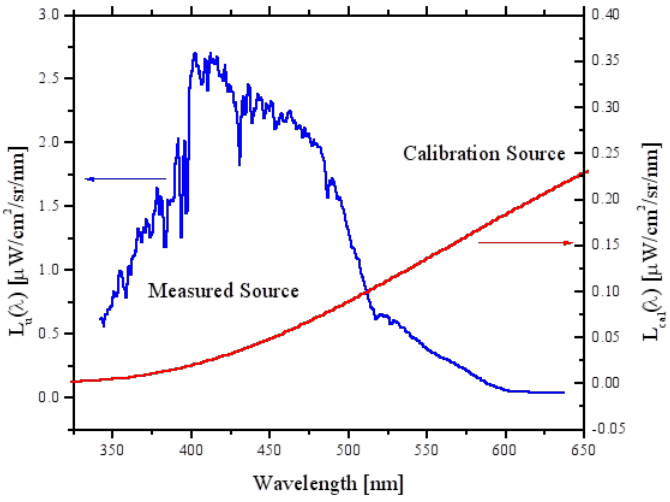

Figure 16. Comparison between the measured (blue) and calibration source (red) at MOBY. From Johnson (2003).

OC-VCAL-RD-25. The *like-to-like* rule shall be followed as much as possible: characterisation/calibration conditions should be as similar as possible to those of the actual measurement in the sea (Johnson et al., 2003). This may require a dedicated calibration facility, such as the Spectral Irradiance and Radiance Responsivity Calibrations with Uniform Sources (SIRCUS; Brown et al., 2000).

OC-VCAL-RU-25. Uncertainties due to conditions violating the *like-to-like* rule shall be introduced in the uncertainty budget. This aspect is probably even more critical when using commercial instruments if manufacturers do not account for environmental sources of uncertainty.

OC-VCAL-RV-25. N/A

4.2. IN SITU PLATFORM

4.2.1. SELF-SHADING AND SUPERSTRUCTURE SHADING

Depending on the design of the radiometer and its deployment system, instrument self-shading and superstructure shading may be a major component of the uncertainty affecting the in situ upwelling radiance. The impact of shading increases towards the red domain and can lead to uncertainties of up to 12% on L_u at 665 nm when uncorrected (MOBY case; Brown et al., 2007). Corrections for self-shading and superstructure shading shall be based on radiative transfer simulations considering accurate modelling of the geometry, illumination angle and optical properties of the water (e.g. Doyle and Zibordi, 2002; Doyle et al., 2003; Mueller, 2007; Vellucci et al., 2014).

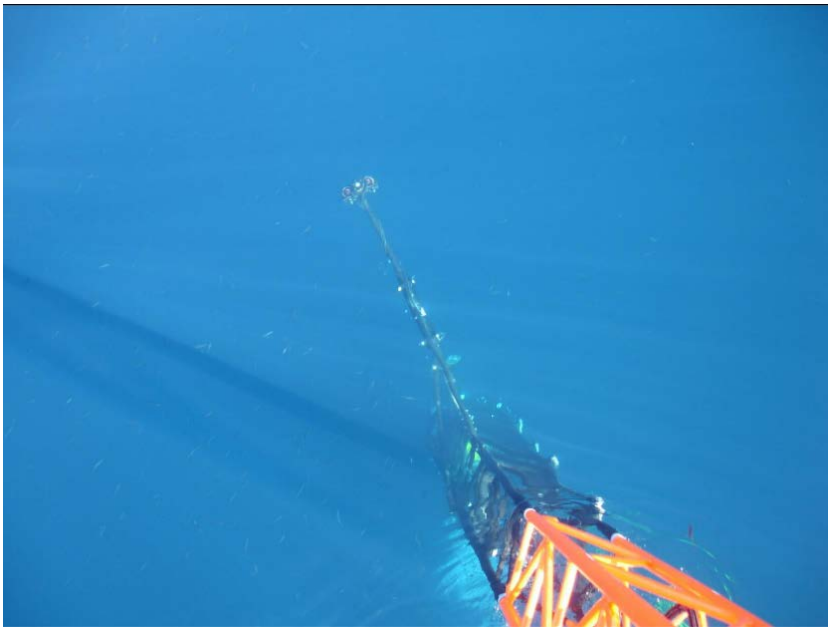

Figure 17. Picture of the shadow of the BOUSSOLE buoy. From Vellucci et al. (2014).

OC-VCAL-RD-26. Instrument self-shading and superstructure shading shall be minimised by design of the radiometer and the platform, and then estimated by accurate radiative transfer modelling to allow correction during deployments.

OC-VCAL-RU-26. Uncertainty of the shading correction shall be kept significantly smaller than the shading error itself which is below 1% in the blue-green bands and below 3% in the red bands.

OC-VCAL-RV-26. Field experiments should empirically validate the radiative transfer simulations to assess the uncertainty in the shading correction.

4.2.2. TILTING

L_u is defined as the upwelling radiance at nadir. As such, if the in-water instrument tilts from nadir, a correction has to be applied to the data for any effect of the tilt or its uncertainty taken into account. The amplitude of tilt depends on the type of platform and environmental conditions. For the example of MOBY, the platform is tethered to a separate mooring buoy, which is fixed to MOBY near

the surface. Thus, MOBY presents very little tilt, as shown in Figure 18 which is a histogram of the MOBY tilt over the full MOBY time series. As can be seen, MOBY tilt is less than 1° for approximately 75% of the measurements, and less than 5° for 96% of the measurements. For field instruments whose tilt significantly impacts the uncertainty budget, a correction for the various resulting effects must be applied, for instance for the shape of the upwelling radiance distribution (BRDF), for the instrument depth, for the shading, etc. In the case of BRDF, the correction depends on relative Sun and instrument geometry, and the optical properties of the water. An example of contour plot of the BRDF correction is shown in Figure 19. As can be seen, for angles less than 1°, the correction is negligible, but by 2° this correction can be as large as 1 %. This example is for waters representative of the MOBY site (Chl = 0.1 mg m^{-3}), 20° solar zenith angle, and 620 nm. The uncertainty of the correction will depend on how large a correction is required, how well the optical properties of the water are known, and how well the BRDF has been modelled with these optical properties and geometry.

OC-VCAL-RD-27. Instrument tilt shall be minimised through the design of the SVC instrument and platform. Accurate tilt/roll measurements shall be performed during the optical measurements.

OC-VCAL-RU-27. For measurements acquired under a significant tilt, the residual uncertainties after tilt corrections (e.g. BRDF correction) must be assessed and held to a level not significantly impacting the overall uncertainty budget (e.g. less than 0.3%).

OC-VCAL-RV-27. Field experiments should empirically validate the tilt corrections (e.g. modelled BRDF correction) at the site.

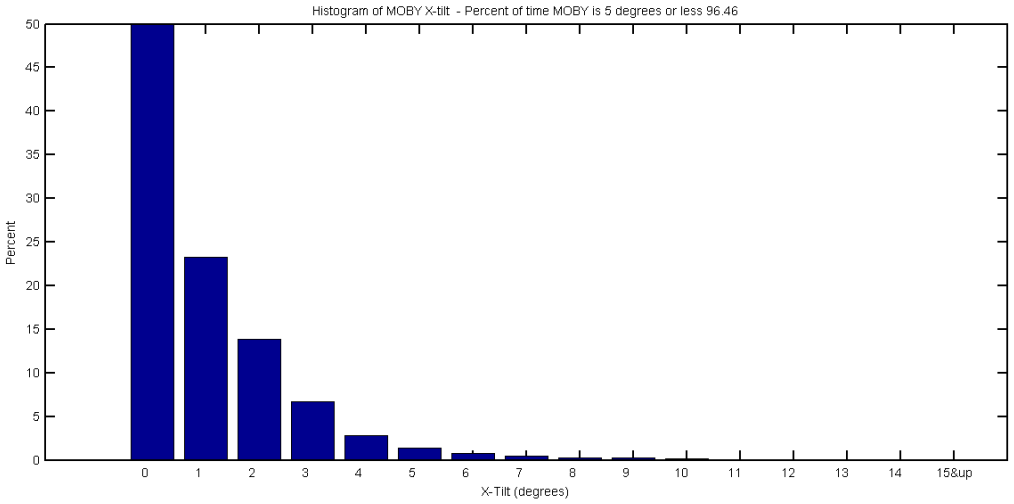

Figure 18. Histogram of MOBY tilt angles over the full MOBY time series. This histogram is for tilt in MOBY's x axis, it is identical to the tilt in the y-axis.

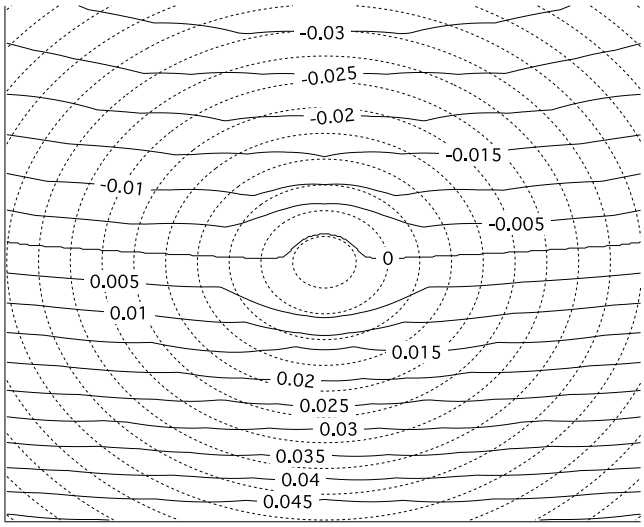

Figure 19. Contour plot of % BRDF correction for a given tilt and azimuth relative to the sun. Each circle represents a 1° change in nadir angle. This example is for clear waters, representative of the MOBY site, 620 nm (the change is more significant at the red wavelengths) and a solar zenith angle of 20°.

4.3. RADIANCE COMPUTATION

4.3.1. MEASUREMENT EQUATION

Underwater instruments on mooring acquire radiometric measurements at several depths and require an extrapolation of the upper most measurement to just below the surface ($z = 0^-$), followed by a propagation of the signal through the water-air interface. The first step generally relies on the exponential decay of the upwelling radiance with depth:

$$L_u(\lambda, 0^-) = L_u(\lambda, z) e^{K_L(\lambda,0,z)z} \tag{30}$$

in which the diffuse attenuation coefficient between two depths z_1 and z_2, is defined as:

$$K_L(\lambda, z_1, z_2) = -\frac{\ln\left(\frac{L_u(\lambda, z_2)}{L_u(\lambda, z_1)}\right)}{z_2 - z_1} \tag{31}$$

A compromise in the measurement depths must be done, as small depths reduce uncertainty in the propagation but induce other sources of uncertainty due to the sea surface state (wave focusing, possibly shading depending on the platform). The BOUSSOLE buoy has two instrumented arms at 4 m and 9 m while MOBY has three arms at 1 m, 5 m and 9 m. Using $K_L(\lambda, z_1, z_2)$ to propagate the upwelling radiance from the shallowest depth to $z = 0^-$ implicitly assumes that the diffuse attenuation is constant in the water column. This extrapolation is typically robust in the blue bands but starts to be wrong from 550 nm with growing error in the red because of the inelastic scattering due to Raman scattering and chlorophyll fluorescence, even in a homogenous medium (Antoine et al., 2008; Voss et al., 2017). A correction on Eqs. (30)-(31) is necessary, either directly on $L_u(\lambda, 0^-)$

(Antoine et al., 2008) or on K_L (Voss et al., 2017), both solutions being based on radiative transfer modelling including Raman scattering and chlorophyll fluorescence (MOBY) or Raman scattering only (BOUSSOLE).

For any wavelength, here omitted for the sake of brevity, the uncertainty of $L_u(0^-)$ does not only depend on the uncertainty of the primary measurement at depth z, $u(L_u(z))$, but also on the uncertainty on K_L, $u(K_L)$, multiplied by the depth:

$$\left(\frac{u(L_u(0^-))}{L_u(0^-)}\right)^2 = \left(\frac{u(L_u(z))}{L_u(z)}\right)^2 + \left(z * u(K_L)\right)^2 \quad (32)$$

Note that the uncertainty due to the depth of the arms varying with the tilt should be added.

For instance, a relative uncertainty for L_u of 1.5% at one meter depth propagates to about 1.8% below the surface when $u(K_L)$ is kept as low as 0.01 m^{-1} as in Voss et al. (2017) (most critical case in the red, above 650 nm). However, propagating from 4 m depth would increase the uncertainty up to 4%.

OC-VCAL-RD-28. Depths of measurements shall be optimised to limit the uncertainty due to the surface effect and the depth extrapolation. The exponential extrapolation shall be systematically corrected for the inelastic scattering at wavelengths above 550 nm, based on radiative transfer simulation.

OC-VCAL-RU-28. The uncertainty due to the depth extrapolation shall be rigorously derived following Eq. (32). For a one meter depth extrapolation, the uncertainty on K_L shall be of the order of 0.01 m^{-1}.

OC-VCAL-RV-28. Verification of the depth extrapolation, its correction and uncertainty shall be assessed at the SVC site using profile measurements (see e.g. Voss et al. 2017); note that it is not recommended to use any concurrent above-water measurements.

The second step consists in propagating the upwelling radiance through the water-air interface:

$$L_w^{IS}(\lambda, \theta_s^t, \theta_v^t, \Delta\varphi^t) = \frac{T_f(ws, \theta_p^t)}{n^2(\lambda, T, S)} L_u(\lambda, 0^-) \quad (33)$$

where $(\theta_s^t, \theta_v^t, \Delta\varphi^t)$ corresponds to the illumination and viewing geometry of the measurement, T_f is the Fresnel transmission through the water-air interface, depending on the wind speed ws, the refracted viewing angle in the water θ_p^t, and the refraction index of seawater n. Values of T_f/n^2 depends on the wavelength, as well as on the temperature (T) and salinity (S) (Voss and Flora, 2017). Uncertainty on these coefficients is often considered as negligible, but must still be justified. For instance a difference in the refractive index at MOBY between 1.34334 (S=40 ppt and T=25°) and 1.34017 (S=30 ppt and T=35°) represents a relative uncertainty of 0.23%, directly transferred on L_w. For SVC purposes, the spectral variation of T_f/n^2 should be included in the calculation.

OC-VCAL-RD-29. Choice of T_f and n shall be justified according to the physical condition at the SVC site. The spectral variation of T_f and n should be included in the calculation of L_w^{IS}.

OC-VCAL-RU-29. Document uncertainty on T_f and n.

OC-VCAL-RV-29. Measure the range of salinity and temperature at the SVC site.

4.3.2. SAMPLING STRATEGY AND DATA REDUCTION

Data reduction consists in producing one representative value of the radiometry measured during a given acquisition time, at a given rate. Statistical filtering removes outliers and fluctuations in the radiometry, due to wave focusing.

OC-VCAL-RD-30. Measurements should be performed over intervals of a few minutes. The variability of the signal due to e.g. wave focusing shall be reduced by filtering over the acquisition time (e.g. by taking the mean or the median). It is recommended to program the in situ acquisition according to the satellite acquisition time over the SVC site (note here that several satellites may be considered, hence scheduling several acquisition times). Regular measurements during the day (e.g. every 15 minutes) are required to assess the temporal variability at the SVC site and to help for QC; more frequent measurements at the time of the satellite overpass (within one hour) may be an indicator of small scale spatial variability.

OC-VCAL-RU-30. Uncertainty of the data reduction shall be assessed by the variability of the measurement during the measurement period, e.g. one standard-deviation. Zibordi and Voss (2014a) reports, after Zibordi et al. (2009), an average coefficient of variation of L_w^{IS} between about 2% and 3% from 443 to 665 nm due to wave perturbations, changes in illumination and marine optical properties.

OC-VCAL-RV-30. N/A

4.4. CHARACTERISATION OF MARINE OPTICAL PROPERTIES

4.4.1. INHERENT OPTICAL PROPERTIES

Further to radiometric measurements, it is necessary to characterise the site in terms of marine IOPs in order to properly handle the various corrections that yield the targeted water-leaving radiance. For instance, absorption should be measured to enable a shading correction. Stratification shall also be characterised (temperature versus depth). The required measurements to support the BRDF correction are detailed separately in section 4.4.2 hereafter. Measurement of backscattering and scattering coefficient, with chlorophyll, would help in the case that alternative ACs are considered in the SVC.

A good example is provided by the BOUSSOLE project, which complements the mooring system by monthly cruises of several consecutive days. Instruments deployed are a CTD plus an “inherent optical properties package”, which includes a 4-band transmissometer (Hobilabs Gamma-4), a

hyperspectral absorption-meter (Hobilabs A-sphere) and a 6-band backscattering meter also equipped with a CDOM fluorometer and a chlorophyll fluorometer (HobiLabs Hydroscat-6). Seawater samples (collected particles on GF/F filters) are also analysed back in the laboratory by HPLC for phytoplankton pigments and by spectrophotometry for particulate absorption, and filtered samples are used for measurement of the CDOM absorption. Vertical profiles of radiometric quantities (Eu and Ed plus surface reference) are also collected with a Biospherical C-OPS profiling radiometer, in order to complement the surface-only radiometry from the BOUSSOLE buoy.

OC-VCAL-RD-31. For underwater systems, the bio-optical conditions at the SVC site shall be characterised, at least in terms of chlorophyll concentration. Absorption shall be measured to enable a shading correction.

OC-VCAL-RU-31. Uncertainty on IOPs affecting the L_w^{IS} measurement and correction shall be assessed (e.g. Chlorophyll or diffuse attenuation coefficient for depth extrapolation and BRDF correction).

OC-VCAL-RV-31. Models using IOPs should be validated.

4.4.2. BIDIRECTIONAL REFLECTANCE DISTRIBUTION FUNCTION (BRDF)

In the context of SVC, the in situ water-leaving radiance measured at nadir must be related to the geometry of the satellite acquisition. Ideally, the directional radiance should be measured with a fish-eye camera to get, for every match-up, the radiance field for the whole hemisphere. In practice, it is much easier to rely on a single directional measurement and a BRDF model, however this requires knowledge of the marine IOPs (e.g. Morel et al., 2002, for Case-1 waters) and induces supplementary uncertainty.

OC-VCAL-RD-32. When implementing a BRDF correction, the marine IOPs at the SVC site shall be characterised, namely the particle scattering phase function, and the absorption and scattering coefficients. Identification of the IOPs for every match-up shall be justified based on this characterisation, either through direct measurements, radiance field inversion or climatological data (in the case of a stable site).

OC-VCAL-RU-32. Uncertainty of the BRDF correction of the in situ upwelling radiance shall be assessed (e.g. Monte-Carlo approach on input angles and chlorophyll concentration).

OC-VCAL-RV-32. Validation of the BRDF correction shall be based on the comparison between BRDF model and radiance distribution measurements (e.g. Voss et al., 2007; Gleason et al., 2012). Examples of existing systems are NURADS from University of Miami (Voss and Chapin, 2005) and the CE600 from LOV (Antoine et al., 2013).

4.5. ATMOSPHERIC MEASUREMENTS

4.5.1. SURFACE IRRADIANCE

The in situ surface spectral irradiance E_d^{IS} is required to determine clarity of the sky during the marine measurements. When it is too different from the theoretical clear-sky value (e.g. Gregg and Carder, 1990), the match-up shall be discarded (see section 5.2.3).

On the other hand, measurement of E_d^{IS} is not strictly required in the gain computation when SVC is formalised in terms of water-leaving radiance. It is not used for instance in the NASA (Franz et al., 2007) or ESA processing (Lerebourg et al., 2011); in this case, marine reflectance, should it be required, is simply computed by using the theoretical E_d of the Level-2 processor. An alternative is to formulate SVC in reflectance, i.e. to adjust the spaceborne sensor on the in-situ remote-sensing reflectance:

$$R_{RS}^{IS} = L_w^{IS}/E_d^{IS} \tag{34}$$

This may be of interest when the time difference between the ground and satellite acquisitions are significantly different; a temporal scaling of L_w^{IS} can then be applied through $L_w^{IS}/E_d^{IS} * E_d$. However this requires measurement of E_d^{IS} at the very same spectral resolution as L_w^{IS}, and may introduce new uncertainties.

OC-VCAL-RD-33. The in situ surface spectral irradiance E_d^{IS} shall be measured at all VIS bands to assess the sky clarity and detect clouds or even sub-pixel clouds possibly not well identified by the satellite data. In this respect, it helps only for a quality control (QC) in the SVC process. When the SVC is formalised in terms of R_{RS}^{IS}, see Eq. 34, E_d^{IS} shall be measured concurrently with L_w^{IS}, at the same spectral bands and resolution.

OC-VCAL-RU-33. Any use of E_d^{IS} in the gain computation (through R_{RS}^{IS}) introduces additional uncertainties (e.g. those associated with the cosine response) that shall be described with same quality as those of the in-water radiance sensor. Note that the uncertainty of R_{RS}^{IS} due to the absolute calibration is expected to be lower than the combined uncertainties of L_w^{IS} and E_d^{IS} if the same lamp and facility are used to calibrate the radiance and irradiance sensors (but in any case not lower than that of L_w^{IS} or E_d^{IS} alone).

OC-VCAL-RV-33. N/A

4.5.2. AEROSOL DETERMINATION

The SVC approach requires very clear maritime atmosphere (low loading in aerosol) to minimise the uncertainty of the AC (aerosol retrieval). This shall be ensured by the site location and data screening in the match-up process. Furthermore it should be remembered that SVC does not use in situ aerosol measurements in the gain computation. Hence, it is not required to have continuous measurements of atmospheric vertical profile (such as with a LIDAR, that would require a substantial effort). Effort should be put on the atmospheric characterisation of the SVC site. This characterisation may also support SVC in the NIR bands, if it is done at the same site. During operation, a regular monitoring,

can be done during monthly cruises; in the example of BOUSSOLE, measurements of the spectral AOT are performed with a handheld sun photometer (CIMEL CE-317 model) when the sun is in direct sight.

OC-VCAL-RD-34. The selection of the site shall be based on climatological datasets derived by a dedicated space mission for aerosol detection and atmosphere sounding, and based on aerosol field measurements, either from an existing LIDAR or AERONET station or specifically dedicated to the SVC selection. OC missions shall not be used as they might be biased and furthermore do not measure Sun extinction (AOT) but apparent optical properties of aerosols (combination of AOT, SSA and APF). During an SVC operation, it is only required to have monthly measurements of spectral AOT in the proximity of the location (for instance during the cruises), e.g. with Microtops (Morys et al., 2001). Additional measurements with more advanced systems, like micro-LIDAR on buoy (e.g. Mariage et al., 2017), could help in the data screening but are not strictly required.

OC-VCAL-RU-34. Uncertainty of this atmospheric characterisation does not directly impact the uncertainty of the SVC gains but directly impacts the total uncertainty budget of the site. We refer to section 3.5 for the uncertainty of atmospheric scattering functions used in the AC algorithm.

OC-VCAL-RV-34. N/A

4.6. OTHER ENVIRONMENTAL CONDITIONS

4.6.1. SPATIAL HOMOGENEITY

A high spatial homogeneity at the SVC site is required so that the point in situ measurement can be consistently compared to the satellite larger footprint acquisition. Obviously this criterion affects the choice of the water types, with oligotrophic waters minimising spatial variability. Spatial variability has been assessed at the BOUSSOLE site by fluorescence measurement (calibrated to chlorophyll HPLC) on a grid of about 2 km around the buoy (Antoine et al., 2008). This variability is linked to the temporal variability at the site and is around 10% in summer (oligotrophic), about 30% in winter and up to 70% in spring (blooms with horizontal gradients) in terms of chlorophyll concentration, in log scale. This variability shall be transferred to Lw uncertainty. At MOBY, an assessment during the Spectral Ocean Radiance Transfer Investigation Experiment (SORTIE ; Voss et al., 2010), suggests a spatial variability of less than 5% on water-leaving radiance over a 6 x 6 km^2 area around the buoy (affected also partially by diurnal variation).

OC-VCAL-RD-35. Spatial variability of geophysical parameters at the SVC site shall be minimised in order to avoid uncertainty at sub-pixel and macro-pixel scale. Assessment of this variability using high spatial resolution spaceborne sensors is not favoured because of their inherent noise. In situ characterisation of the site should be preferred. In parallel, short-term temporal variability (within one hour) measured at the site can be used as an indicator of spatial variability.

OC-VCAL-RU-35. Uncertainty due to spatial variability can be related to the coefficient of variation (C_v) in the match-up protocols (see section 5.2).

OC-VCAL-RV-35. N/A

4.6.2. TEMPORAL STABILITY

High stability is a fundamental requirement for SVC supporting climate change investigations (Zibordi and Mélin, 2017). Temporal stability is required for the period between the in-situ measurement and the satellite overpass: high stability ensures that the measured water-leaving radiance is a good representation of the satellite pixel footprint at the time of observation. This factor is also related to the spatial homogeneity, as a site that is spatially homogeneous, will likely also exhibit sufficient temporal stability for the near simultaneous SVC process.

OC-VCAL-RD-36. Temporal stability of the atmospheric and marine conditions at the SVC site are required as much as possible to minimise uncertainty in the SVC gains. Also, they are strongly recommended to ease the QC analysis of the data.

OC-VCAL-RU-36. Temporal stability of the atmospheric and marine conditions shall be taken into account everywhere in the uncertainty budget of the gain computation, for instance by a Monte-Carlo approach; this refers notably to the BRDF correction, the depth-extrapolation, the temporal interpolation at the time of satellite overpass, the atmosphere characterisation, etc.

OC-VCAL-RV-36. Temporal stability of the SVC gains shall be analysed with respect to temporal and spatial variability of the atmospheric and marine conditions.

4.6.3. WEATHER AND PHYSICAL CONDITIONS

Ensuring low cloudiness is an obvious requirement to maximise the number of useful satellite acquisitions in the SVC process (see e.g. Zibordi and Mélin, 2017, for a recent assessment of clear sky conditions over various potential sites). Regarding the atmosphere, legacy requirements from Gordon (1998) indicates very clear atmosphere (AOT lower than 0.1 in the visible) with non-absorbing maritime aerosols; this may be refined according to the actual uncertainty budget of the atmospheric scattering functions, as described in section 3.5.

Moderate wind speed at sea level limits the formation of whitecaps as well as probability of Sun glint occurrence due to the surface roughness. Requirements on the ocean current depend on the platform design: for instance the BOUSSOLE buoy is located near the centre of a cyclonic circulation that characterises the Ligurian Sea (Antoine et al. 2006), with current < 20 cm/s limiting systematic tilt.

OC-VCAL-RD-37. The SVC site shall be located in a region minimising cloud coverage, with very clear and stable maritime atmosphere (in particular not impacted by absorbing aerosols) and low wind speed. Depending on the platform design, fixed mooring may have to be located in a zone with weak ocean currents to limit systematic tilting (example of BOUSSOLE).

OC-VCAL-RU-37. Uncertainty due to each environmental factor shall be assessed, see e.g. OC-VCAL-RU-12 for uncertainty due to the atmospheric component and OC-VCAL-RU-27 for uncertainty due to tilt. Data screening in the match-up process shall also reduce these uncertainties but, also, the number of matchups, see section 5.2.

OC-VCAL-RV-37. N/A

4.6.4. EXTERNAL CONTAMINATION (LAND, DEPTH)

Presence of land surface in the vicinity of the SVC site may induce adjacency effect in the satellite data, i.e. the contamination of the ocean radiometry by surrounding land pixels through the scattering in the atmosphere, as well as the loss of the marine signal that would exist without land (Santer and Schmechtig 2000). This effect depends on the brightness and distance of the land surface, on the viewing and illumination geometry, and on the aerosol properties of the atmosphere. Avoidance of adjacency effects shall be ensured by locating the SVC site sufficiently far from the coast. Accurate estimates of the radiometric contamination are achievable with three-dimensional radiative transfer simulations (Bulgarelli et al. 2014), to possibly correct it but the residual uncertainty needs to be added to the total SVC budget.

Another source of contamination of the water-leaving radiance may be the light reflected from the sea bottom. This is particularly critical for very clear waters, as targeted by SVC. Hence deep waters (depth larger than 1000 m) are required.

Both BOUSSOLE, located about 59 km from the shore with a water depth of about 2400 m, and MOBY, located 20 km from Lanai's coast in 1200 m of water, are safe from these sources of contamination.

OC-VCAL-RD-38. The SVC site shall be located far enough from land to avoid adjacency effect, as well as in deep waters to avoid the effect of the sea bottom.

OC-VCAL-RU-38. When the previous requirement is not met, the residual uncertainties on the adjacency correction (for satellite data) and bottom correction (both satellite and in situ data) shall be assessed and added to the overall SVC uncertainty budget thanks to accurate radiatrive transfer modelling.

OC-VCAL-RV-38. N/A

4.6.5. ILLUMINATION ANGLE

The illumination angle, defined by the latitude of the calibration site and the time of observation, has various effects on the SVC process. First, a large range of solar zenith angle induces a wide range of variability in the atmospheric path radiance, and may help to investigate the effects of illumination conditions on the gains. However, growing solar zenith angles generally decrease the performance of the AC, especially when they are beyond 70° and need to account for atmospheric sphericity in the RTM. This induces a larger uncertainty in the SVC gains, with possible systematic differences between targets illuminated from different angles. Those angles are typically excluded from the SVC

matchups. From the in situ point of view, larger solar zenith angles can also cause more uncertainty in the downwelling irradiance measurements due to tilt and cosine collector imperfections, as well as in the BRDF correction. On the other hand, it should be acknowledged that extremely small solar zenith angles may cause problems with instrument self-shading.

OC-VCAL-RD-39. Care shall be taken on the range of the illumination angles at the SVC site during the year, as too large angles may induce systematic uncertainty in the AC and the SVC gain computation, and extremely small angles may induce instrument self-shading.

OC-VCAL-RU-39. Uncertainties related to the solar zenith angle shall be assessed, on both the satellite (AC) and in situ sides.

OC-VCAL-RV-39. Variability of the individual gains with respect to the zenith solar angle shall be monitored in order to detect any trends and possibly screen data for some geometrical conditions.

5. REQUIREMENTS ON THE SVC DATA PROCESSING

5.1. IN SITU DATA POST-PROCESSING

5.1.1. QUALITY CONTROL

The in situ data processing, from raw counts to calibrated water-leaving radiance L_w^{IS}, needs to be completed by a Quality Control (QC) step, whose goal is to ensure consistency of each measurement and appropriateness for vicarious calibration. Dubious data resulting from any instrument failure or environmental factor (bio-fouling, cloud coverage, etc.) shall be detected by inspecting the time-series of raw data, processed data, and derived quantities such as the diffuse attenuation coefficient. The QC shall also rely on ancillary data and justified thresholds, when environmental conditions are known to increase the uncertainty in L_w^{IS} (e.g. the tilt angle should be lower than 10° at BOUSSOLE, Antoine et al., 2008). To screen out overcast sky conditions, comparison between the measured E_d^{IS} at 443 nm and the theoretical clear-sky value (Gregg and Carder, 1990) can be limited to within +/- 10%. More detailed radiometric QC protocols can be found in Mueller (2003) and specifically in Kuwahara et al. (2003) for moored buoys.

OC-VCAL-RD-40. The data processing and the QC shall be a combination of automated routine and visual inspection to ensure highest quality. Both approaches are required for SVC data. This includes inspection of time-series, from raw counts to processed data, to detect any anomalous daily measurement. Ancillary data shall be continuously recorded (e.g. sea surface state, sky condition) to select optimal data for SVC.

OC-VCAL-RU-40. Uncertainty of the provided L_w^{IS} shall be computed after the QC. When several levels of the QC and data quality are provided, several levels of uncertainty shall be also provided.

OC-VCAL-RV-40. N/A

5.1.2. SPECTRAL INTEGRATION

We refer to section 4.1.1.2 where the spectral integration has been introduced.

OC-VCAL-RD-41. The in situ water-leaving radiance needs to be spectrally integrated against the SRF of the spaceborne sensor as in Eq. (28). When the surface irradiance E_d^{IS} is used in the SVC process, it shall also be integrated similarly.

OC-VCAL-RU-41. As per OC-VCAL-RU-14.

OC-VCAL-RV-41. N/A

5.1.3. NORMALISATION

For being ingested in the gain computation, the in situ radiance L_w^{IS} has to be normalised. In a SVC approach, the normalisation process shall be the same as that used in the processing algorithm for satellite radiance.

OC-VCAL-RD-42. The in situ water-leaving radiance shall be fully normalized, i.e. including the BRDF effects (Morel et al., 2002). This means that Eq. (12) shall be applied to get L_{wN}^t, importantly by taking the solar zenith angle at time of the in situ measurement for $t_{g,down}^{IS}$, t_{down}^{IS}, μ_s^{IS} and C_Q^{IS}.

OC-VCAL-RU-42. As per OC-VCAL-RU-32.

OC-VCAL-RV-42. N/A

5.1.4. RADIANCE TO REFLECTANCE CONVERSION

For methodological reason, the Level-2 processor may require the computation of SVC gains in terms of reflectance ratio (MERIS case, Lerebourg et al., 2011). This does not preclude, however, to calibrate the sensor in the radiance unit, as discussed in section 3.3.1 and in requirement OC-VCAL-RD-6. In such a case, the fully-normalised targeted marine reflectance shall be computed by:

$$\rho_{wN}^t(\lambda_i) = \frac{L_{wN}^t(\lambda_i)}{F_0(\lambda_i)} \tag{35}$$

5.2. MATCH-UP PROTOCOLS

A match-up consists in the extraction of concurrent satellite data and the in situ measurements. In this process, protocols shall ensure the maximum comparability between ground and space acquisition.

5.2.1. TIME DIFFERENCE

OC-VCAL-RD-43. When the in situ acquisition is not programmed to exactly match the satellite overpass (see OC-VCAL-RD-30), the difference in time between ground and space acquisitions (Δt) shall be minimised. The exact threshold depends on the temporal variability at the site and can be optimised considering the various measurements during the day. Over a clear homogeneous water mass, a baseline is Δt=+/- 3 hours (Bailey and Werdell, 2006).

OC-VCAL-RU-43. Uncertainty due to any temporal mismatch between the satellite and in situ measurements shall be included in the targeted L_{wN}^t (for instance standard-deviation during (Δt).

OC-VCAL-RV-43. N/A

5.2.2. SIZE OF MACRO-PIXEL

OC-VCAL-RD-44. The size of the box around the in situ location shall be computed in number of pixels, and not in km, in order to minimise the satellite radiometric noise. For OC sensors such as SeaWiFS (in native 1.1 km resolution), and over homogeneous oceanographic target, a statistically reliable size is 5 x 5 pixels (Bailey and Werdell 2006, Franz et al., 2007). For mission with lower SNR (e.g. ESA/S2), the number of pixels can be chosen to increase SNR to a comparable level of reference mission (e.g. S3/OLCI). This size relates to the pixels where individual SVC gains are computed; data extraction and screening over a larger box may be required, see OC-VCAL-RD-45.

OC-VCAL-RU-44. Variability of individual SVC gains computed in the macro-pixel relates to various effects such as actual geophysical heterogeneity, radiometric noise, uncertainty propagation by the AC, etc. This variability is generally not transferred to the SVC uncertainty budget but shall be inspected to simply accept or discard the match-up. After data screening (see section 5.2.3), spatial homogeneity shall be assessed through the coefficient of variation C_v in the macro-pixel (ratio between standard-deviation and mean) of the satellite L_w; this quantity incorporates the effect of sensor noise and AC. Values of C_v higher than about 0.15 (after a preliminary filtering, Bailey and Werdell, 2006) or 0.2 (directly on the 5 x 5 pixels, Zibordi and Mélin, 2017) require exclusion of the match-up.

OC-VCAL-RV-44. The distribution of pixel-by-pixel gains in the macro-pixel shall be analysed to validate the choice of its size and relevance of the statistical filtering.

5.2.3. DATA SCREENING

Data screening for SVC shall follow the protocols for validation of OC satellite data (e.g. Bailey and Werdell, 2006), with however more stringent criteria. For instance, Franz et al. (2007) discard the match-up as soon as any pixel is flagged by either a navigation problem, or a contamination issue (land, cloud, cloud shadow, stray light) or a Level-2 problem (atmospheric correction failure). For OLCI, the question of duplicated detectors shall also be considered, as the duplicated radiometry within the macro-pixel affects artificially the statistics.

Match-ups contaminated by whitecaps and Sun glint shall also be discarded. For medium resolution sensor, Sun glint is generally directly flagged in the Level-2 processor through a wave slope distribution model (Cox and Munk, 1954) and the knowledge of the wind speed just above sea level. It should be noted that it cannot be processed by the usual way with high resolution data (S2/MSI): the effect of sea surface roughness (swell, wave-height) induces strong variability in the radiometric field between adjacent pixels. This is an open issue which needs further investigation.

Because aerosols can be transported over very long distance, it is required to carefully screen-out the atmosphere for the dusts; when the information is not available from ancillary data, the aerosol model detected by the OC sensor shall be used (e.g. using the absorbing aerosol flag).

The existing SVC protocols, also remove any macro-pixels with mean chlorophyll concentrations above 0.2 mg /m^3, and the retrieved AOTs in the NIR greater than 0.15 (Franz et al., 2007). The protocols also constrain the viewing geometry to below 56° zenith angle, and solar geometry to below 70° zenith. They require all pixels in the macro-pixel box to pass these criteria.

OC-VCAL-RD-45. SVC requires a severe data screening to ensure the best consistency between the sea-truth and satellite observations. This screening shall consider the Level-1 flags (navigation problem, saturation, dead pixel, duplicated pixel…), the Level-2 flags relevant for OCR (adjacency contamination, cloud, cloud shadow, haze, Sun glint, atmospheric correction failure, absorbing aerosol …) and ancillary data (e.g. threshold on wind speed to limit whitecaps). Thresholds on chlorophyll concentration, AOT, observation geometry are also required. All pixels in the macro-pixel need to meet these criteria.

OC-VCAL-RU-45. Varying the thresholds and criteria of the data screening may be used to increase confidence in the representativeness of the match-up (Feng et al. 2009).

OC-VCAL-RV-45. N/A

5.3. VICARIOUS GAINS COMPUTATION

5.3.1. INDIVIDUAL GAINS

Computation of pixel-by-pixel SVC gains and of their associated uncertainties shall follow the methodology already introduced in sections 1.5 and 2.3, respectively. Provision of an individual gain per match-up is a matter of statistical averaging. Franz et al. (2007) have used the mean of the semi-interquartile range (MSIQR) to remove the effect of outliers in the macro-pixel. This filtering can be completed by considering the actual uncertainty of each single gain.

OC-VCAL-RD-46. Individual gains at pixel level shall be computed following Eqs. (11)-(13)-(15). Computation of a unique gain per match-up shall result from statistical averaging and filtering, like a MSIQR, and possibly by considering the uncertainty at pixel level.

OC-VCAL-RU-46. Uncertainty of the individual gains, per pixel, shall be computed as Eq. (26). Uncertainty at match-up level can be deduced using the same averaging as that of the gain values. This computation shall distinguish the systematic and random components of the uncertainty.

OC-VCAL-RV-46. Verification of individual gain, at pixel level, shall follow requirement OC-VCAL-RV-8.

5.3.2. NUMBER OF MATCH-UPS AND MISSION AVERAGE GAIN

The required number of match-ups is determined by the convergence of the individual gain time-series towards a stabilised value (Franz et al., 2007). In the past, at least one year of observation has been necessary to obtain valid gains (IOCCG, 2012), and even between two and three years for SeaWiFS at MOBY (Franz et al., 2007). NASA is now targeting to derive gain in the first year of operation, with the uncertainties lower than what has been achieved previously (NASA, 2014).

The mission-averaged gain $\bar{g}$ may be computed in different ways, according to the weights assigned in Eq. (23), and depending on the intended impact of SVC. In general, a simple arithmetic average is used ($w = 1$), after outliers removal (e.g. MSIQR). But summing Eq. (16) over all match-ups shows

that other weightings are more appropriate to remove the systematic bias. A first choice is to remove the bias in absolute value:

$$\sum_{n=1}^{N} L_w^{\overline{cal}} - L_w^t = 0 \Leftrightarrow \bar{g} = \frac{\sum_{n=1}^{N} \frac{L_t}{t_g t_{up}} g}{\sum_{n=1}^{N} \frac{L_t}{t_g t_{up}}} \tag{36}$$

Another choice consists in removing the bias in relative value:

$$\sum_{n=1}^{N} \frac{L_w^{\overline{cal}} - L_w^t}{L_w^t} = 0 \Leftrightarrow \bar{g} = \frac{\sum_{n=1}^{N} \frac{L_t}{t_g t_{up} L_w^t} g}{\sum_{n=1}^{N} \frac{L_t}{t_g t_{up L_w^t}}} = \frac{\sum_{n=1}^{N} \frac{L_t}{t_g t \mu_s C_s C_Q^t L_{wN}^t} g}{\sum_{n=1}^{N} \frac{L_t}{t_g t \mu_s C_s C_Q^t L_{wN}^t}} \tag{37}$$

Alternatively, it may be relevant to account for the uncertainty of the individual gain in the averaging by:

$$\bar{g} = \frac{\sum_{n=1}^{N} \frac{1}{u(g)} g}{\sum_{n=1}^{N} \frac{1}{u(g)}} \tag{38}$$

Where $u(g)$ is defined in Eq. (26). An interesting feature of the last formulation is that, when the relative uncertainty of the in situ measurement is identical for all match-ups (i.e. when $u(L_{wN}^t)/L_{wN}^t$ and $u(C_Q^t)/C_Q^t$ are assumed to be fixed), it simplifies exactly to Eq. (37), so that it amounts to removing the bias in relative value.

OC-VCAL-RD-47. For climate applications, maximising the number of high-quality match-ups is a general requirement which shall drive the selection of the SVC site (see e.g. Zibordi et al., 2015; Zibordi and Mélin, 2017). The required number of match-ups shall be determined by taking into account the real uncertainty in the vicarious gains at match-up level and the averaging process; for instance, with a constant uncertainty of 3.5% on individual gains, assumed to be random, 50 match-ups are necessary to reach a 0.5% uncertainty on the mission average gain - importantly, systematic uncertainty (bias) does not cancel out when adding more match-ups and shall be rigorously considered. The required number of satellite observations to produce these high quality match-up depends strongly on the SVC site(s) (cloud coverage, glint perturbation, spatial homogeneity, etc.) and shall be assessed by climatological study on past archive (see Zibordi and Mélin, 2017). A more ambitious target is to derive the mission average gain in the first year of operation; however, climate-oriented applications generally need longer time-series, so that in practice match-up criteria can be relaxed in the early phase of mission for providing a tentative SVC, to be consolidated after a longer period; alternatively marine reflectance models applied over stable oceanographic regions may be used for such a purpose (e.g. Werdell et al., 2007). Last, the averaging process shall minimise the effects of outliers and correspond to the desired effect of SVC, e.g. for removing the systematic bias in absolute or relative value.

OC-VCAL-RU-47. Statistical tests (like χ^2 test) shall be implemented to demonstrate the relevance of the averaging. For climate-oriented applications, stabilisation of the mission average gain shall be within 0.1%. The uncertainty of the mission average gain shall be computed as in Eq. (24).

OC-VCAL-RV-47. N/A

6. REQUIREMENTS ON THE SVC OPERATION AND SERVICE

6.1. FIELD OPERATIONS AND MAINTENANCE

To some extent, the field operations and maintenance are driven by the specific instrument characteristics. For example, if the SVC instrument is a free-floating drifting instrument, it is likely there is no operational requirement for maintenance that can be performed after deployment. So far permanent moorings, such as BOUSSOLE and MOBY, have been considered to be well adapted to provide stable personnel, equipment and methodologies. Hence, the experience of BOUSSOLE and MOBY is here described, to provide guidance on the operational requirements.

6.1.1. RADIOMETER ROTATION

The MOBY protocol has been to have two identical systems available, with each system being alternately deployed at the mooring site with 3 (initially) to 4 (currently) month deployments. Because of logistical considerations, such as only one mooring buoy available, there is no field overlap of the instruments. However, because the Lanai site has very stable optical conditions, the continuity between instruments can be monitored. The MOBY project replaces the mooring buoy on a 2-year rotation.

The BOUSSOLE protocol includes bi-annual rotations of the instrumented buoy (currently closer to 9-12 months) with monthly servicing and science cruises to the site, plus cleaning operations in-between those monthly cruises (so that the frequency of instrument cleaning is close to 15 days). The mooring part of the buoy is replaced on a 3-year rotation cycle.

Ideally, overlap in instrumentation might be desirable, but has been impractical to date because MOBY and BOUSSOLE have one mooring. Thus, only one instrument can be in place at a time. Occasional overlaps happen at MOBY, if the new instrument is deployed on the mooring and the old instrument is being towed by the ship before it is recovered, but this is not a frequent occurrence because of ship-time cost.

OC-VCAL-RD-48. The required frequency of in situ instrument rotation shall be defined for minimising the uncertainty on the L_w^t measurement, depending on the effective marine conditions at the site and instrument performance. According to existing systems and experiences, a 4 to 6 months (maximum) deployment is recommended. Too frequent rotations and handling may however induce human operator error. In order to secure the rotation frequency, it is required to have three identical systems; this redundancy can be limited, though, to the strict necessary components. System replacement shall be planned in advance to ensure long-term time series.

OC-VCAL-RU-48. When stable optical conditions are ensured, continuity between deployments shall be monitored; any discontinuity shall be corrected whenever possible, and residual uncertainty transferred to the uncertainty budget.

OC-VCAL-RV-48. N/A

6.1.2. ROUTINE MAINTENANCE

Any instrument left in the field for extended periods will require routine maintenance during the deployment. Bio-fouling on MOBY is decreased both through antifouling paint on all non-optical surfaces, exposed copper near the collectors, and bromine powder in a container next to the collector. There are internal calibration sources (LEDs and incandescent sources) that are used during each data measurement. In addition, diver operations occur monthly to clean the optical surfaces. During these diver operations, a field calibration source is applied to each optical collector. In general the uncertainty of this diver calibration is too large to be useful for more than a tracking measurement. BOUSSOLE follows a similar procedure to limit bio-fouling. The buoy superstructure is coated with an antifouling paint, and the radiometers housings are covered by copper tape. Optical surfaces are cleaned by divers about every two weeks during field operations to the buoy. These measures allow minimising bio-fouling contamination, and are combined with a data screening that allows either correcting for bio-fouling whenever possible (see Figure 20) or eliminating corrupted data if necessary.

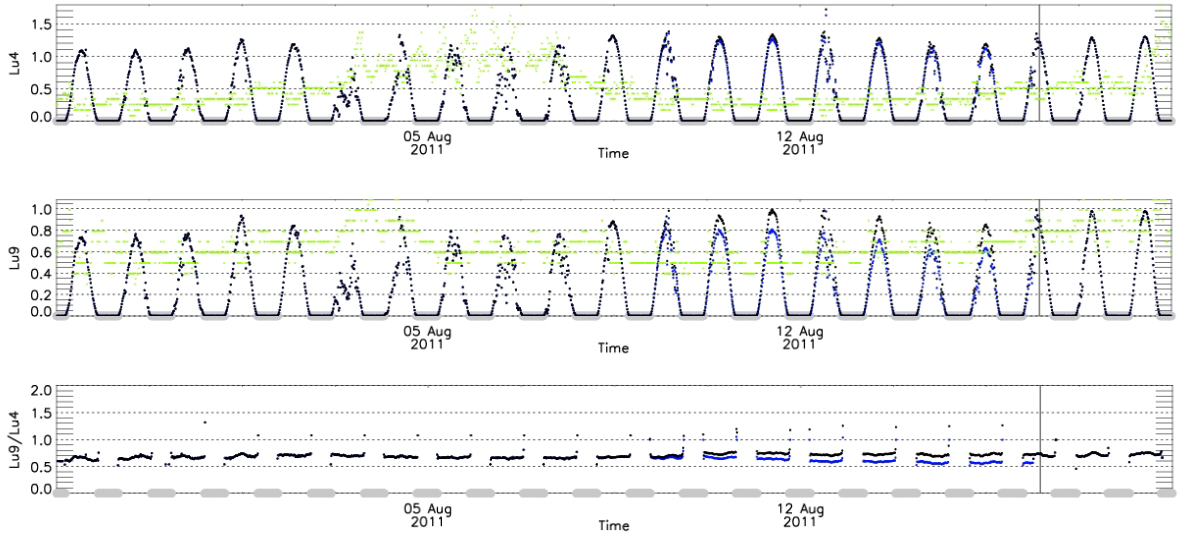

Figure 20. Time-series of BOUSSOLE Lu(412) at 4m depth (top), 9m (middle) and ratio of both (bottom) in August 2011 (blue dots) with associated Chlorophyll-a fluorescence (green dots, relative scale). The black vertical line on the right-hand side corresponds to the day of a diver cleaning. Black dots correspond to the radiometry after correction for bio-fouling (here by matching the values before and after cleaning, and applying an exponential correction starting at the last measurement before cleaning). Grey lines on the time axis indicate nighttime.

This maintenance requires the site to be located near islands or any coastal location that allows keeping transit times to the site below workable limits, which certainly depends on the distance from the coast and the characteristics of available vessels (how much equipment can be embarked, how many staff, and maximum speed). On the other hand, it should be far enough away to avoid adjacency effects and far enough away from casual recreational boating to minimise physical and radiometric perturbation (MOBY lessons learnt).

OC-VCAL-RD-49. To ensure operational activity and favour the routine maintenance, the SVC site shall be located at a reasonable distance from coast and from a laboratory facility, while as much

as possible far away from recreational boating. In-water systems shall limit bio-fouling by the use of antifouling paint and copper around the instrument; new approaches with UV LEDs are also being investigated. The system shall also be cleaned by divers at least on a monthly basis (and more regularly in case of blooms). It is recommended to have available divers for checking the status of the mooring and instrumentation, and possibly document with pictures.

OC-VCAL-RU-49. Uncertainty due to bio-fouling and of any bio-fouling correction shall be assessed.

OC-VCAL-RV-49. Comparison before and after each cleaning shall help to verify the proper data screening or bio-fouling correction.

6.1.3. AUTONOMOUS FIELD OPERATIONS

OC-VCAL-RD-50. The site shall be equipped by an electronic device recording and storing all measured data (optical but also environmental data) and, obviously, the necessary power supply to operate. Data related to the status of the platform (such as pressure, tilt angle, depth, strain of the mooring cable if any, battery voltage, disk space) and status of the radiometer shall be transmitted continuously to the ground station to check the nominal operation of the SVC site. Scientific data used for the SVC itself (radiometry and possibly other measurement) may be transferred at lower rate.

OC-VCAL-RU-50. N/A

OC-VCAL-RV-50. N/A

6.1.4. UNCERTAINTY PROPAGATION

OC-VCAL-RD-51. It is required to analyse measured spectra and provide an uncertainty estimate for each single data measurement.

OC-VCAL-RU-51. N/A

OC-VCAL-RV-51. N/A

6.2. DATA ACCESS AND TIMELINES

6.2.1. DATA ACCESS

OC-VCAL-RD-52. For being traceable, the data shall be publicly and freely available on a website in standard scientific format (e.g. text file or NetCDF), together with the documentation on measurement protocols, field operations and quality level. Data includes the raw data (inputs to the in situ data processing code), the Lw data and history of the radiometric calibration. Automated

graphs of all measured parameters shall be posted on the website. The full processing code of in situ data shall be an open-source community processor available on the web, so that any user can check and recompute Lw. As additional service, Lw and LwN in space instrument SRFs per band shall be made available for the participating space missions.

OC-VCAL-RU-52. N/A

OC-VCAL-RV-52. N/A

6.2.2. DATA QUALITY LEVELS AND VERSIONING

OC-VCAL-RD-53. The different quality levels of data shall be clearly documented, with detailed protocols (e.g. limit on tilt angle, etc.). The exact levels are currently not harmonised among existing systems (e.g. "good", "bad", "questionable" level of MOBY); such harmonisation shall be part of the SVC development in collaboration with international entities (Space Agencies, IOCCG, etc.) and could follow, for instance, the AERONET-OC system (Level-1, 1.5 & 2). A rigorous version management system shall be implemented to keep track of the various processing levels and reprocessing versions (numbering, date, etc.).

OC-VCAL-RU-53. Different levels of uncertainty shall be associated with the different levels of data quality.

OC-VCAL-RV-53. N/A

6.2.3. LATENCY

The latency in the field data delivery likely depends on the targeted application and the required level of quality. For instance, from the NOAA experience, the quick delivery of MOBY data with lower quality is of high value for Near real-time (NRT) monitoring of the VIIRS mission (Figure 21). Conversely, higher level of quality is expected for SVC and long-term studies.

OC-VCAL-RD-54. The required latency in in situ data delivery depends on the operational phase of SVC and quality level of data. In the early phase of space missions, quick delivery of SVC measurements is required (about one week), acknowledging that the data may be of lower quality. Consolidated SVC gain computation, relying on higher quality in situ measurement, shall be done after post-calibration, i.e. after several months (depending on system rotation). It is also required that the SVC site contributes to validation and QC activities. For NRT monitoring of the space mission performance, daily delivery is recommended, again with a possible lower quality level.

OC-VCAL-RU-54. N/A

OC-VCAL-RV-54. N/A

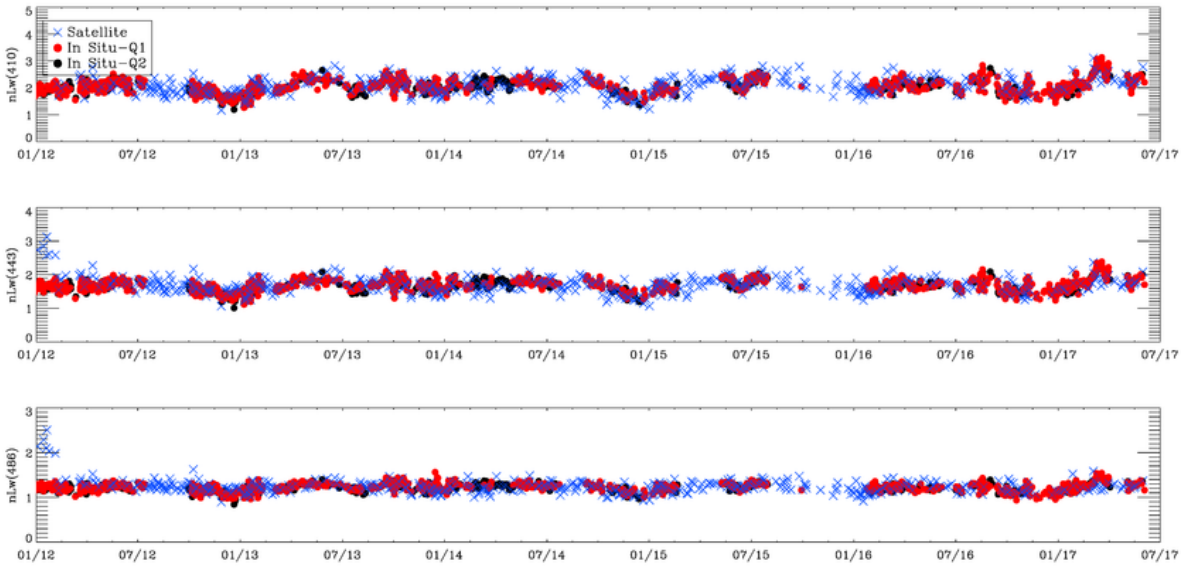

Figure 21. Example of NOAA's continuous NRT monitoring of VIIRS water-leaving radiance (blue cross, at 410, 443 and 486 nm from top to bottom) against MOBY data (red dots, and black dots for highest quality) between January 2012 and June 2017.

6.3. GROUND SEGMENT OPERATIONS

6.3.1. EARTH-OBSERVATION DATA

OC-VCAL-RD-55. Match-ups extraction shall be automatically and continuously available to support NRT validation. This can also be used to detect any problem of either the satellite sensor or the in situ instrument. When producing the SVC gains, the satellite and in situ data shall be additionally manually inspected.

OC-VCAL-RU-55. N/A

OC-VCAL-RV-55. N/A

6.3.2. PROCESSING ALGORITHM AND CAPABILITY

OC-VCAL-RD-56. The complete Level-2 processor with source code (algorithm and auxiliary data) shall be available to allow the computation of its associated SVC gains. Space Agencies shall have the capability to easily and quickly reprocess the mission whenever the SVC gains need to be updated or tested.

OC-VCAL-RU-56. N/A

OC-VCAL-RV-56. N/A

6.3.3. SVC PROCESSOR

Theoretically, the adjustment of mission average SVC gains is expected to be less than the uncertainty of the instrumental calibration. This has always been the case with MERIS for instance (Lerebourg et al., 2011). If not, then it indicates that some uncertainties are not well considered in either the SVC process or the instrument calibration.

OC-VCAL-RD-57. The SVC calculation should be embedded in the operational L2 sensor processing code to ensure exact replication of all relevant L2 processing steps during SVC computations. Ideally, the code shall be part of a community processor publicly available. This does not preclude that each agency may process the data by itself.

OC-VCAL-RU-57. The SVC processor shall include a module to derive the exact gain uncertainty budget, at pixel, matchup and mission level.

OC-VCAL-RV-57. It shall be verified that values of SVC gains, including their uncertainty, are within the instrumental calibration uncertainty. Close collaboration shall exist between the SVC team and the team in charge of the space instrumental calibration.

6.4. INTERNATIONAL HARMONISATION

Harmonisation between the worldwide SVC infrastructures managed by different agencies is highly encouraged, regarding measurement protocols, methodology for the uncertainty budget, processing code and, ideally, the instrument itself. Hence it is recommended to develop strong link between the expected European SVC programme and international frameworks such as CEOS (i.e. the Ocean Colour Radiometry Virtual Constellation) and the IOCCG.

OC-VCAL-RD-58. The full equivalence between the SVC sites and the derived gains shall be assured and drive the level of the international cooperation. International harmonisation of measurement protocols and methodologies for uncertainty assessment is required. Harmonisation of SVC infrastructures operated by different agencies is desirable as the harmonization is difficult when technologies are too different. Interagency collaboration shall include activities such as training and experience sharing between the different SVC infrastructures (the SVC infrastructure shall follow the recommendations of the INSITU-OCR white paper and be part of the IOCCG working group on SVC). Sharing of processing codes is recommended. It is recommended that field activities include intercomparisons of Lu measurements using a dedicated transfer radiometer (e.g. profiler) deployed at the participating SVC sites and potential research activities. It is worth noting that to be useful, the radiometric quality of such a transfer instrument should be equivalent to that of the SVC systems.

OC-VCAL-RU-58. N/A

OC-VCAL-RV-58. N/A

6.5. HUMAN AND MANAGEMENT ASPECTS

6.5.1. MANUFACTURING

OC-VCAL-RD-59. The instrument can be either bought off the shelf or developed in-house (at the laboratory in charge of SVC), as far as all technical requirements are met, including the regular characterisation, calibration and maintenance. A potential issue for manufacturers might be to maintain expertise if only few SVC instruments are sold. In case of commercial instrument, a very close relationship between the manufacturer and the laboratory is required.

OC-VCAL-RU-59. See OC-VCAL-RU-10.

OC-VCAL-RV-59. N/A

6.5.2. SERVICE OPERATION

OC-VCAL-RD-60. The SVC infrastructure, being an essential contributor to the performance of the S2 and S3 missions, is required to be managed as a sustainable and operational service for Copernicus. Duration of the service shall be aligned on that of the Copernicus programme. This also means that long-term funding is required. From MOBY and BOUSSOLE experience, the cost is not only driven by equipment, but also by staff costs and characterisation, calibration and maintenance activities (including ship time). Contingency funding is required in case of emergencies (buoys drift, boat strikes…). Additional funding is required for a research component to continuously improve the characterization of the SVC infrastructure and advance the SVC services (see section 6.5.3)..

OC-VCAL-RU-60. N/A

OC-VCAL-RV-60. N/A

6.5.3. EVOLUTIONARY AND SCIENCE COMPONENT

Success of the MOBY and BOUSSOLE projects relies deeply on the strong link between operation (strict provision of data for satellite SVC) and research activities. This mutual benefit between operational and science objectives shall be a model for any future SVC infrastructure.

OC-VCAL-RD-61. In parallel of its operational aspect, it is critical for the SVC programme to include an evolutionary component, to ensure flexibility and scientifically up to date SVC. It shall allow research activities at the site, possibly funded by other programmes.

OC-VCAL-RU-61. N/A

OC-VCAL-RV-61. N/A

6.5.4. HUMAN RESOURCES MANAGEMENT

In terms of human resources management, running a long-term operational SVC programme requires maintaining the knowledge in the SVC process and in the daily in situ operations. It is thus required to have training and maintenance of expertise over the long-term. Another key aspect in the success of the current two SVC sites (MOBY and BOUSSOLE) has been the joint collaboration with national metrology institutes (NIST and NPL, respectively). The SVC team shall follow this example and include this expertise to ensure establishing a rigorous SI-traceability in the sea-truth measurement.

OC-VCAL-RD-62. To ensure an operational service, the SVC field infrastructure shall be led by a Principal Investigator (PI) together with a sustainable team with demonstrated long-term history of working on SVC science and technology (instrument) development. Training of the team shall be continuously offered to ensure both redundancy and long-term continuation in human expertise; redundancy can be for instance ensured thanks to two PIs sharing a full time equivalent position. Finally, development and operation of the SVC infrastructure shall be done jointly with a NMI.

OC-VCAL-RU-62. N/A

OC-VCAL-RV-62. N/A

7. CONCLUSION: THE WAY TOWARDS A EUROPEAN SVC PROGRAMME

Europe, via its Copernicus programme, has now invested in a decade long commitment to operational ocean colour observations from space. A complementary investment in SVC will allow the best utilisation of these assets and fulfilment of the promise of quality marine services. SVC requires a dedicated programme with a set of strict requirements that answer to the needs of decades of future ocean colour observations. The programme also requires a long-term sustained investment in dedicated in situ measurement infrastructure and its calibration and validation activities.

With Sentinel-3A being already in orbit since February 2016, and Sentinel-3B planned for launch in early 2018, this expected European SVC programme should start as soon as possible: “climate change measurements place stringent requirements on accuracy, precision, and stability of our observations. To reduce the risk of not meeting these requirements, a calibration plan from beginning to end-of-life (i.e., ground to on-orbit operations) should be developed as early as possible (preferably during instrument design)” (Ohring et al., 2003).

Five steps are envisioned in this programme. The phases listed hereafter follow the European space industry standards (ECSS); this presentation is, however, not restrictive, as another phasing could be proposed, should the programme be implemented by other trusted-entities:

- Step1: Scientific, technical and operational requirements (Phase 0); this report constitutes the main baseline of this first step.
- Step2: Preliminary design, project plan and costing (Phase A & B).
- Step 3: Technical definition, specifications, detailed design (Phase C).
- Step 4: Development, testing and demonstration in the field (Phase D).
- Step 5: Operation (phase E).

The main priority identified by the ocean colour community for the operational phase is to ensure sustainable resources (staff, knowledge and infrastructure) to build long-term data series over multi-mission lifetime.

8. TABLE OF SYMBOLS

Symbol	Definition	Dimension/unit
λ	Wavelength (continuous variable)	nm
λ_i	Discrete theoretical wavelength of satellite sensor band i	nm
λ_j	Discrete theoretical wavelength of in situ sensor band j	nm
θ_p^{IS}	Refraction angle in the seawater	deg.
θ_s	Solar zenith angle	deg.
θ_s^{IS}	In situ solar zenith angle	deg.
θ_v	View zenith angle	deg.
θ_v^{IS}	In situ view zenith angle	deg.
$\Delta\varphi$	Relative azimuth angle	deg.
$\Delta\varphi^{IS}$	In situ relative azimuth angle	deg.
μ_s	Cosine of solar zenith angle	dimensionless
μ_s^{IS}	Cosine of in situ solar zenith angle	dimensionless
$\rho_f(n, \theta_s^{IS}, w_s)$	Fresnel reflection at the water surface	dimensionless
$\rho_w(\lambda_i, \theta_s, \theta_v, \Delta\varphi)$	Bidirectional marine reflectance (not corrected for the BRDF effect)	dimensionless
σ	Standard deviation (statistical parameter)	*as of the variable*
χ^2	Chi-squared test (statistical hypothesis)	dimensionless
$C_Q(\lambda_i, \theta_s, \theta_v, \Delta\varphi)$	Corrective factor of the surface BRDF effect applied to L_{wN} (correction from in situ to satellite geometry)	dimensionless
$C_Q^t(\lambda_i, \theta_s, \theta_v, \Delta\varphi)$	Corrective factor of the surface BRDF effect applied to L_{wN}^t (correction from in situ to satellite geometry)	dimensionless
$C_Q^{IS}(\lambda_i, \theta_s, \theta_v, \Delta\varphi)$	Corrective factor of the surface BRDF effect applied to L_{wN}^{IS} (correction from in situ to satellite geometry)	dimensionless
$C_s(time)$	Corrective factor of the 'Sun-Earth' distance varying with time (applied to F_o)	dimensionless
$C_s^{IS}(time)$	Corrective factor of the 'Sun-Earth' distance varying with in situ time (applied to F_o)	dimensionless
C_v	Coefficient of variation	dimensionless
$E_d^{IS}(\lambda_i)$	In situ surface spectral irradiance	W. m^{-2}.nm^{-1}
$F_0(\lambda_i)$	Mean extraterrestrial solar spectral irradiance	W. m^{-2}.nm^{-1}
$g(\lambda_i)$	Individual vicarious gain (i.e. pixel-by-pixel)	dimensionless
$\bar{g}(\lambda_i)$	Mission average vicarious gain	dimensionless
k	Coverage factor defining the confidence interval of a value taken by a variable	dimensionless
$K_L(\lambda, z)$	Spectral diffuse attenuation coefficient at depth z (in water)	m^{-1}

$L(\lambda_i)$	Spectral radiance at a given discrete band λ_i	W. m^{-2}.sr^{-1}.nm^{-1}
$L(\lambda)$	Spectral radiance (continuous spectrum)	W. m^{-2}.sr^{-1}.nm^{-1}
$L_a(\lambda_i, \theta_s, \theta_v, \Delta\varphi)$	Spectral radiance for a pure aerosol atmosphere	W. m^{-2}.sr^{-1}.nm^{-1}
$L_{path}(\lambda_i, \theta_s, \theta_v, \Delta\varphi)$	Spectral radiance for a pure scattering atmosphere (molecules+aerosols)	W. m^{-2}.sr^{-1}.nm^{-1}
$L^t_{path}(\lambda_i, \theta_s, \theta_v, \Delta\varphi)$	True (or targeted) spectral radiance for a pure scattering atmosphere (molecules+aerosols)	W. m^{-2}.sr^{-1}.nm^{-1}
$L_R(\lambda_i, \theta_s, \theta_v, \Delta\varphi)$	Spectral radiance for a pure molecular (Rayleigh) atmosphere	W. m^{-2}.sr^{-1}.nm^{-1}
$L_{Ra}(\lambda_i, \theta_s, \theta_v, \Delta\varphi)$	Spectral radiance for the 'Rayleigh-aerosol' coupling term	W. m^{-2}.sr^{-1}.nm^{-1}
$L_t(\lambda_i, \theta_s, \theta_v, \Delta\varphi)$	Spectral radiance at TOA	W. m^{-2}.sr^{-1}.nm^{-1}
$L^t_t(\lambda_i, \theta_s, \theta_v, \Delta\varphi)$	True (or targeted) spectral radiance at TOA	W. m^{-2}.sr^{-1}.nm^{-1}
$L_u(\lambda, 0^-)$	Upwelling spectral radiance just below the water surface	W. m^{-2}.sr^{-1}.nm^{-1}
$L_u(\lambda, z)$	Upwelling spectral radiance at depth z (in water)	W. m^{-2}.sr^{-1}.nm^{-1}
$L_w(\lambda_i, \theta_s, \theta_v, \Delta\varphi)$	Water-leaving spectral radiance	W. m^{-2}.sr^{-1}.nm^{-1}
$L_w^{\overline{cal}}(\lambda_i, \theta_s, \theta_v, \Delta\varphi)$	Satellite water-leaving spectral radiance after applying mission average vicarious gain	W. m^{-2}.sr^{-1}.nm^{-1}
$L_w^{IS}(\lambda_j, \theta_s^{IS}, \theta_v^{IS}, \Delta\varphi^{IS})$	In situ water-leaving spectral radiance	W. m^{-2}.sr^{-1}.nm^{-1}
$L^t_w(\lambda_i, \theta_s, \theta_v, \Delta\varphi)$	True (or targeted) water-leaving spectral radiance	W. m^{-2}.sr^{-1}.nm^{-1}
$L_{wN}(\lambda_i, \theta_s, \theta_v, \Delta\varphi)$	Fully normalized water-leaving spectral radiance	W. m^{-2}.sr^{-1}.nm^{-1}
$L^t_{wN}(\lambda_i, \theta_s, \theta_v, \Delta\varphi)$	True (or targeted) fully normalized water-leaving spectral radiance	W. m^{-2}.sr^{-1}.nm^{-1}
$n(\lambda_i, T, S)$	Spectral refractive index of seawater as function of water body temperature (T) and salinity (S)	dimensionless
N	Number of match-ups in the vicarious gain averaging	dimensionless
$R_{RS}^{IS}(\lambda_i)$	In situ remote sensing reflectance	dimensionless
S	Seawater salinity	ppt
$SRF_i(\lambda)$	Satellite sensor spectral response function of band λ_i	dimensionless
$SRF_j^{IS}(\lambda)$	Field sensor spectral response function of band λ_i	dimensionless
T	Seawater temperature	deg. C
$T_f(\theta_p^{IS}, w_s)$	Fresnel transmission through the 'water-air' interface	dimensionless
t$(\lambda_i, \theta_s, \theta_v)$	Total (upward+downward) atmospheric transmittance (accounting for molecules and aerosols scatterers)	dimensionless
$t^t(\lambda_i, \theta_s, \theta_v)$	True (or targeted) total (upward+downward) atmospheric transmittance (accounting for molecules and aerosols scatterers)	dimensionless
$t_{down}(\lambda_i, \theta_s, \theta_v)$	Total (direct+diffuse) downward atmospheric transmittance (accounting for molecules and aerosols scatterers)	dimensionless
$t_{down}^{IS}(\lambda_i, \theta_s, \theta_v)$	In situ total (direct+diffuse) downward atmospheric transmittance (accounting for molecules and aerosols scatterers)	dimensionless

$t_g(\lambda_i, \theta_s, \theta_v)$	Total (upward+downward) atmospheric gaseous transmittance	dimensionless
$t_g^t(\lambda_i, \theta_s, \theta_v)$	True (or targeted) total (upward+downward) atmospheric gaseous transmittance	dimensionless
$t_{g,down}^{IS}(\lambda_i, \theta_s)$	In situ downward atmospheric gaseous transmittance	dimensionless
$t_{up}(\lambda_i, \theta_s, \theta_v)$	Total (direct+diffuse) upward atmospheric transmittance (accounting for molecules and aerosols scatterers)	dimensionless
$u(x)$	Standard uncertainty (*k=1*) of any quantity x	*as of the variable*
$u(x, y)$	Standard covariance (*k=1*) of any two quantities x and y	*as of the variables*
u_r	Random part of total uncertainty u	*as of the variable*
u_s	Systematic part of total uncertainty u	*as of the variable*
$w(\lambda_i)$	Weighting coefficient of individual gains	dimensionless
w_s	Wind speed just above sea level	$m.s^{-1}$
z	Depth in water	m

9. LIST OF ACRONYMS

AC	Atmospheric Correction
AAC	Alternative Atmospheric Correction (OLCI)
AERONET	AErosol RObotic NETwork
AERONET-OC	Ocean Colour component of AERONET
AOT	Aerosol Optical Thickness
APF	Aerosol Phase Function
BOA	Bottom Of the Atmosphere
BOUSSOLE	BOUée pour l'acquiSition d'une Série Optique à Long termE (buoy for the acquisition of a long-term optical series); (field instrument)
BRDF	Bidirectional Reflectance Distribution Function
Cal/Val	Calibration and Validation
CCD	Charge-Coupled Device
CDOM	Coloured Dissolved Organic Matter
CDR	Climate Data Record
CEOS	Committee on Earth Observation Satellite
CMEMS	Copernicus Marine Environment Monitoring Service
CMUG	Climate Modelling User Group
CNSA	Chinese National Space Administration
COCTS	Chinese Ocean Colour and Temperature Scanner (on-board CNSA/HY-1B satellite)
COMS	Communication, Ocean, and Meteorological Satellite (South Korean satellite)
CTD	Conductivity, Temperature and Depth instrument
CZI	Coastal Zone Imager (on-board CNSA/HY-1B satellite)
DOP	Degree Of Polarization
ECSS	European Cooperation for Space Standardization
ENVISAT	ENVIronment SATellite (ESA satellite)
EO	Earth Observation
ESA	European Space Agency
EU	European Union
EUMETSAT	European Organisation for the Exploitation of Meteorological Satellites (Darmstadt, Germany)
FIDUCEO	FIDelity and Uncertainty in Climate data records from Earth Observations (funded by H2020)
FOV	Field Of View
FRM	Fiducial Reference Measurement
FWHM	Full-Width-at-Half-Maximum
GCOS	Global Climate Observing System
GEO-CAPE	GEOstationary Coastal and Air Pollution Event (future NASA mission)
GOCI	Geostationary Ocean Color Imager (on-board South Korean COMS)
GSFC	Goddard Space Flight Center (NASA Institute, Greenbelt, MA)
GUM	Guide to the expression of Uncertainty in Measurement
H2020	Horizon 2020 EU programme for research and innovation
HPLC	High Performance Liquid Chromatography (method to determine chlorophyll content)
HY-1B	Hai-Yang 1B (CNSA satellite)
HyspIRI	Hyperspectral Infrared Imager (future NASA mission)

INSITU-OCR	International Network for Sensor Inter-comparison and Uncertainty assessment for OCR
IOCS	International Ocean Colour Science
IOCCG	International Ocean-Colour Coordinating Group
IOP	Inherent Optical Property
ISRO	Indian Space Research Organization
JCGM	Joint Committee for Guides in Metrology
JRC	Joint Research Centre (Ispra, Italy)
LANDSAT-8	LAND SATellite-8 (NASA satellite for land applications)
LED	Light Emitting Diode
LIDAR	LIght Detection And Ranging
LISCO	Long Island Sound Coastal Observatory (near Northport, NY)
LOV	Laboratoire d'Océanographie de Villefranche/Mer (Villefranche/Mer, France)
MERIS	MEdium Resolution Imaging Spectrometer (on-board ESA/ENVISAT satellite)
MetEOC	Metrology for Earth Observation and Climate (joint research project coordinated by a network of NMIs across Europe)
MOBY	Marine Optical BuoY (field instrument)
MODIS	MODerate resolution Imaging Spectroradiometer (on-board NASA/Terra & NASA/Aqua EO satellites)
MRTD	Mission Requirements Traceability Document
MSI	Multi-Spectral Instrument (on-board ESA/S2 satellite)
MSIQR	Mean of the semi-interquartile range
NASA	National Aeronautics and Space Administration
NetCDF	Network Common Data Form
NIR	Near InfraRed part of the solar spectrum
NIST	National Institute of Standards and Technology (Gaithersburg, MD)
NMI	National Metrology Institute
NN	Neural Network
NOAA	National Oceanic and Atmospheric Administration
NPL	National Physical Laboratory (Teddington, UK)
NRT	Near real-time
NURADS	Upwelling RADiance distribution camera System (field instrument)
OC	Ocean Colour
OC-CCI	Ocean Colour Climate Change Initiative (ESA project)
OC-VCAL	Ocean Colour Vicarious Calibration
OCM-2	Ocean Colour Monitor-2 (on-board ISRO/OceanSat-2)
OCR	Ocean Colour Radiometry
OLCI	Ocean and Land Colour Instrument (on-board ESA/S3 satellite)
OSPREy	Optical Sensors for Planetary Radiant Energy (field instrument)
PACE	Plankton, Aerosol, Cloud, ocean Ecosystem (future NASA mission)
PDF	Probability Density Function
PI	Principal Investigator
ppt	Part per thousand (‰)
PROBA-V	Project for On-Board Autonomy-Vegetation (VEGETATION instrument on-board ESA/PROBA satellite)
QA4EO	Quality Assurance Framework for Earth Observation (ESA Workshop)
QC	Quality Control
RAMSES	RAdiation Measurement Sensor with Enhanced Spectral resolution (field instrument

	developed by TriOS)
RD	Requirement Description
RFP	Request For Proposals
RTM	Radiative Transfer Model
RU	Requirement Uncertainty
RV	Requirement Verification
S2	Sentinel-2 (ESA satellite)
S3	Sentinel-3 (ESA satellite)
S3VT	S3 Validation Team (ESA working group)
SDF	Stray light Distribution Function
SeaWiFS	Sea-viewing Wide Field-of-view Sensor (on-board GeoEye's OrbView-2 satellite)
SI	International System of Units
SIO	South Indian Ocean
SLA	Service Level Agreement
SLSTR	Sea and Land Surface Temperature Radiometer (on-board ESA/S3 satellite)
SNPP	Suomi National Polar-orbiting Partner-ship weather satellite (NASA satellite)
SNR	Signal to Noise Ratio
SO	Successive Orders of the scattering code (radiative transfer code)
SPG	South Pacific Gyre
SPMR	SeaWiFS Profiling Multichannel Radiometer (field instrument)
SRF	Spectral Response Function
SSA	Single Scattering Albedo
STAIRS	Spectrally Tuneable Absolute Irradiance and Radiance Source (i.e. the NPL system for calibrating radiometric detectors in radiance, irradiance or power mode)
SVC	System Vicarious Calibration
SWIR	Short-Wave InfraRed part of the solar spectrum
TOA	Top of the Atmosphere
TriOS	Tri-Optical Sensors company (Rastede, Germany)
USA	United States of America
UV	Ultra-Violet part of the solar spectrum
VIIRS	Visible Infrared Imaging Radiometer Suite (on-board NASA/SNPP)
VIM	Vocabulário Internacional de Metrologia (International Vocabulary of Metrology)
VIS	Visible part of the solar spectrum
WGCV	Working Group on Calibration and Validation (CEOS programme)

10. REFERENCES

Ahmad, Z., B.A. Franz, C.R. McClain, E.J. Kwiatkowska, P.J. Werdell, E.P. Shettle, and B.N. Holben, 2010. "New aerosol models for the retrieval of aerosol optical thickness and normalized water-leaving radiances from the SeaWiFS and MODIS sensors over coastal regions and open oceans", *Applied Optics*, **49**: 5545-5560.

Ahmed, S., A. Gilerson, S. Hlaing, A. Weidemann, R. Arnone, and M. Wang, 2013. "Assessment of VIIRS Ocean Color data retrieval performance in coastal regions", In *Proceedings of International Ocean Colour Science* (IOCS'2013), Darmstadt, Germany, 06-08 May 2013.

Antoine, D., and C. Mazeran, 2017. "System vicarious calibration for satellite ocean colour observations: Review of historical and contemporary approaches", *Presentation at International Workshop on "Options for future European satellite OCR vicarious adjustment infrastructure for S3/OLCI and S2/MSI series"*, ESA/ESRIN, Frascati, Italy, 21-23 February 2017.

Antoine, D., and A. Morel, 1999. "A multiple scattering algorithm for atmospheric correction of remotely-sensed ocean colour (MERIS instrument): Principle and implementation for atmospheres carrying various aerosols including absorbing ones", *International Journal of Remote Sensing*, **20** (9): 1875-1916.

Antoine, D., M. Chami, H. Claustre, F. D'Ortenzio, A. Morel, G. Bécu, B. Gentili, F. Louis, J. Ras, E. Roussier, A.J. Scott, D. Tailliez, S.B. Hooker, P. Guevel, J.-F. Desté, C. Dempsey, and D. Adams, 2006. "BOUSSOLE: a joint CNRS-INSU, ESA, CNES and NASA ocean colour calibration and validation activity", In *NASA Technical Memorandum*, N° 2006-214147, Greenbelt (MD), 61p.

Antoine, D., F. D'Ortenzio, S.B. Hooker, G Bécu, B. Gentili, D. Tailliez, and A.J. Scott, 2008. "Assessment of uncertainty in the ocean reflectance determined by three satellite ocean color sensors (MERIS, SeaWiFS and MODIS-A) at an offshore site in the Mediterranean Sea (BOUSSOLE project)", *Journal of Geophysical Research*, **113**, C07013.

Antoine, D., P. Guevel, J.-F. Desté, G. Bécu, F. Louis, A.J. Scott, and P. Bardey, 2008b. "The BOUSSOLE buoy: A new transparent-to-swell taut mooring dedicated to marine optics: Design, tests and performance at sea", *Journal of Atmospheric & Oceanic Technology*, **25**: 968-989.

Antoine D., A. Morel, E. Leymarie, A. Houyou, B. Gentili, S. Victori, J.-P. Buis, N. Buis, S. Meunier, M. Canini, D. Crozel, B. Fougnie, and P. Henry, 2013. "Underwater radiance distributions measured with miniaturized multispectral radiance cameras", *Journal of Atmospheric & Oceanic Technology*, **30** (1): 74-95.

Austin, R.W., 1974. "The remote sensing of spectral radiance from below the ocean surface", In *Optical Aspects of Oceanography* (N.G. Jerlov and E.S. Nelson, Eds.), Academic Press, New-York (NY): 317-344.

Austin, R.W., and G. Halikas, 1976. "The index of refraction of seawater", *Scripps Institution of Oceanography Report*, N^{o} 76-1, San Diego (CA), 64p.

Aznay, O., R. Santer, and F. Zagolski, 2014. "Validation of the atmospheric scattering functions used in the atmospheric correction over ocean", *International Journal of Remote Sensing*, **35** (13): 4984-5003.

Bailey, S.W., and P.J. Werdell, 2006. "A multi-sensor approach for the on-orbit validation of ocean color satellite data products", *Remote Sensing of Environment*, **102**: 12-23.

Bailey, S.W., S.B. Hooker, D. Antoine, B.A. Franz, and P.J. Werdell, 2008. "Sources and assumptions for the vicarious calibration of ocean color satellite observations", *Applied Optics*, **47**: 2035-2045.

Bell, S, 2011. "A beginner's guide to uncertainty of measurement", *National Physical Laboratory (NPL) Measurement Good Practice Guide N° 11, Issue 2*, Teddington, UK.

Bialek, A., C.L. Greenwell, E.R. Woolliams, N. Fox, and G. Zibordi, 2013. "Hidden secrets of absolute radiometric calibration", In *Proceedings of International Ocean Colour Science* (IOCS'2013), Darmstadt, Germany, 06-08 May 2013.

Bialek A., V. Vellucci, B. Gentili, D. Antoine, C. Underwood, N. Fox, 2016. "An uncertainty budget for the BOUSSOLE radiometry, as derived using a monte carlo method", In *Proceedings of Ocean Optics XXIII Conference*, Victoria (BC), Canada, 23-28 October 2016.

Bouvet M., and F. Ramoino, 2010. "Equalization of MERIS level-1b products from the 2nd reprocessing", In *ESA/ESTEC Technical Note*, TN TEC-EEP/2009.521, Noordwijk, The Netherlands.

Brown, S.W., G.P. Eppeldauer, and K.R. Lykke, 2000. "NIST facility for spectral irradiance and radiance responsivity calibrations with uniform sources", *Metrologia*, **37**: 579-582.

Brown, S.W., S.J. Flora, M.E. Feinholz, M.A. Yarbrough, T. Houlihan, D. Peters, Y.S. Kim, J. Mueller, B.C. Johnson, D.K. Clark, 2007. "The marine optical buoy (MOBY) radiometric calibration and uncertainty budget for ocean colour satellite sensor vicarious calibration", In *Proceedings of SPIE on Optics & Photonics*, *Sensors, Systems, and Next-Generation Satellites XI*, Florence, Italy, 17-20 September 2007.

Bulgarelli, B., V. Kiselev, and G. Zibordi, 2014. "Simulation and analysis of adjacency effects in coastal waters: A case study", *Applied Optics*,. **53**: 1523-1545.

Casal, T., C. Donlon, P. Goryl, P. Femenias, R. Schaarroo, A. O'Caroll, E. Kwiatkowska, H. Wilson, 2014. "Sentinel-3 scientific validation team implementation plan", *ESA/ESRIN report*, EOP-SM/2641/CD-cd, Issue 1.4, Frascati, Italy.

Cox, C., and W. Munk, 1954. "Measurement of the roughness of the sea surface from photographs of the Sun's glitter", *Journal of the Optical Society of America*, **44**: 838-850.

Delwart, S., and L. Bourg, 2001. "Radiometric calibration of MERIS", In *Proceedings of SPIE on Sensors, Systems, and Next-Generation Satellites XV*, Prague, Czech Republic, September 16-19, 2011.

Deschamps, P. Y., M. Herman, and D. Tanre, 1983. "Modelling of the atmospheric effects and its application to the remote sensing of ocean colour", *Applied Optics,* **22**: 3751-3758.

Doerffer, R., and H. Schiller, 2007. "The MERIS Case 2 water algorithm", *International Journal of Remote Sensing*, **28** (3): 517-535.

Donlon, C., 2011. "Sentinel-3 mission requirements traceability document (MRTD)", *ESA/ESRIN report*, EOP-SM/2184, CD-cd, Issue1, Frascati, Italy.

Doyle, J.P., and G. Zibordi, 2002. "Optical propagation within a three-dimensional shadowed atmosphere-ocean field: application to large deployment structures", *Applied Optics,* **41**, 4283-4306.

Doyle, J.P., S.B. Hooker, G. Zibordi, and D. van der Linde, 2003. "Validation of an in-water tower shading correction scheme", In *SeaWiFS Postlaunch Technical Report Series* (S.B. Hooker and E.R. Firestone, Eds.), NASA/GSFC, TM-2003-206892, Greenbelt, MD, vol. 25, 33p.

Eplee, R.E. Jr., W.D. Robinson, S.W. Bailey, D.K. Clark, P.J. Werdell, M. Wang, R.A. Barnes, and C.R. McClain, 2001. "Calibration of SeaWiFS. II. vicarious techniques", *Applied Optics*, **40**: 6701-6718.

Feinholz, M.E., S.J. Flora, M.A. Yarbrough, K.R. Lykke, S.W. Brown, B.C. Johnson, and D.K. Clark, 2009. "Stray light correction of the marine optical system", *Journal of Atmospheric & Oceanic Technology*, **26**: 57-73.

Feinholz, M.E., B.C. Johnson, K.J. Voss, M.A. Yarbrough, and S.J. Flora, 2017. "Immersion coefficient for the marine optical buoy (MOBY) radiance collectors", *Journal of Research of the National Institute of Standards & Technology*, **122**: 9p.

Feng, H., D. Vandemark, J.W. Campbell, and B.N. Holben, 2009. "Evaluation of MODIS ocean colour products at a northeast United States coast site near the Martha's Vineyard Coastal Observatory", *International Journal of Remote Sensing*, **29**: 4479-4497.

Flora, S.J., S. Brown, B.C. Johnson, 2006. "MOBY/AHAB wavelength resolution question", *MOBY/AHAB Review Meeting*, July 18, 2006.

Fox, N., 2010. "A guide to expression of uncertainty of measurements", *National Physical Laboratory (NPL)-QA4EO guide*, ref. QA4EO-QAEO-GEN-DQK-006, Issue 4.0, Teddington, UK.

Franz, B.A., E.J. Ainsworth, and S. Bailey, 2001. "SeaWiFS vicarious calibration: an alternative approach using in situ observations of oceanic and atmospheric optical properties", In *In Situ Aerosol Optical Thickness Collected by the SIMBIOS Program (1997–2000): Protocols, Data QC, and Analysis* (G.S. Fargion, R.A. Barnes, and C.R. McClain, Eds.), NASA/GSFC Technical Memorandum, 209982, Greenbelt (MD): 88-96.

Franz, B.A., S.W. Bailey, P.J. Werdell, and C.R. McClain, 2007. "Sensor-independent approach to the vicarious calibration of satellite ocean colour radiometry", *Applied Optics*, **46**: 5068–5082.

GCOS, 2011. "Systematic observation requirements for satellite-based data products for climate", *Supplemental details to the satellite-based component of the "Implementation Plan for the Global Observing System for Climate in Support of the UNFCCC (2010 update)"*, December 2011, published by *World Meteorological Organization* (WMO), GCOS-154, Geneva, Switzerland.

GCOS, 2016. "The global observing system for climate: Implementation needs", published by *World Meteorological Organization* (WMO), GCOS-200, Geneva, Switzerland.

Gergely, M., and G. Zibordi, 2014. "Assessment of AERONET-OC Lwn uncertainties", *Metrologia*, **51** (1): 40-47.

Gleason, A.C.R., K.J. Voss, H.R. Gordon, M. Twardowski, J. Sullivan, C. Trees, A. Weidemann, J.F. Berthon, D. Clark, Z.P. Lee, 2012. "Detailed validation of the bidirectional effect in various Case I and Case II waters", *Optics Express*, **20** (7): 7630-7645.

Gordon, H.R., 1987. "Calibration requirements and methodology for remote sensors viewing the ocean in the visible", *Remote Sensing of Environment*, **22**: 103–126.

Gordon, H.R., 1997. "Atmospheric correction of ocean color imagery in the Earth observing system era", *Journal of Geophysical Research*, **102D**: 17081-17106.

Gordon, H.R., 1998. "In-orbit calibration strategy for ocean colour sensors", *Remote Sensing of Environment*, **63** (3): 265–278.

Gordon, H.R., and M. Wang, 1994. "Retrieval of water-leaving radiance and aerosol optical thickness over the oceans with SeaWiFS: A preliminary algorithm", *Applied Optics*, **33**: 443-452.

Gregg, W.W., and K.L Carder, 1990. "A simple spectral solar irradiance model for cloudless maritime atmospheres", *Limnology & Oceanography*, **35**: 1657-1675.

Hooker, S.B., G. Bernhard, J.H. Morrow, C.R. Booth, T. Comer, R.N. Lind, and V. Quang, 2012. "Optical sensors for planetary radiant energy (OSPREy): Calibration and validation of current and next-generation NASA missions", *NASA Technical Memorandum*, 2012–215872, NASA/GSFC, Greenbelt, MD.

IOCCG, 2008. "Why ocean colour?", In *The Societal Benefits of Ocean-Colour Technology* (T. Platt, N. Hoepffner, V. Stuart, and C. Brown, Eds.), *Reports of the International Ocean-Colour Coordinating Group*, No. 7, IOCCG, Dartmouth (NS), Canada.

IOCCG, 2010. "Atmospheric correction for remotely-sensed ocean-colour products". M. Wang (Ed.), *Reports of the International Ocean-Colour Coordination Group*, No. 10, IOCCG, Darmouth (NS), Canada.

IOCCG, 2012. "Mission requirements for future ocean-colour sensors",In *Reports of the International Ocean-Colour Coordinating Group*, No. 13, IOCCG (C.R. McClain and G. Meister, Eds.), Dartmouth (NS), Canada.

IOCCG, 2013a. "In-flight calibration of satellite ocean-colour sensors", R. Frouin (Ed.), *Reports of the International Ocean-Colour Coordinating Group*, No. 14, IOCCG, Dartmouth (NS), Canada.

IOCCG, 2013b. "Report from the IOCCG workshop on ocean colour system vicarious calibration for science and operational missions", *Reports of the International Ocean-Colour Coordinating Group*, ESA/ESRIN, Frascati, Italy.

JCGM, 2008. "Evaluation of measurement data", *Guide to the expression of Uncertainty in Measurement* (GUM), JCGM 100:2008 (ISO/IEC Guide 98-3).

JCGM, 2011. "Evaluation of measurement data", *Supplement 2 to the "Guide to the expression of Uncertainty in Measurement* (GUM)*" – Extension to any number of output quantities*, JCGM 102:2011 (ISO/IEC Guide 98-3-2).

JCGM, 2012. "International vocabulary of metrology", *Basic and General Concepts and Associated Terms (VIM)*, 3rd edition, JCGM 200:2012.

Johnson, B.C., 2003. "Radiometric metrology for remote sensing", In *Proceedings of International Workshop on Radiometric and Geometric Calibration*, 2-5 December 2003, Gulfport (Miss).

Johnson, B.C., S.W. Brown, and J.P. Rice, 2003. "Metrology for remote sensing radiometry", *In Post-Launch Calibration of Satellite Sensors-Proceedings of the International Workshop on Radiometric and Geometric Calibration*, 2–5 December 2003, Gulfport (Miss), (S.A. Morain, A.M. Budge, and Taylor & Francis Group, Eds.), London, UK.

Johnson, B.C., H. Yoon, J.P. Rice, and A.C. Parr, 2014. "Principles of optical radiometry and measurement uncertainty". In *Optical Radiometry for Ocean Climate Measurements* (G. Zibordi, C. Donlon, and A. Parr, Eds.), Academic Press, Amsterdam, The Netherlands.

Knaeps, E., A.I. Dogliotti, D. Raymaekers, K. Ruddick, and S. Sterckx, 2012. "In situ evidence of non-zero reflectance in the OLCI 1020 nm band for a turbid estuary", *Remote Sensing of Environment*, **120**: 133-144.

Kratzer, S., E.T. Harvey, and P. Philipson, 2014. "The use of ocean colour remote sensing in integrated coastal zone management: A case study from Himmerfjärden, Sweden", *Marine Policy*, ISSN 0308-597X, vol. 43: 29-39.

Kuwahara, V., P.G. Strutton, T.D. Dickey, M.R. Abbott, R.M. Letelier, M.R. Lewis, S. McLean, F.P. Chavez, A. Barnard, J. Ruairidh Morrison, A. Subramaniam, D. Manov, X. Zheng, and J.L. Mueller, 2003. "Radiometric and bio-optical measurement from moored and drifting buoys: measurement

and data analysis protocols", In *Ocean Optics Protocols for Satellite Ocean Colour Sensor Validation*, *NASA Technical Memorandum*, Chapter 3, Rev.-4, Vol.-VI (J.L. Mueller, G.S. Fargion, and C.R. McClain, Eds.), NASA/GSFC, Greenbelt, MD.

Kwiatkowska, E.J., B.A. Franz, G. Meister, C.R. McClain, and X. Xiong, 2008. "Cross calibration of ocean colour bands from moderate resolution Imaging spectroradiometer (MODIS) on Terra platform", *Applied Optics*, **47** (36): 6796-6810.

Lenoble, J., M. Herman, J.L. Deuzé, B. Lafrance, R. Santer, and D. Tanré, 2007. "A successive order of scattering code for solving the vector equation of transfer in the Earth's atmosphere with aerosols", *Journal of Quantitative Spectroscopy & Radiative Transfer*, **107**: 479-507.

Lerebourg, C., C. Mazeran, J.P. Huot, and D. Antoine, 2011. "Vicarious adjustment of the MERIS ocean colour radiometry", ESA/ESRIN MERIS ATBD-2.24 Issue 1.0, Frascati, Italy.

Levick, A.P., C.L. Greenwell, J. Ireland, E. Woolliams, T. Goodman, and N. Fox, 2014. "Spectral radiance source based on supercontinuum laser and wavelength tunable bandpass filter: The spectrally tunable absolute irradiance and radiance source (STAIRS)", *Applied Optics*, **53** (16): 3508-3519.

Mangin, A., C. Brockmann, O. Fanton d'Andon, F.-R. Martin-Lauzer, S. Peters, N. Dwyer, K. Ruddick, 2014. "The FP7 space projects prospective", *Copernicus Coastal Service White Paper*.

Mariage, V., J. Pelon, F. Blouzon, S. Victori, N. Geyskens, N. Amarouche, C. Drezen, A. Guillot, M. Calzas, M. Garracio, N. Wegmuller, N. Sennéchael, and C. Provost, 2017. "IAOOS microlidar-on-buoy development and first atmospheric observations obtained during 2014 and 2015 arctic drifts", *Optics Express*, **25** (A): 73-84.

Mazeran, C., C. Brockmann, A. Ruescas, F. Steinmetz, and M. Zühlke, 2017. "A revisit of system vicarious calibration for non-standard ocean colour algorithm: Application to SeaWiFS, MODIS and MERIS data processed by POLYMER", (Submitted).

Mélin, F., 2016. "Impact of inter-mission differences and drifts on chlorophyll-a trend estimates", *International Journal of Remote Sensing*, **37** (10): 2061-2079

Mélin, F., G. Sclep, T. Jackson, and S. Sathyendranath, 2016. "Uncertainty estimates of remote sensing reflectance derived from comparison of satellite data sets", *Remote Sensing of Environment*, **177**: 107–124.

Merchant, C., J. Mittaz, E. Woolliams, R. Roebeling, Y. Govaerts, and T. Block, 2016. "Fidelity and uncertainty in climate data records from Earth observations (FIDUCEO) vocabulary", Technical Note, Issue 1.2, 12 April 2016.

Meroni, M., L. Busetto, L. Guanter, S. Cogliati, G. Crosta, M. Migliavacca, C. Panigada, M. Rossini, and R. Colombo, 2010. "Characterization of fine resolution field spectrometers using solar Fraunhofer lines and atmospheric absorption features", *Applied Optics*, **49**: 2858-2871.

Morel, A., and B. Gentili, 1996. "Diffuse reflectance of oceanic waters: 3.-Implication of bidirectionality for the remote-sensing problem", *Applied Optics*, **35**: 4850-4862.

Morel, A., D. Antoine, and B. Gentili, 2002. "Bidirectional reflectance of oceanic waters: Accounting for Raman emission and varying particle phase function", *Applied Optics*, **41**, 6289-6306.

Morys, M., F.M. Mims III, S. Hagerup, S.E. Anderson, A. Baker, J. Kia and T. Walkup, 2001. "Design, calibration and performance of MICROTOPS II handheld ozone monitor and Sun photometer", *Journal of Geophysical Research*, **106**: 14573-14582.

Mueller, J.L., and R.W. Austin, 2003. "Characterization of oceanographic and atmospheric radiometers", *NASA/GSFC Technical Memorandum*, 211621, Greenbelt (MD), vol. II, Issue 4.2: 17-33.

Mueller, J.L., 2003. "In-water radiometric profile measurements and data analysis protocols", In *Ocean Optics Protocols for Satellite Ocean Colour Sensor Validation*, *NASA Technical Memorandum*, Chapter-2, Rev.-4, Vol.-III (J.L. Mueller, G.S. Fargion, and C.R. McClain, Eds.), NASA/GSFC, Greenbelt, MD.

Mueller, J., 2007. "Self-shading corrections for MOBY upwelling radiance measurements", *Final Technical Report to NESDIS*, NOAA Grant NA04NES44000007, 33p.

NASA, 2014. "ROSES 2014 research announcement", *Topic A.3: Ocean Biology and Biogeochemistry: Ocean Color Remote Sensing Vicarious (In Situ) Calibration Instruments*. Amended 21 March 2014.

Ohring, G., B. Wielicki, R. Spencer, B. Emery, and R. Datla, 2004. "Satellite instrument calibration for measuring global climate change", *National Institute of Standards and Technology (NIST) Report*, Gaithersburg (MD), NISTIR 7047, 101p.

Ohring, G., 2007. "Achieving satellite instrument calibration for climate change (ASIC)", *Report of the Workshop from NOAA, NIST, NASA, NPOESS, and SDL-USU,* National Conference Center at Lansdowne, West Virginia (WV), 16-18 May 2006.

Quan, X., and E.S. Fry, 1995. "Empirical equation for the index of refraction of seawater", *Applied Optics*, **34**: 3477-3480.

Santer, R., and C. Schmechtig, 2000. "Adjacency effects on water surfaces: primary scattering approximation and sensitivity study", Applied Optics, **39:**, 361-375.

Sentinel-3 CalVal Team, 2016. "Sentinel-3 OLCI-A pre-flight spectral response functions", ESA/ESTEC Technical Note, ref. S3-TN-ESA-OL-660, Noordwijk, The Netherlands.

Steinmetz, F, D. Ramon, P.-Y. Deschamps, 2012. "POLYMER atmospheric correction algorithm", ESA/ESRIN/OC-CCI Algorithm Theoretical Basis Document (ATBD), Issue 1.3, Frascati, Italy.

Talone, M., G. Zibordi, I. Ansko, A. Banks, and J. Kuusk, 2016. "Stray light effects in above-water remote-sensing reflectance from hyperspectral radiometers", *Applied Optics*, **55**: 3966-3977.

Tanré D., Deroo C., Duhaut P., Herman M., Mocrette J.J., Perbos J. and Deschamps P.Y., 1990, "Description of a computer code to Simulate the Satellite Signal in the Solar Spectrum: The 5S code", *International Journal of Remote Sensing*, 11: 659-668.

Vanhellemont, Q., and K. Ruddick, 2015. "Advantages of high quality SWIR bands for ocean colour processing: Examples from Landsat-8", *Remote Sensing of Environment*, **161**: 89-106.

Vellucci, V., E. Leymarie, B. Gentili, D. Antoine, 2014. « Shadowing corrections of BOUSSOLE radiometric measurements", In *Proceedings of SPIE*, *Ocean Optics XXII Conference*, Portland (ME), 27-31 Octobre 2014.

Vermote, E., D. Tanré, J.L. Deuzé, M. Herman, and J.J. Morcrette, Second simulation of the satellite signal in the solar spectrum, 6S: an overview, *I.E.E.E. Transactions on Geoscience and Remote Sensing*, 35 (3), 675-687, 1997.

Voss, K.J., and A.L. Chapin, 2005. "Upwelling radiance distribution camera system, NURADS", *Optics Express*, **13** (11): 4250-4262.

Voss, K.J., A. Morel, and D. Antoine, 2007. "Detailed validation of the bidirectional effect in various Case 1 waters for application to Ocean Color imagery", *Biogeosciences*, **4**: 781-789.

Voss, K.J., S. McLean, M. Lewis, B.C. Johnson, S.J. Flora, M.E. Feinholz, M.A. Yarbrough, C. Trees, M. Twardowski, D. Clark, 2010. "An example crossover experiment for testing new vicarious calibration techniques for satellite ocean colour radiometry", Journal of Atmospheric & Oceanic Technology, **27**: 1747-1759.

Voss, K.J., and N. Souaidia, 2010. "POLRADS: Polarization radiance distribution measurement system", *Optics Express*, **18**: 19672-19680.

Voss, K.J., B.C. Johnson, M.A. Yarbrough, and A. Gleason, 2015. "MOBY-Net: An ocean colour vicarious calibration system", ESTF, June 2015, Pasadena (CA).

Voss, K.J., and S.J. Flora, 2017. "Spectral dependence of the seawater-air radiance transmission coefficient", Journal of Atmospheric & Oceanic Technology, **34**: 1203-1205.

Voss, K.J., H.R. Gordon, S.J. Flora, B.C. Johnson, M.A. Yarbrough, M.E. Feinholz, and T. Houlihan, 2017. "A method to extrapolate the diffuse upwelling radiance attenuation coefficient to the surface as applied to the marine optical buoy (MOBY)", *Journal of Atmospheric & Oceanic Technology*, **34**: 1423-1432.

Wang, M., and H.R. Gordon, 2002. "Calibration of ocean colour scanners: How much error is acceptable in the near infrared?", *Remote Sensing of Environment*, **82**: 497-504.

Wang, M., K.D. Knobelspiesse, and C.R. McClain, 2005. "Study of the sea-viewing wide field-of-view sensor (SeaWiFS) aerosol optical property data over ocean in combination with the ocean colour products", *Journal of Geophysical Research*, **110**, D10S06.

Wang, M., W. Shi, L. Jiang, and K.J. Voss, 2016. "NIR- and SWIR-based on-orbit vicarious calibrations for satellite ocean color sensors", Optics Express, **24**: 20437-20453.

Werdell, P., S. Bailey, B. Franz, A. Morel, and C. McClain, 2007. "On-orbit vicarious calibration of ocean colour sensors using an ocean surface reflectance model", *Applied Optics*, **46**, 5649-5666.

White, D.R., M.T. Clarkson, P. Saunders, and H. Yoon, 2008. "A general technique for calibrating indicating instruments", *Metrologia*, **45**: 199-210.

Woolliams, E., A. Hueni, and J. Gorrono; 2015. "Intermediate uncertainty analysis for Earth observation (instrument calibration)", *Course of the European Metrology for Earth Observation and Climate project* (MetEOC), version 2.

Yoon, H.W., J.J. Butler, T.C. Larasen, and G.P. Eppeldauer, 2003. "Linearity of InGaAs diodes", *Metrologia*, **40** (S): 154-158.

Zibordi, G., 2006. "Immersion factor of in-water radiance sensors: Assessment for a class of radiometers", *Journal of Atmospheric & Oceanic Technology*, **23**: 302-313.

Zibordi, G., J.-F. Berthon, F. Mélin, D. D'Alimonte, and S. Kaitala, 2009a. "Validation of satellite ocean colour primary products at optically complex coastal sites: Northern Adriatic Sea, northern Baltic Proper and Gulf of Finland", *Remote Sensing of Environment*, **113**: 2574-2591.

Zibordi, G., B.N. Holben, I. Slutsker, D. Giles, D. D'Alimonte, F. Mélin, J.-F. Berthon, D. Vandemark, H. Feng, G Schuster, B.E. Fabbri, S. Kaitala, and J. Seppala, 2009b. "AERONET-OC: A network for the validation of ocean colour primary radiometric products", *Journal of Atmospheric & Oceanic Technology*, **26**: 1634-1651.

Zibordi, G., F. Mélin, K.J. Voss, B.C. Johnson, B. Franz, E. Kwiatkowska, J-P. Huot, M. Wang, and D. Antoine, 2015. "System vicarious calibration for ocean colour climate change applications: Requirements for in situ data", *Remote Sensing of Environment*, **159**: 361-369.

Zibordi, G., and K.J. Voss, 2014a. “In situ optical radiometry in the visible and near infrared”, In *Optical radiometry for ocean climate measurements*, *Experimental Methods in the Physical Sciences* (G. Zibordi, C. Donlon, and A. Parr, Eds.), Academic Press, Amsterdam, The Netherlands.

Zibordi, G., and K.J. Voss, 2014b. “Requirements and strategies for in situ radiometry in support of satellite ocean colour”, In *Optical Radiometry for Oceans Climate Measurements*, *Experimental Methods in the Physical Sciences* (G. Zibordi, C.Donlon and A. Parr, Eds.), Academic Press, Amsterdam, The Netherlands.

Zibordi, G., and F. Mélin, 2017. “An evaluation of marine regions relevant for ocean color system vicarious calibration”, *Remote Sensing of Environment*, **190**: 122-136.

Zibordi, G., F. Mélin, and M. Talone, 2017a. “System vicarious calibration for Copernicus ocean colour mission: Requirements and recommendations for an European Site”, *Joint Research Centre (JRC) Technical Note, EUR 28433 EN*, Ispra, Italy.

Zibordi, G., M. Talone, K.J. Voss, and B.C. Johnson, 2017b. “Impact of spectral resolution of in situ ocean colour radiometric data in satellite matchups analyses”, *Optics Express* (in press).

Zibordi, G., M. Talone, and L. Jankowski, 2017c. “Response to temperature of a class in situ hyperspectral radiometers”, *Journal of Atmospheric & Oceanic Technology* (in press).